Influence of Parametric Modelling of Wing Subsystems on the Aircraft Design and Performance

Nithin Kodali Rao

Technische Universiteit Delft

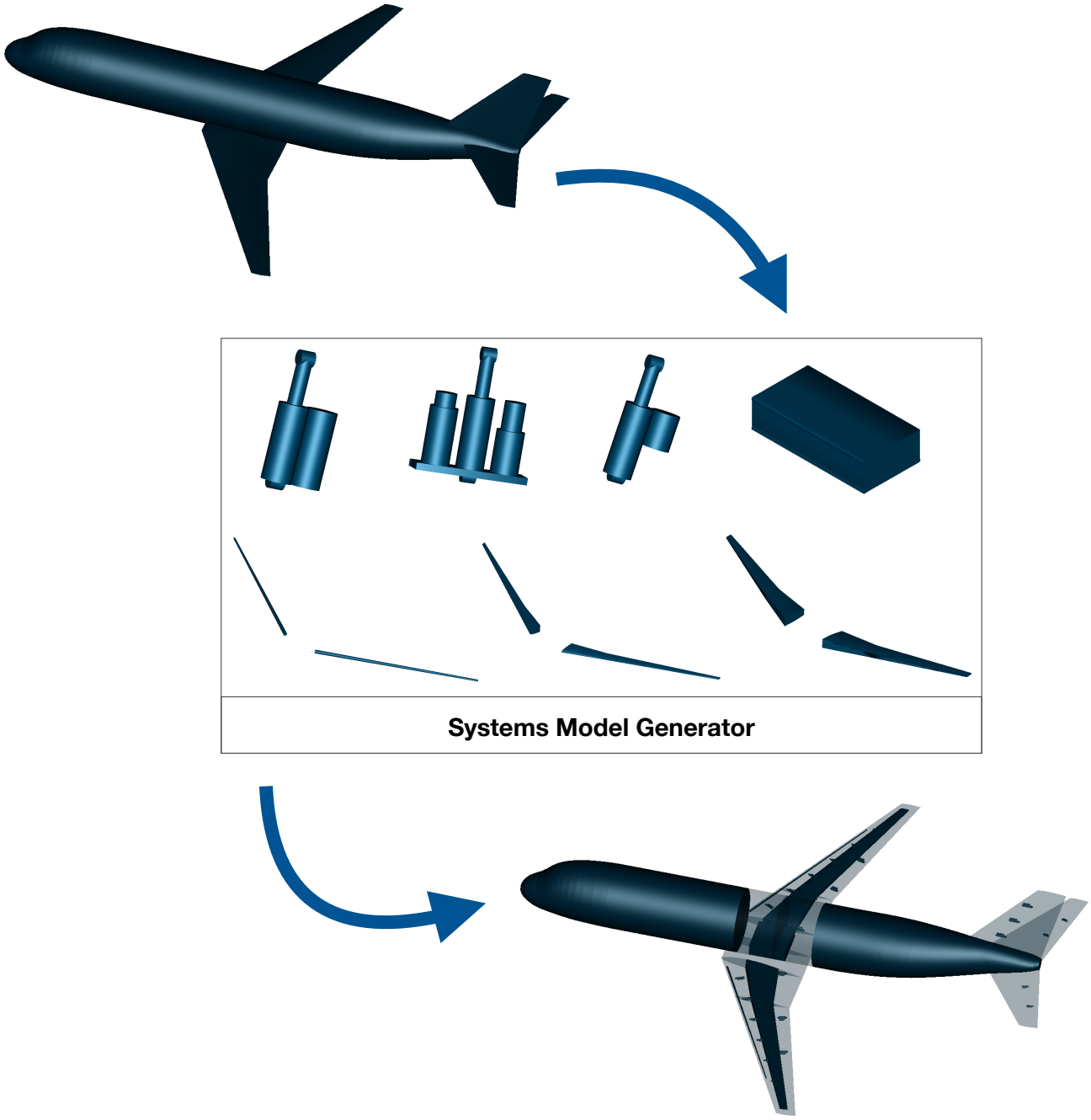

TU Delft Delft University of Technology

DLR

Influence of Parametric Modelling of Wing Subsystems on the Aircraft Design and Performance

by

Nithin Kodali Rao

in partial fulfillment of the requirements for the degree of

Master of Science
in Aerospace Engineering

at the Delft University of Technology,
to be defended publicly on Monday December 18, 2017 at 13:30 hr.

Supervisors:	Dr. ir. M. Voskuijl,	TU Delft
	P.S. Prakasha,	DLR
Thesis committee:	Prof. dr. ir. L.L.M Veldhuis,	TU Delft
	Dr. ir. C. Borst,	TU Delft
	Dr. ir. M. Voskuijl,	TU Delft

An electronic version of this thesis is available at http://repository.tudelft.nl/.
Student number: 4465571
Thesis registration number: 172#17#MT#FPP

TU Delft Delft University of Technology

DLR

Summary

Aircraft design methodologies have been significantly developing from the past few years with the advancements in knowledge based techniques. These methods enable the storage of design knowledge and rules, and reuse them to create different types of designs, thus preventing the designer to perform repetitive tasks. Tasks such as parametric modelling of components, such as the aircraft wing can be automated by storing the modelling processes and the design rules in a knowledge base. With this process, variants of the wing with different geometric parameters can then be generated in a short duration by simply varying certain top-level requirements. It is necessary to extend these design techniques to model aircraft systems in the conceptual design stage. This, not only decreases the time of design realisation but also presents a scope to assess the effects of various inter-dependencies due to systems and make appropriate changes, in the early stages of aircraft design. Developing and demonstrating a framework which aids to assess the influence of the wing subsystems, namely the flight control actuators, fuel tanks and anti-ice elements; on the aircraft design and performance in the conceptual design stage is the aim of the thesis.

This thesis presents a combination of physics based and knowledge based design methodologies to size the wing subsystems and position them in the airframe. Consequently, the methods are integrated into the conceptual aircraft design process to enable multidisciplinary design with supporting domains. The methods are aimed to aid the design of conventional systems architectures and More Electric Aircraft (MEA) systems architectures as well. With these methodologies, the Systems Model Generator (SMG) application is developed in Python to facilitate semi-automatic wing subsystems sizing and orientation in the airframe based on top-level aircraft requirements, initial aircraft design parameters and system specific parameters. The subsystem models generated with the proposed methodology for short-medium range civil transport aircraft are verified and validated as well. Knowledge based systems and subsystems selection are implemented to facilitate semi-automated systems, subsystems and architecture selection, based on the aircraft configuration and systems specific requirements. Methods for automatic iterative fuel tanks sizing and intersection detection are implemented to further reduce the overall design time and make the tool more suitable for integrated sizing.

With the multidisciplinary design framework, the conceptual parametric models, volume, mass, power consumption and position of the subsystems in the airframe are generated and propagated in the conceptual aircraft design stage; thus bridging the conceptual and the preliminary design stages. In the proposed framework, the domains of aircraft design generation, systems selection and sizing, subsystems selection and sizing, engine sizing and mission simulation are considered for the multidisciplinary design process. The domains are integrated with the DLR CPACS-RCE framework.

A case study to demonstrate the process of integrated parametric subsystems sizing of the aircraft, with the proposed framework is presented. The aim of this case study is to assess the influence of the MEA systems architecture relative to the conventional systems architecture for a short-medium range transport aircraft, similar to the Airbus A320-200. In this case study, the quantitative influence of the subsystems' parameters on the aircraft design and performance parameters is determined and analysed. The subsystems' parameters constitute the mass, power consumption, volume and location of the subsystems in the airframe and the aircraft design parameters constitute the aircraft masses such as the overall empty mass and the fuel mass for the mission. The generation and propagation of the design and performance parameters of the aircraft through each domain of the framework are presented and analysed as well with the case study. In this case study, it is observed that the MEA systems architecture results in a lower mission fuel mass relative to the conventional systems architecture by nearly 2.3%. Furthermore, these results are compared with literature and observed to be in the similar range of 2-7%. Thus, the validated aircraft design framework presented in this thesis enables to substantially increases and propagate the design knowledge of aircraft systems, in the early design stages.

Acknowledgements

This Master's thesis concludes my 24 month journey of becoming a Master of Aerospace Engineering at Delft University of Technology. During this period, I was honoured to work with people across different nations and domains. I am grateful to my family, who have provided me moral and emotional support in my life. I am also grateful to my friends who have supported me along the way.

I have spent the past 15 months at DLR, starting as an intern and then extending the opportunity to a Master's thesis. I would like to thank my supervisor from DLR, Prajwal Shiva Prakasha, firstly for giving me this valuable opportunity and for the patient guidance, encouragement and advice he has provided throughout my time as his student. I have been extremely lucky to have a supervisor who cared so much about my work, and who responded to my questions and queries so promptly. His valuable insights on aircraft systems, project planning and presentation skills helped me throughout my projects. I would like to thank Matthias Strack who shared his knowledge on DLR tools such as CPACS and RCE, which were major enablers for my work at DLR. I would like to extend this gratitude to all my colleagues at DLR who supported me with technical and non technical work which lead to the successful completion of my projects from a professional and academic perspective. Most importantly, my friends at DLR made my time more valuable and created a mutual learning experience. A very special mention goes out to all down at DLR and for the AGILE project for helping and providing the funding for the work.

I would like to express my sincere gratitude to my advisor Dr. ir. Mark Voskuijl for his continuous support during my thesis, for his patience, motivation, enthusiasm, and immense knowledge. His guidance helped me in all the time of research and writing of this thesis. I could not have imagined having a better advisors and mentors. Mark's ideas and feedback on aircraft design and research methodologies were pivotal in shaping this thesis. Frequent communication over long distances with regard to thesis progress is not easy; I however never realised this during my whole thesis due to Mark's and Prajwal's timely support and availability.

Besides my advisors, I would like to thank the rest of my thesis committee: Prof. dr. ir. L.L.M. Veldhuis and Dr. ir. C. Borst, for their encouragement and valuable time to provide insightful comments and constructive feedback.

My time as an Aerospace Engineering student at TU Delft would be unforgettable as I have learnt certain skills, values and knowledge which would be unique forever in a certain way as this is where it all began. This was made partly possible by my university professors, who through their courses, teaching methodologies and experience imparted the necessary knowledge and skills that allowed me to achieve this proficiency. My friends and colleagues at TU Delft who supported me, worked with me on projects, and proofread my work with constructive feedback were one of the reasons for my constant motivation. To all my family, friends, colleagues, professors and mentors: This wouldn't have been possible without your support. Thank you. With these experiences, memories and inspiration, I embark on future endeavours.

Nithin Kodali Rao
Delft, December 2017

Contents

List of Figures

List of Tables

Nomenclature

Acronym	Designation
AEA	All-Electric Aircraft
AIS	Anti-Ice System
APU	Auxiliary Power Unit
ATA	Air Transport Association of America
BWB	Blended-Wing Body
CAD	Computer Aided Design
CAFFE	Collaborative Application Framework For Engineering
CPACS	Common Parametric Aircraft Configuration Schema
CRISPS	Collaborative Research Initiative into Secondary Power Systems
DEE	Design Engineering Engine
DLR	Deutschen Zentrums für Luft- und Raumfahrt
DOE	Design Of Experiments
DSM	Design Structure Matrix
E	Electric
ECS	Environmental Control System
EH	Electric and Hydraulic
EMA	Electro Mechanical Actuator
EMM	Engine Modelling Module
ETAIE	Electro-Thermal Anti-Ice Element
FCS	Flight Control System
FSMS	Flight Simulation and Mission Simulation
FUS	Fuel System
GALEQ	Galley Equipment
H	Hydraulic
HAAIE	Hot-Air Anti-Ice Element
HTP	Horizontal Tail Plane
IATA	International Air Transport Association
IDEA	Integrated Digital Electric Aircraft
IR	Infra-Red
KBE	Knowledge Based Engineering
KBSS	Knowledge Based System Selection
KBSUS	Knowledge Based SUbSystem Selection
LGS	Landing Gear System
MALE	Medium Altitude Long Endurance
MDOPT	Multidisciplinary Design Optimisation System
MEA	More-Electric Aircraft
MICADO	Multidisciplinary Integrated Conceptual Aircraft Design and Optimization
Misc	Miscellaneous
MMG	Multi Model Generator
MTOM	Maximum Take-Off Mass
OEM	Operating Empty Mass
P	Pneumatic
PGDS	Power Generation and Distribution System
RCE	Remote Component Environment
SFC	Specific Fuel Consumption
SMG	Systems Model Generator

SSM	Systems Synthesis Module
TL	Technology Level
TLAR	Top Level Aircraft Requirements
TRS	Thrust Reverser System
TU Delft	Technische Universiteit Delft
UAV	Unmanned Aerial Vehicle
VTP	Vertical Tail Plane
XML	eXtensible Markup Language
ZFM	Zero Fuel Mass
ZLM	Zero Landing Mass

Symbols

Greek symbols

Symbol	Designation	Unit
α	Angle of attack	$[deg]$
δ	Maximum deflection angle	$[deg]$
λ_{cs}	Width to depth ratio of the control surface	$[-]$
ρ	Density	$[kg/m^3]$
σ_{max}	Maximum allowable stress	$[N]$
υ	Velocity	$[m/s]$

Others

Symbol	Designation	Unit
$Area_{protection}$	Area of protection	$[m^2]$
c_{cs}	Width (span) of the control surface	$[m]$
C_{hinge}	Hinge coefficient	$[-]$
$C_{h,\alpha}$	Hinge coefficient of angle of attack	$[-]$
$C_{h,\gamma}$	Hinge coefficient of deflection	$[-]$
$C_{h,0}$	Hinge coefficient at zero deflection	$[-]$
c_{mac}	Mean aerodynamic chord of the wing	$[m]$
$c_{mean\ chord}$	Mean chord of the control surface	$[m]$
C_{slat}	Mean chord of the slat	$[m]$
$C_{slat\ ref}$	Reference mean chord of the slat	$[m]$
d	Diameter of the accumulator	$[m]$
d_{pic}	Distance of the piccolo tube from the slat leading edge	$[m]$
dia_{pic}	Diameter of the piccolo tube	$[m]$
$dia_{pic\ ref}$	Reference diameter of the piccolo tube	$[m]$
EOP	Extent of protection	$[-]$
F^*	Scaling factor for force	$[-]$
k^*	Scaling factor of the piccolo tube	$[-]$
k_0	Constant 0 for anti-ice element sizing	$[-]$
k_1	Constant 1 for anti-ice element sizing	$[-]$
k_2	Constant 2 for anti-ice element sizing	$[-]$
l	Length of the accumulator	$[m]$
l^*	Scaling factor for length	$[-]$

M_{hinge}	Hinge moment	$[Nm]$
r^*	Scaling factor for radius	$[-]$
$S_{ref,cs}$	Reference area of the control surface	$[m^2]$
x	Value of the required parameter	$[-]$
x_{ref}	Value of the reference parameter	$[-]$
x^*	Scaling ratio	$[-]$

1

Introduction

1.1. Background

Aircraft design is a complex multidisciplinary process involving various domains, hence inaccuracies in predictions of parameters of a single domain cause a snowball effect in other domains and lead to a flawed design.The process is spread across a large time frame, typically over a span of 10 years. Realising some of the design restrictions in the later stages of design leads to grounding the project or to make fixes that are not a part of the design. This is expensive and often leads to a decrease in the final performance of the aircraft, if the design ever goes into production. This is a part of the diverging-converging aircraft design process, where the aircraft design diverges initially with a large number of possible solutions and starts to converge with fixing each design solution [7]. It is hence required to consider a large number of design possibilities and compute the parameters of all the domains accurately from the early design stages. However, the in-availability of design data in these early stages leads to inaccurate predictions. The current methodologies limit these estimations in the early stages, this is evident by the delay of major aircraft deliveries such as the A380, A350 and Boeing 777. It is hence necessary to develop new design methods that improve the knowledge regarding different domains of design in the early stages. This aids to make necessary changes to the domains and design the supporting technologies accordingly in the initial stages. One such domain is the aircraft systems, which contributes to nearly 30% of the Operating Empty Mass (OEM) [8] and requires off-takes from the engine such as the shaft power and bleed-air to function.

The conventional systems, such as the hydraulic fight control system, which have been improved and optimised through the past decade have reached a technological saturation [15]. This trend is similar to other complementary technologies, common for the conventional tube and wing aircraft configuration. According to the IATA (International Air Transport Association) technological roadmap of 2013 [9], novel system technologies such as the All Electric Aircraft (AEA) systems architecture, hybrid laminar flow control system or the fly-by-light system are expected to be available within the next five years and integrated with the aircraft over the next decade. These technologies are not only vital for environmental impact but also to lower the design, development and operating costs of the aircraft. A similar technological goal was set for the More Electric Aircraft (MEA) systems architecture for applicability before 2020. This was partially achieved by the A350, A380 and the Boeing 787. The Boeing 787 is relatively advanced as the bleed-air system was totally eliminated by electrifying the pneumatic systems, thus making the engines bleed-less. However, this trend was not adopted by the latter A350. Introducing novel technologies is highly risky from an economic perspective for aircraft organizations. This is due to the technological uncertainty of initial models of novel systems, which are usually not very robust. This process of technological saturation and the resources for improving novel technologies is addressed by the S-curve, proposed by Foster [10]. Considerable changes in the overall performance of the aircraft are only achievable if these risks are taken by introducing novel technologies. This introduction is only possible if the knowledge of the uncertainties is available in the initial design stages.

Besides the civil aviation sector, a considerable growth has been achieved in the Unmanned Aerial Vehicle (UAV) sector in the past few years. The size of UAVs range from micro air vehicles, which fit

in the human palm to Long Endurance High Altitude (HALE) UAVs which carry out transcontinental missions across the Atlantic. As the name suggests, these aircraft are unmanned. This narrows down the design requirements to the on-board systems and the payload for the design mission. Thus the design and configuration of a UAV is dictated predominantly by the systems.

Due to this vitality of systems in the design and development of aircraft, it is crucial to size the systems[1] and subsystems[2] simultaneously with the aircraft in an integrated framework from the early stages of design.

In this chapter, systems sizing in the conceptual design stages is addressed and the objective for this research is formulated. In Section 1.2, the aircraft design process is outlined with the importance of systems sizing in the early design stages. In Section 1.3, the scope of the research and the primary objective along with the sub-objectives are addressed. Finally, the structure of this thesis report with an overview is presented in Section 1.4.

1.2. Aircraft design and systems

1.2.1. Aircraft design process

The aircraft design process is generally grouped into three stages. The conceptual design stage, the preliminary design stage and the detailed design stage ([11], [12]). In the conceptual design stage, different aircraft configurations and concepts are evaluated and sized. Different trade-offs are considered and the configuration that brings the most value for the requirements is chosen. As the data about the aircraft is very limited at this stage, the geometry and the performance parameters such as the fuel consumption are computed with various empirical methods based on historic data. It usually takes a few weeks to months with nearly 1% of the engineering staff to complete the conceptual design stage [13].

In the preliminary design stage, further design and analysis of the chosen concepts is carried out and the configuration is fixed. Due to the availability of a large number of aircraft design and performance parameters at this stage, high fidelity analysis and physics based methods are employed to get detailed properties of the aircraft. Preliminary design usually takes from a few months to years, with nearly 9% of the engineering staff contributing to it [13].

The final stage of design before production is the detailed design stage. Each and every component that would be present in the aircraft is designed in this stage. The design is fine tuned and the performance is evaluated accurately. With the completion of this stage, product drawings are released to manufacturers. The detailed design stage takes a few years to complete with nearly 90% of the engineering staff [13].

The design process at each stage is multidisciplinary, consisting domains such as aerodynamics, structures, propulsion, systems etc.The design is iterated through each domain till a design convergence is reached at each stage. The fidelity of computation at each stage varies based on the available data. Moreover, this design process is done on various scales such as on a fleet scale, an aircraft scale or on a component scale. For instance, conceptual design is always carried out on an aircraft scale but the detailed design is carried out on a component scale as each component is designed and analysed exclusively. To visualise this design space, La Rocca and Van Tooren [14] proposed the three dimensions of aircraft design. The design space has three axes containing disciplines, scale and fidelity, similar to the representation in Figure 1.1.

To put the design stages on this design axis in a perspective, in the conceptual design stage, the fidelity is usually empiric due to the in-availability of data, the scale is aircraft and the computations are carried out for each of the domains. One of the main aims of the conceptual design stages is to assess the effects of each domain on the other domains, thus studying the trade-offs that need to be made. Similarly, in the preliminary design stage, the fidelity is usually semi physics or advanced physics methods with computations on a component scale. In the detailed design stage, full physics based methods are used for computations on a component scale. The components are made as efficient and as reliable as certification demands.

One of the problems with the current methods in the conceptual design stages is that the use of empirical methods based on statistics from historic data. This method not only is less accurate but also

[1] In the scope of this research, a system is defined as an on-board system as a whole, such as the flight control system or the anti-ice system.

[2] A subsystem is defined as a part of the system; the flight control actuators are subsystems of the flight control system.

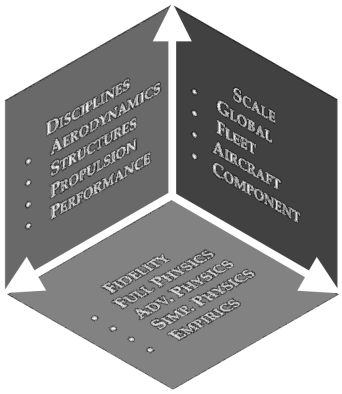

Figure 1.1: The three dimensions of aircraft design [1]

restricts the assessment of new technologies. These limitations can be addressed with an example of sizing the on-board systems. Aircraft systems, just as any other electronics have become lighter, smaller and more efficient. The latest commercial aircraft Boeing produced was the 787 in 2007 and that of Airbus was the A350X in 2010. The 787 unlike any of the previous aircraft, totally eliminates bleed-air requirement for the systems, replacing the Environmental Control System (ECS) and the Anti-Ice System (AIS) with equivalent electric systems. This constitutes the MEA systems architecture, which is a step towards the All-Electric Aircraft (AEA) systems architecture, which is the total electrification of the on-board systems. This shift towards the AEA architecture is not a distant reality any more due to the exponential developments in electronics during the past decade. This ever changing trend limits evaluating the properties of the systems of the future aircraft designs based on the past aircraft models. If done so, it would indeed lead to an over or under estimation of certain parameters. Two limitations arise with over estimation. Firstly, it causes a snowball effect on the other domains, thus increasing the overall inaccuracy of the parameters. The second problem is that novel technologies such as the MEA systems cannot be assessed due to the limitations of the current methods. The repercussions of systems on the overall aircraft design and performance is presented in the following subsection.

1.2.2. Impact of systems on overall aircraft design and performance

Aircraft systems are the on-board systems that contribute to the aircraft's control, performance, safety and comfort. The systems on a civil aircraft are usually referenced by the Air Transport Association (ATA) chapters. Each system is designed to perform specific functions. For instance, the flight control system is responsible for providing the required control surface actuation. Similarly, the anti-ice system is responsible for maintaining the wing and other components free of ice formation. The fuel system is responsible for the safe storage and distribution of fuel. As the on-board systems weight nearly 30% of the OEM, occupy volume in the airframe and consume all the shaft power generated by the engines; they indeed impact the design and performance of the aircraft in different ways.

The direct impact of the systems is the effect of the off-takes they derive from the engine for their functioning. These off-takes may be in the form of shaft power for hydraulic and electric systems, and bleed air for pneumatic and environmental control systems. Engine off-takes contribute to nearly 5% increase in the fuel consumption [15]. The increase in Specific Fuel Consumption (SFC) is also linear to the shaft power off-takes. Bleed air off-takes have a higher impact on the aircraft as the bleed air off-take decreases the core mass flow to the engine, thus reducing the engine performance as well.

Indirectly, the systems' mass, volume and the position in the airframe cause a snowball effect on the overall aircraft design and performance. For instance, larger actuators for flight control may require a wing with higher thickness or a redesign of the actuator, thus increasing the OEM. This influences the Maximum Take-off Mass (MTOM). To automate the generation of these subsystem parameters and propagate the effects to the complementary domains, a design and analysis framework is proposed and demonstrated in this thesis. The motivation for the development and the objectives of this researched are presented in the following section.

1.3. Research scope and objective

The aim of this research is to demonstrate a method which would enable automatic sizing and orientation of the subsystems with the airframe from a volumetric perspective. To automate the parametric modelling of the subsystems, the geometric parameters need to be related to the aircraft and subsystem specific parameters. These methods need to be developed into a computer program and the proposed framework needs to be simulated with complementary domains in an integration environment. Domains for aircraft design generation, system selection and sizing, subsystem selection and sizing, engine sizing and mission simulation are considered in this research. Pre-existing tools at DLR are used to perform the functions of these complementary domains. Translating these requirements, the following research objective was defined.

> *Develop a framework that enables automated parametric sizing of the subsystems in an integrated aircraft design process, within a multidisciplinary environment.*

This research objective is divided into several sub-objectives

1. Develop a conceptual multidisciplinary aircraft design framework, capable of propagating the subsystems' parameters.
2. Develop methodologies that facilitate automatic generation of subsystems' parametric models based on aircraft and subsystem specific parameter.
3. Develop an object-oriented computer program based on these methodologies to automate the design process.
4. Verify and validate the developed subsystem models with sensitivity analyses.
5. Recreate the developed conceptual design framework in an integration environment.
6. Demonstrate a case study with this framework by comparing a conventional systems architecture to an MEA systems architecture for a short-medium range transport aircraft.

Fulfilling these sub-objectives would fulfil the main research objective, which aims at improving the overall aircraft design process.

1.4. Overview and report structure

This chapter presented an overview on the aircraft design process and the importance of aircraft systems sizing in the conceptual design stage. Further more, the scope of the research; developing a framework for integrated sizing of aircraft subsystems with the aircraft was discussed and the research objective was formulated.

In Chapter 2, the state of the art in integrated sizing of systems and volumetric modelling of aircraft subsystems is presented. The applicability of each of the models in the conceptual design stage is addressed. The chapter is concluded with grounds for a requirement of a novel methodology. The proposed framework with this novelty and the implementation is introduced and elaborated in Chapter 3. The various domains of multidisciplinary design and their integration is also presented in detail. The parametric models of the subsystems and the rules for sizing are described in Chapter 4. In Chapter 5, the validation and the sensitivity analysis of the models is presented at a system, subsystem and an aircraft level. The case study generated with the proposed framework in presented in Chapter 6. The conclusions of this research and recommendations for future work are proposed in Chapter 7.

2

State of the art

2.1. Introduction

In Chapter 1, the main objective of this research is presented along with the background information relating to aircraft design and the vitality of integrated systems sizing with the aircraft. In this chapter, the state of the art in integrated systems sizing approaches and parametric modelling methods of the aircraft subsystems are discussed. Various dissertations have addressed different aspects of systems and subsystems design. The work on integrated sizing of the systems with the aircraft is discussed is Section 2.2 and the parametric sizing of the subsystems is discussed in Section 2.3. Each research is described in brief and critically analysed to infer the methods, novelty and limitations which aid in identifying improvements necessary to bridge the current research gap. The observations and conclusions of the current research along with the novelty of the current methodology is presented in Section 2.4

2.2. Integrated sizing of systems with the aircraft

Sizing the systems with the aircraft in an integrated environment was a topic of interest in the past few years. Lammering [15] proposed a methodology to model the systems and the systems architecture. In his research, each system was modelled as a function of mass and power consumption (based on the mission) with semi physics based methods. Additionally, the approach also included computations of the center of gravity of each of the system. The systems were classified based on traditional ATA chapters.The methods were integrated with an existing aircraft design environment called Multi Disciplinary Integrated Conceptual Aircraft Design and Optimization (MICADO). This integration enables the modelling of different system architectures. Computations of mass and power consumption of the systems and assessing their influence on the overall aircraft design follows. Thus, different system architectures can be generated and assessed in the early stages of design with this framework. Lammering also addressed the limitations of regression based computations of the SFC which fail to take into account the engine type though the engine off-takes were considered. Hence, he used engine performance analysis tool called GasTurb based on which the polynomial curves were fitted. The computed system properties were fed back into MICADO to resize the aircraft. The ”snowball” effects of the systems architecture on the aircraft were determined with this process as well. Lammering also demonstrated how new technology such a hybrid laminar flow technology could be integrated and the effects were assessed on the overall aircraft design. The methodology was validated against present methods and literature as well, for an aircraft similar to the Airbus A320 and the other similar to the Boeing 777. The sensitivity of the computed parameters for varying inputs was demonstrated. He identified the trends of mass and power consumption of the systems which were influenced by system specific parameters such as the recirculation factor of the Environmental Control System (ECS), aircraft design parameters such as the cabin dimensions and top level aircraft requirements such as the design range. Some of the limitations in his research were that various system architectures were not assessed and the systems were idealised as points and virtually positioned only on a 2D axis.

To tackle the problem of systems sizing in the conceptual design, Chakraborty [16] developed a modular environment linking system sizing and analysis with aircraft sizing, including novel system

architectures for which historic data is unavailable. Rather than classifying the systems with ATA chapters, he classified them into two groups based on their functions, namely the power consuming systems and the power generation and distribution systems. The novel systems included equivalent electric systems of all the conventional systems. Chakraborty presented explicit methods through which different conventional and novel system architectures can be modelled. The performance of different system architectures was investigated along with the variations of these parameters with the aircraft size. The sensitivities of the performance of the novel architectures was assessed with technological uncertainties and limitations, this can be considered as one of the salient features of this work. The methods proposed were computationally inexpensive, semi-physics based, sensitive to technological progress and all the inputs could be obtained at the early stages of design. However, in this research only nine power consuming systems were considered and major systems such as the fuel system and the galley equipment which consume high power were beyond the scope.

2.3. Parametric sizing of subsystems

Manjulury et. al. [2] demonstrated parametric modelling of flight control surfaces with a Knowledge Based Engineering (KBE) methodology by associating a Computer Aided Design (CAD) tool (CATIA [17]) with a knowledge base. CAD templates of the flight control surfaces were created in CATIA based on associative modelling. This enabled a top-down assembly design, where modifications to one component would affect the the whole system, thus reflecting the modifications on the other components as well. The parameters of each of the parts were associated with "rules [1]" and "reactions [2]", which could be triggered by the user by changing the input values in the user interface. For example, the user inputs for an aileron constitute the length of the aileron, distance from the centre of the wing etc.

This framework was integrated with the RAPID tool [18], thus allowing the generation of CAD models of the flight control surfaces for a predefined aircraft model. The framework is capable of generating geometric models of the ailerons, elevators, rudder and flaps. The constructed surface models were tested with different aircraft. A user interface was created with excel so as to integrate the tools and ease the design process. Besides modelling the control surfaces, a flap mechanism was integrated which allowed the extension and retraction of the flap with the change in actuator stroke. An aerodynamic model replicating the CAD model was created in Tornado [19], which was capable of updating automatically with the CAD model. This analysis determined the aerodynamic forces required to deflect the control surfaces. These forces were fed down to the simulation tool Dymola [20] in which the dynamic model of the control surfaces was simulated. The dynamic model computes the force required for actuating the actuator and feeds it to the optimiser, which then picks the best actuator for the flap from the actuator component library, for a specific flap configuration. An excel interface was developed to integrate the CAD tool, the aerodynamics tool and the simulation tool. This tool is one of the first of its kind, capable of generating automatic CAD models for the flight control surfaces, as presented in Figure 2.1. Moreover, the user interfaces enabled integration and automation of the design and analysis, besides easing the usability of the framework. In this research, however, the dimensions of the flight control surfaces were not generated in an automated way from an initial aircraft sizing method, nor the design iterated till convergence. Only the Electro Mechanical Actuator (EMA) was considered and that was limited to the flap as well. The effects of choosing a specific actuator on the performance of the aircraft or the influence of modelling the control surfaces in the early stages of design were beyond the scope of this research.

Inés [3] presented a framework that enabled recurrent design and integration of the flight control system in a short period of time. CAD templates of the flight control actuators and the associated hydraulic system were created with a KBE methodology. This framework was integrated with the RAPID tool [18] to enable automatic integration of the generated CAD models with the pre-existing aircraft geometry. The methods used to create the templates were similar to the model presented in the previous paragraph [2] . The flight control actuators, the piping, the hydraulic pump, the hydraulic

[1] A "Rule" in CATIA is a set of instructions based on conditional statement where the relationships between the parameters in controlled.

[2] The "Reaction" feature in CATIA triggers actions such as creation, deletion, insertion, replacement, drag and drop of an object with a change in the input parameter.

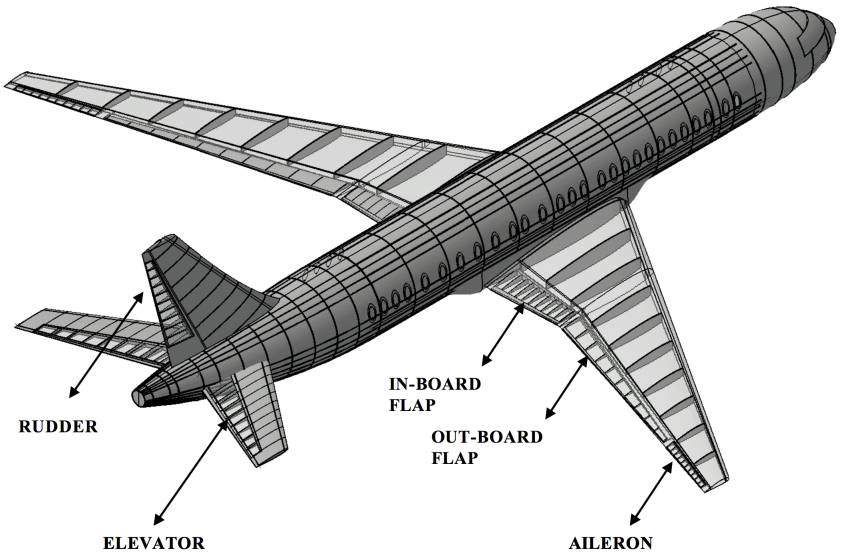

Figure 2.1: Parametric models of the flight control surfaces [2]

tank, the regulating valve, the hydraulic accumulator, the hydraulic conductors and the Auxiliary Power Unit (APU) are modelled in the scope of this thesis. The integrated model is presented in Figure 2.2 and the model of the hydraulic actuator is presented in Figure 2.3. An excel interface was created to input the parameters such as the number of actuators required for each control surface, rotary radius, length of the actuator, definition and redundancy of the hydraulic system etc. The hydraulic actuators were scaled based on the hinge moment required, however the scaling laws of any of the remaining systems were not discussed. The novelty of this research is that the framework enables automatic redesign and integration of the flight control system on changing the required parameters in the input file. This is one of the works where CAD is used in the early stages of design to integrate the aircraft systems. One of the limitations of this research is the use of only hydraulic actuators. In reality, aircraft use Electro Hydrostatic Actuators (EHA) and EMAs as well. Moreover the flight control actuators were not integrated with the flight control surfaces, if done, this would enable to assess the effects of position and orientation based on the functionality and the available space. The scaling laws of the remaining systems were not presented, hence it is assumed that static models were used which restrict the sizing of the systems based on the aircraft parameters. This method presented a huge potential to assess the effects of volume and mass of the generated systems on the overall aircraft design, however those analyses were beyond the scope of this research.

Manjulury et. al. [4], in their work presented a framework for the parametric modelling of the EHA and EMA for flight control. CAD templates were created in CATIA for EHA and EMA models with KBE methods. This framework enable automatic sizing of the actuator models based on few input parameters such as hinge moment, actuator stroke etc. The sizing of actuators was based on methods proposed by Frischemeier [21]. The components of the EHA are the fixed displacement pump, electric motor, accumulator and power electronics. It is assumed that the motor and the pump are positioned in the axis parallel to the hydraulic cylinder. The accumulator is assumed as a cylinder and its volume is determined within some limits of l/d of the accumulator where l and d are the length and diameter of the accumulator. The actuator force, the maximum allowable stress in the material, the maximum system pressure, the control surface hinge moment, the actuator hinge arm, the swept angle, the maximum loaded velocity of the actuator, the nominal speed of the motor and the power of the motor are the parameters required to determine the dimensions of the EHA with semi-physics based methods. The parametrised models are presented in Figure 2.4. This was the first research which introduced a framework to enable automatic generation and modification of parametric models of EHAs and EMAs. Due to the complexity of the actuator models, the scope of the research was limited to just creating a framework for the actuator models. Integration into an aircraft with the control surfaces or the influence of the actuator properties on the aircraft design or performance were not addressed.

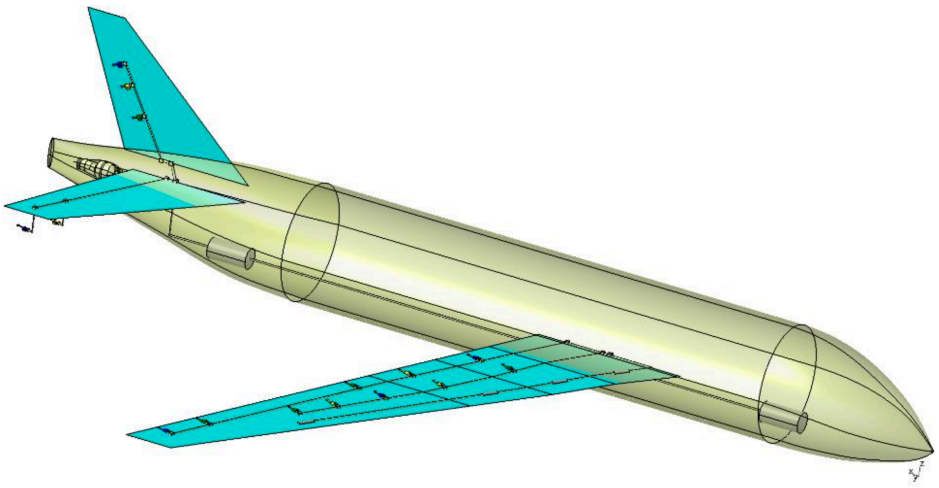

Figure 2.2: Parametric model of the aircraft hydraulic system [3]

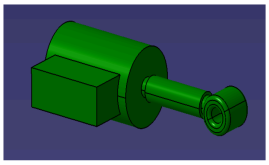

Figure 2.3: Parametric model of the hydraulic actuator [3]

López et. al. [5] proposed a framework based on KBE methods for parametric sizing of the fuel system in the conceptual design stage of aircraft. CAD templates for the aircraft fuel system were created in this framework. The methodology allows modifications to the layout and the geometry of the systems with few user inputs. This included generation of geometries of the fuel tanks, the piping, the pressurisation system, the engine feed system which enabled fuel storage, engine feed, fuel pressurisation, re/de fuelling and venting. Wing tanks, fuselage tanks and aft tanks were defined for fuel storage. The sizing of the wing tanks is based on wing geometry and the desired combination of fuel pumps and refuel stations. These tanks are bordered by the wing skin, front spar, rear spar and wing ribs. The wing tank geometry is defined by 11 parameters, enabling geometries and configurations similar to the ones seen in contemporary civil aircraft. The method enables sizing of two types of fuel pumps, centrifugal and cartridge canister types. The transfer pumps are defined by 4 parameters for geometry and 2 parameters for positioning. The fuel pump is modelled with 9 parameters. One parameter for pump type , one for redundancy, 6 for sizing and positioning one pump and one more to position the second pump. A single refuel station can be added with one parameter. The position of the main central tank was defined relative to the wing reference planes and origin. The fuel tanks are bordered by the inner surface of the fuselage and the central wing box. Feed pumps can be specified in a particular tank and the cross-feed connections automatically connect to it. The redundancy of the feed pump can be set with a parameter. The transfer pumps are present in the central tank and can be moved and placed with 5 parameters. The tail tanks are bordered with the stabiliser surface and the rear spar. The transfer pumps can be placed anywhere in the tank, provided they are attached to the bottom surface. Cross-feed piping was also an integral part of this research. During the condition of an inoperative engine(s), it is required for the fuel available elsewhere to be utilised by the operative engine(s), this is the function of the cross-feed system. This is done by connecting the feed pumps of different tanks. One of the four configurations can be selected with a single input based on the requirements. The system piping length can also be determined within this method. A transfer system connects every tank of the aircraft with each other through their transfer pumps. The venting system is represented by two surge tanks outboard the wing and a rectangular surge box, the size and position of which can be modified by the user. For all the fuel tanks, besides analysing the fuel capacity of a fully filled tanks, the possibility of analysing a partially filled tanks at a specific attitude and propagating

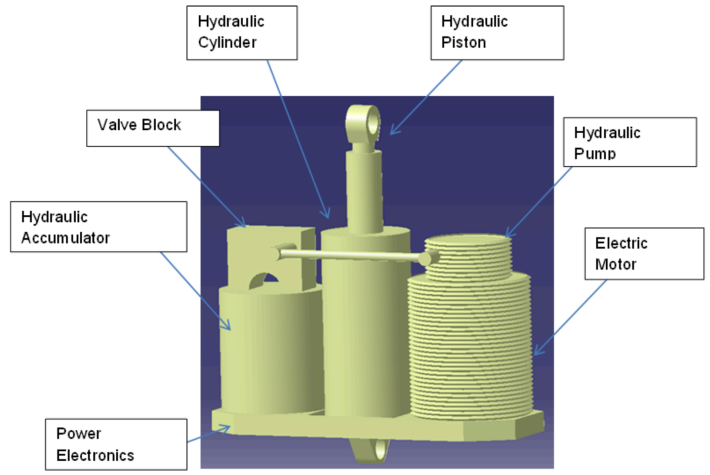

(a) EHA parametric model

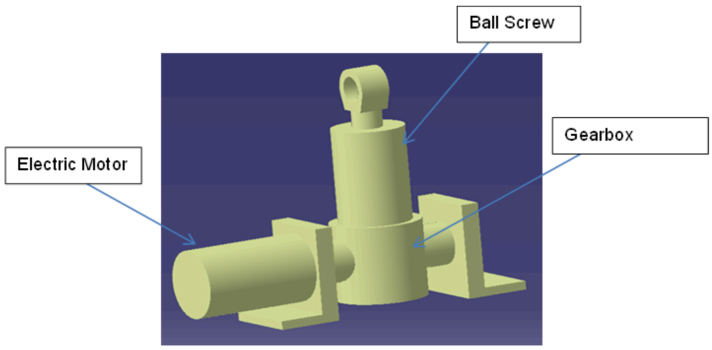

(b) EMA parametric model

Figure 2.4: Actuator models [4]

its values for stability analyses is discussed as well.

This framework was integrated with RAPID [18] to enable the instantiation of these components as seen in Figure 2.5 in a pre-existing aircraft geometry created by the tool. The parametric definition of the fuel tank was capable of propagating throughout the design stages. The automatic generation of CAD templates of the fuel system based on input parameters is the first of its kind. The fuel system model is very complex as well, covering most of the functions of the system and the components related to it. The ability of the framework to generate different configurations and extract data such as the fuel capacities at different filled fractions at different attitudes and the length of the piping is novel as well. The mass and position of the fuel tanks play an important role in the aircraft sizing. However, in this research the effects of different fuel tank configurations or material of the fuel tanks on the aircraft design were not assessed, though the possibility of assessing the influence of the fuel capacity was discussed.

Fuchte et. al. [6] in their research, developed a tool for the placement of systems inside the aircraft's fuselage. The objective of this research was to estimate the effects of location of certain systems on system routing. It was claimed that this determination of the various possibilities of the system routing would enable to make better predictions for the weight and the geometry of the aircraft. The system components and the connectors were placed in the fuselage based on knowledge patterns. Within the scope of this research, the environmental control system, the water and waste system and parts of the electrical power system were placed in a detailed geometrical model of a fuselage. The effects of changing architectures of the fuselage systems were presented as well. The fuselage model considered has detailed structural components including the cabin with the fixtures and the overhead stowage bins. The fuselage model was in the Common Parametric Aircraft Configuration Schema (CPACS) format, thus enabling interaction with different supporting tools. The large components such as the mixer unit, the

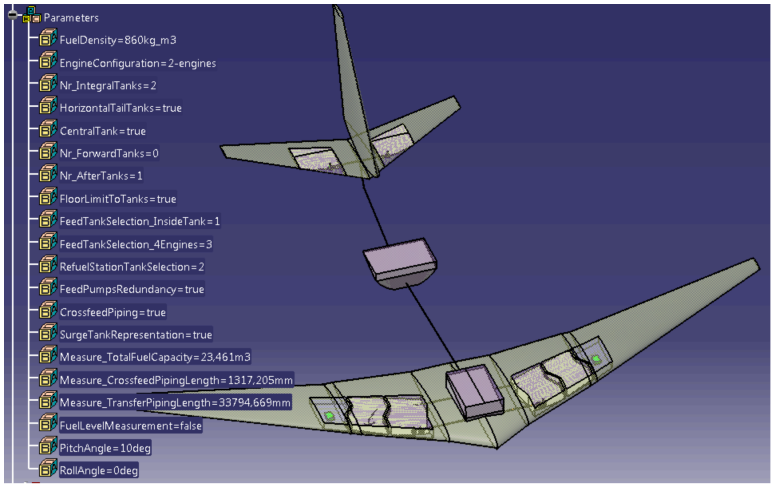

Figure 2.5: Fuel system generated by RAPID [5]

water and waste system and the power tanks were restricted in their placement to only a few possible locations. Hence, different architectures were made with the combination of the possible positions of these systems. These positions were considered based on design rules from previous aircraft. The possible locations for the mixer unit were in front of the main wing box and behind the landing gear bay. The possible locations for the water and waste tanks were in the rear of the fuselage, between the cargo hold and the pressure bulk head.

The connections between the placed systems were routed based on a path finding algorithm. Each connection was defined by a start and an end point. The path finding algorithm then finds the route in the available location and blocks the required volume at each frame location. The areas are separated into squares of 2.54 cm length, forming a 2-D matrix. The algorithm then, based on the mapped field determines if a block is free or occupied and if free, if it is sufficiently large to place the duct. One of the assumptions is that each duct occupies a square field and the minimum cross section required for a duct is the area of a single cell of the matrix. The generation of ducting for the ECS and the water and waste system was demonstrated with this method. One of the configurations is presented in Figure 2.6.

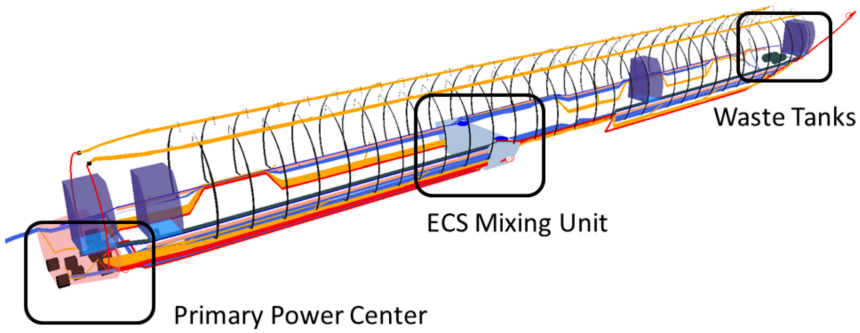

Figure 2.6: Placement of fuselage components [6]

To demonstrate the usability of this model, a few case studies were presented. For the ECS, it was assumed that the aircraft has two temperature zones. Three different ECS architectures were considered based on the placement of the mixing unit. In the first, the mixing unit of the ECS was placed in front of the wing box, in the second behind the main landing gear and in the third, just in front of the main bulk head. The possibility of varying temperature zone locations or the placement of the engines (wing mounted or fuselage mounted) was the reason for these configurations to be considered. Similarly, the possible locations of the power centre were also varied. Possible locations were the front section of the fuselage just below the cockpit and the section of the fuselage just behind the main landing gear bay. The power centre is connected to local distribution centres and to the generators.

The first systems architecture for the case study was with the mixer unit in the front of the centre section, the water and waste tanks at the rear in front of the aft bulk head and the power centre in the front, below the flight deck. The ECS ducting was with local riser ducts with feed lines below the cabin surface. This layout is analogous to that of an A320. The second architecture considered was with mixer unit in the aft, behind the main cargo hold, the fresh water tanks in the front , the waste water tanks in front of the centre wing box and the power centre behind the main landing bay as seen in Figure 2.7. The ECS ducting was with two main riser ducts. For the two architectures presented, the surface area and length of the ducting for each of the system was assessed as it correlates with the weight. Based on the results presented, it was inferred that the second architecture lead to higher ducting surface areas for the ECS and the water and waste systems. Besides, the ducting length and the surface area for increasing the number of temperature zones from 1 to 3 was also presented. It was inferred that with increasing the number of temperature zones, the complexity of the ECS would increase but the weight penalty due to the increased ducting would be minimal. This method enabled the assessment of different system architectures in the initial design stages. However, this method was limited to only determining the incremental ducting surface areas for different configurations of three systems in the fuselage. The architectures were considered for only a single aircraft with fixed geometry, this limits the flexibility of the tool to assess the impact of configuration on aircraft with different geometry. The method even lacks coupling with complementary tools to assess the overall impact of the architectures.

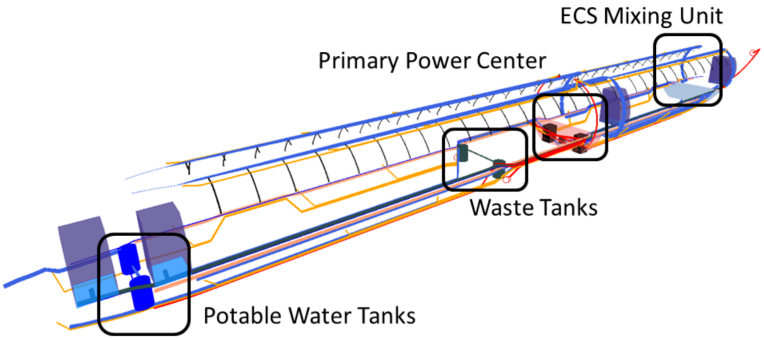

Figure 2.7: Varying the position of fuselage components [6]

Anti-ice systems were seldom addressed from a design perspective in the aircraft conceptual design stage in previous research. However, a few design, analysis and optimisation studies [22–25] provide insights into the preliminary geometry of these systems. The piccolo tube system consists of a tube with holes aligned along the wing span inside the slat close to the leading edge. Bleed air at high temperature is passed through the tube. This hot air gets impinged on the leading edge of the slat through the holes in the tube, thus heating the leading edges of the slat, maintaining the desired surface temperature. The cross section of a Piccolo tube is presented in Figure 2.8a . In an electro-thermal anti-ice system, a heating strip is stuck on the leading edge of the slat along the span. The heating strip works on the principle of electro-thermal heating. The geometry of a typical electro-thermal heating element is presented in Figure 2.8b.

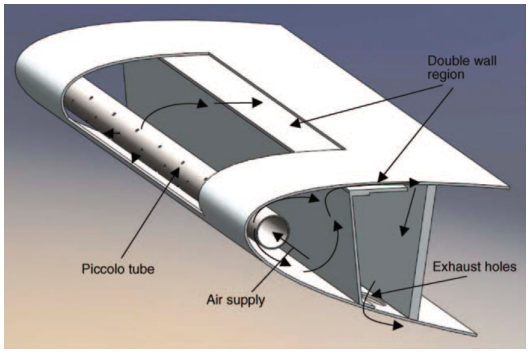

(a) Piccolotube anti-ice system [22]

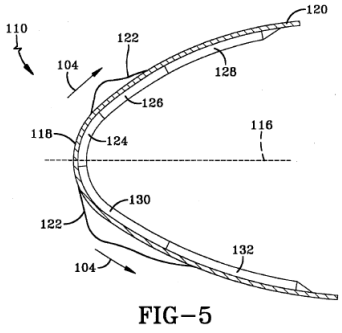

(b) Electro-thermal anti-ice system [25]

Figure 2.8: Anti-ice system models

2.4. Observations from the literature and the novelty of the proposed methodology

Based on the observations from the state of the art, some conclusions are drawn which would aid in determining the present research gap and thus identify the need for a novel approach. The observations are summarized in the following table (Table 2.1).

Scope \ Literature	Chakraborty [16]	Lammering [15]	RAPID [3] ([2], [3], [4], [5])	Fuchte [6]
Systems	FCS, ECS, AIS, LGS, TRS, EPGDS, HPGDS, PPGDS, EPGDS	ATA-100	FCS, FUS	ECS Ducting
Integrated sizing [4]	✓	✓	-	-
Parametric modelling	-	-	✓	✓
Case study [5]	✓	✓	-	✓
Systems' mass	✓	✓	✓	✓
Systems' power consumption	✓	✓	-	-

Table 2.1: Summary of the state of the art

The observations made in Table 2.1 are summarized as follows.

1. Geometry, similar to other subsystem parameters such as mass and power consumption, changes rapidly during the aircraft sizing process. Thus, it is required that this geometric change of the subsystems is propagated to other domains to enable the sizing if the aircraft with these considerations.
2. Present methods are stand-alone templates that generate CAD models of the specific subsystems based on KBE methods. Accurate geometries can be generated with ease, provided the dimensions and other system specific parameters are know. This is of advantage during the late preliminary design stage when more information regarding the design is exposed. This limits the usage of these methods during the initial sizing in the conceptual design stage.
3. The geometry generated during the conceptual design stage is not for manufacturing and just for sizing and visualisation. Hence detailed modelling of the components is not required.
4. The state of the art only consists methods for automating the geometric modelling of specific subsystems. However, the effects of the geometry on the overall design and performance of the

[3] Research limited to on-board systems
[4] Multidisciplinary design with propagation of parameters, enabling snowball effects
[5] Case study with quantitative results

aircraft from a subsystem, system and aircraft level was beyond the scope of the prior research as the methods were never integrated into a multidisciplinary aircraft design process.

5. A single model that determines the geometry, mass and power consumption of the subsystems doesn't exist. Uniting these methods under a common platform would facilitate easy integration of the methods into the aircraft design framework.

To overcome the discussed limitations, the unique aspects of this research are the ones that the previous research has never addressed or addressed to an insufficient level. Some of the novel characteristics of this research are presented:

1. To size the subsystems accurately within the available volume, it is required to consider all the subsystems within a control volume such as all the wing subsystems or all the fuselage subsystems. In this thesis, the considered control volume is the wing (and the empennage).
2. To integrate the methods into the overall aircraft design process, a process is developed in the scope of the current thesis to determine the required systems and subsystems; constituting the systems (and subsystems) architecture. This eliminates the time consumed for manual selection and contributes in automating design decisions as well. In this thesis, the design decisions are stored in a knowledge base which facilitates automatic systems, subsystems and architecture selection based on minimal input parameters.
3. The wing subsystems comprise the fuel tanks, the flight control actuators and the anti-ice elements. Existing methods support the sizing of the flight control actuators and the fuel tanks, however new methods are developed in this research for sizing the anti-ice elements.
4. The sized parametric models of the subsystems are positioned and oriented in the airframe to assess the volumetric effects and gain space allocation knowledge.
5. To avoid intersection of the subsystems in the airframe, a methodology is developed to detect the intersections, thus enabling the designer resize/reposition the subsystems, based on this knowledge.
6. Fuel tanks can be placed in the wing, in the horizontal stabiliser or in the fuselage. Besides manual selection, a methodology for iterative sizing and positioning is developed. This method considers parameters such as the available volume in the airframe, required fuel mass to accommodate and the possible locations for the fuel tanks.
7. Due to the gradual increase of electrification of aircraft systems, the equivalent electric subsystem models are developed as well.
8. The influence of the parametric models can only be quantified if sized simultaneously with the aircraft within an integrated multidisciplinary framework. This is the main focus of this research and is demonstrated by a case study with the proposed framework.

2.5. Chapter summary

From the conclusions drawn based on the state of the art, it is evident that a novel methodology is required to integrate the subsystem sizing methods in the overall aircraft design process. The limitations of the present methods are addressed along with the required novelty to overcome this research gap. Based on these conclusions, the novel framework developed as a part of this research, along with the development of the parametric sizing domain is presented in the following chapter.

3

Approach

3.1. Introduction

In Chapter 2, the state of the art in parametric modelling of subsystems and integrated systems sizing with the aircraft design are discussed. The chapter is concluded with the limitations of the current methods and the necessary novelty of the proposed framework. In this chapter, the proposed framework in this research is introduced and described in detail. The concept of integrated parametric sizing of subsystems with the aircraft is presented in Section 3.2. The assumptions and the subsystem models developed in the scope of this research are discussed in Section 3.3. The development of the subsystems sizing domain, which is a corner stone of the proposed framework is presented in Section 3.4. The implementation of the proposed framework, with the respective enablers is described in Section 3.5. The chapter is summarised in Section 3.6.

3.2. Integrated parametric sizing approach

The integration of a specific domain, such as subsystems sizing in the aircraft design process in highly challenging as the design process is multidisciplinary. The introduction of a new subsystem causes a change in the performance of the aircraft and so to the design. The design needs to be recomputed amongst various domains till the design convergence is reached. Different aircraft design frameworks exist to facilitate this process. Multi Disciplinary Design Optimisation System (MDOPT) by Boeing [26], DesignCompiler 43 by the University of Stuttgart, Collaborative Application Framework for Engineering (CAFFE) [27] and Design Engineering Engine (DEE) from TU Delft [28] are some frameworks that enable multidisciplinary aircraft design. DEE, in specific is focussed on integrated parametric sizing and analysis of the aircraft (and components) with KBE methodologies. KBE methodologies need tools called KBE tools which are capable of generating and manipulating geometry. A KBE tool is a platform which combines the parametric modelling capability of a CAD tool with programming capability [13]. A framework, similar to DEE is proposed in this research, in specific for parametric sizing of subsystems. However, the framework is demonstrated with an initial conceptual sizing approach. This keeps the geometric sophistication at minimum and individual subsystems' configurations fixed, thus eliminating the need for specific KBE tools. However, the framework can be adopted with KBE methodologies as well, with an MMG (Multi Model Generator) capable of subsystems sizing. The overview of the proposed framework is presented as a flowchart in Figure 3.1. Each of the domains is described in the following subsections.

Top Level Aircraft Requirements (TLAR) are the set of requirements for the aircraft which are decided by the aircraft producing organization. These requirements are often derived for configuration, payload, range, operating costs and emissions. Requirements such as payload, range, take-off field length, service-ceiling and cruise mach number relate to the performance requirements. The payload requirements consist parameters such as the number of passengers or payload mass. The requirements can be extended to system and subsystem specific requirements, engine requirements and mission requirements. Some of the driving parameters for these requirements include technological progress, competition, demand and regulations. Airlines, government, airports and the regulating authorities are

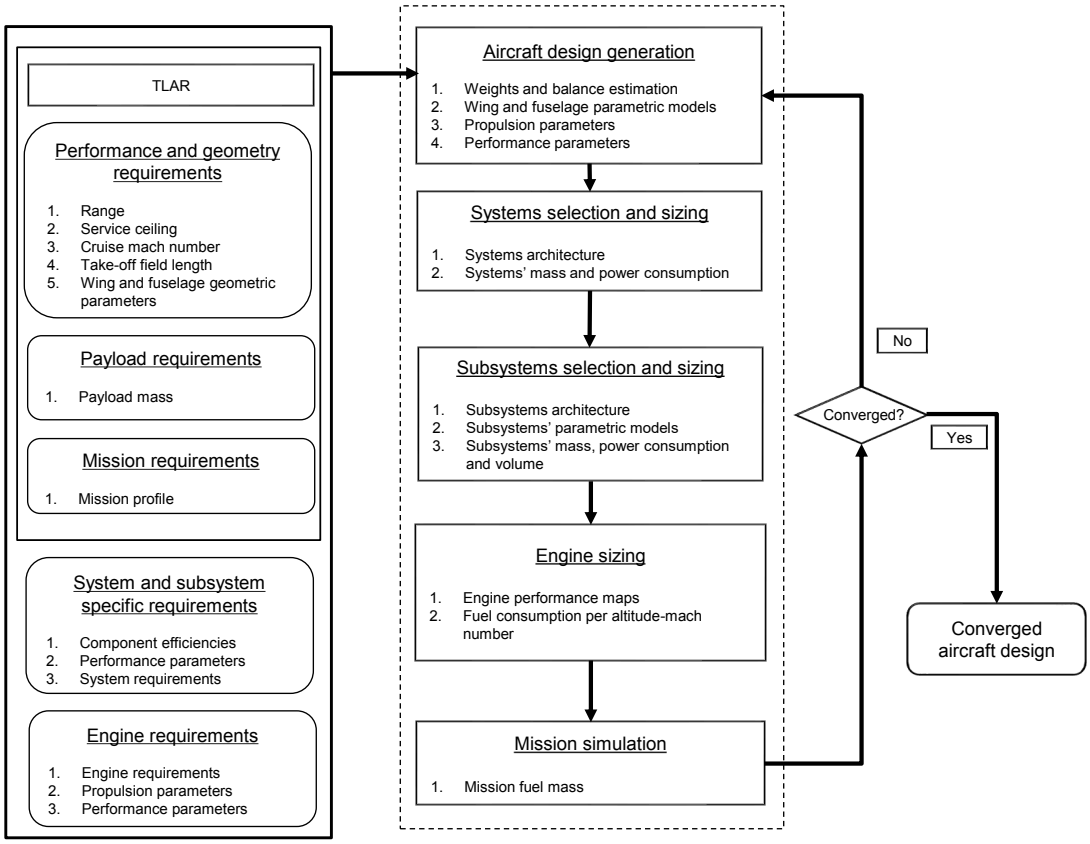

Figure 3.1: Framework of the sizing methodology

some of the major stakeholders that influence the driving parameters of the requirements.

Aircraft design generation follows the TLAR. This design consists of aircraft geometry, mass estimations, aerodynamic, structural, propulsion and performance parameters. The parametric models of the lifting surfaces and the fuselage constitute the aircraft parametric model. The mass estimations constitute the maximum take-off mass, operating empty mass, payload and fuel masses with their compositions. The lift to drag ratios and the respective aerodynamic coefficients constitute the aerodynamic parameters. Thrust requirements at different stages such as at take-off, cruise and landing comprise the propulsion requirements. This is the first conceptual design model estimated from TLAR with statistical data and handbook methods.

System selection and sizing is the domain in which, the on-board systems for the aircraft are selected and sized. Based on the the systems requirements, TLAR and the aircraft design parameters determined in the previous domain, the required systems and the actuation mechanism for each system are selected. This constitutes the systems architecture. Consequently, each of the systems in the architecture is sized to determine the mass and power consumption at system and architecture level. The power consumption constitutes the electrical power, hydraulic power and bleed air requirement.

Subsystem selection and sizing is the core domain developed as a part of this thesis. The subsystems for each of the systems in the systems architecture are selected and sized in this domain. The subsystems selection, similar to the systems selection depends on the subsystem specific requirements, TLAR and the aircraft design parameters. With the subsystems architecture, each of the subsystem is then sized to compute the parametric model, geometry, mass and power consumption. The parameters are determined at subsystem level and architecture level as well. The development of this domain is presented in Section 3.4

In the **Engine sizing** domain, the aircraft engine is sized and simulated to generate the performance maps. Besides the engine requirements, aircraft propulsion parameters (computed in the initial sizing process such as the maximum thrust) and the systems off-takes such as the overall shaft power and bleed air requirement (computed in the preceding domains) are vital to determine the engine parameters. One of the major parameters computed in this domain includes the fuel consumption of the engine for the design mission.

In the **Mission simulation** domain, the aircraft is simulated for the flight mission defined in the initial requirements with the major aim of determining the mission fuel consumption. This translates into the mission fuel mass. Besides the mission requirements; the aircraft parametric model, design masses, performance parameters, engine performance map and aerodynamic parameters are required to determine the required fuel mass for the mission.

Within the **framework**, the design parameters are generated and propagated through each of the domain, with the domains with higher fidelity methods replacing the parameters computed by the initial estimations. The design is iterated till the MTOM is converged.

The framework is represented as a Design Structure Matrix (DSM) in Figure 3.2 to better present the interconnection amongst the domains involved. The black squares represent the interaction of the parameters and the dotted border represents design iteration. The DSM is recreated in Chapter 6 with the specifics of the parameters exchanged in the presented case study.

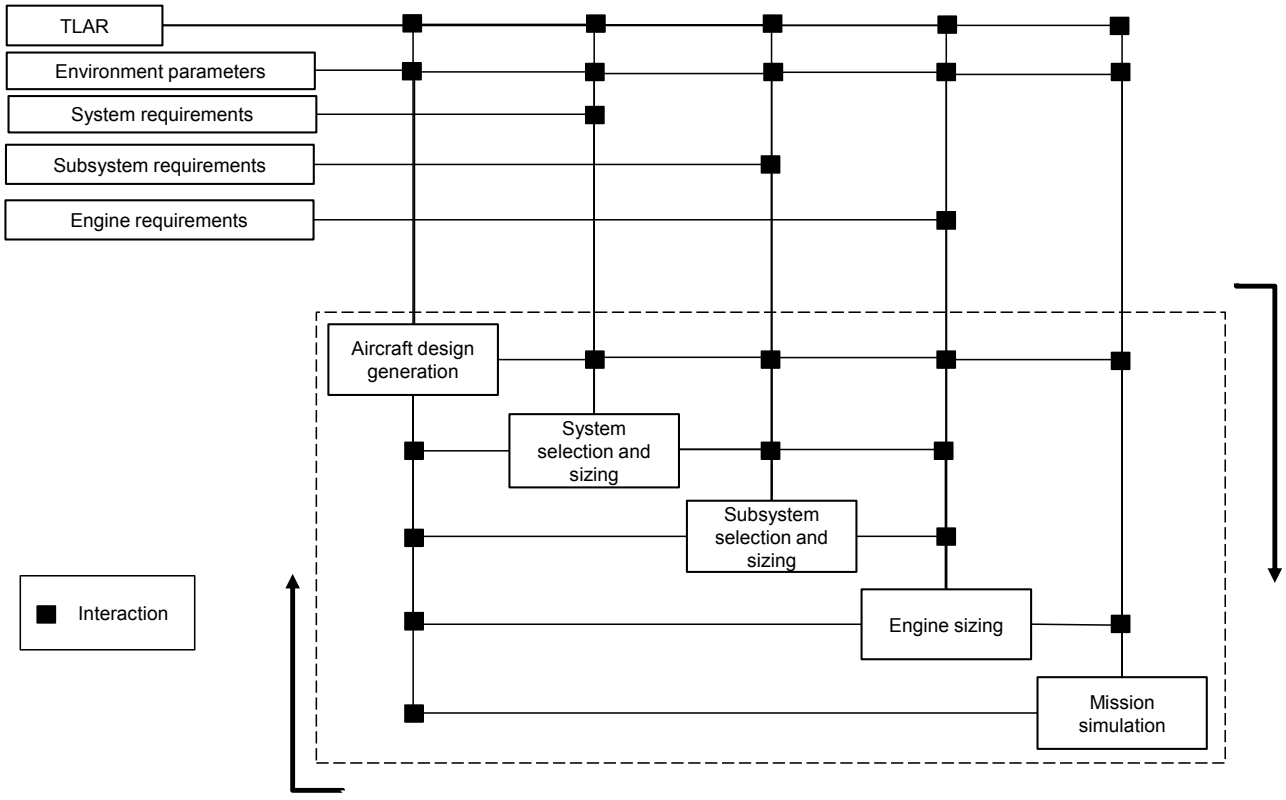

Figure 3.2: Design structure matrix of the framework

Summarising the DSM; with the intial design generated with the TLAR, the aircraft parametric model [1] and geometric parameters are propagated to the systems selection and sizing domain. The on-board systems architecture, mass and power consumption are determined and propagated to the subsystems selection and sizing domain. Here, the mass and the power consumption of the subsystems

[1]The parametric models of the fuselage, wing, horizontal tailplane and the vertical tailplane, are referred to in this thesis as the aircraft parametric model.

are computed and replaces the specific systems' parameters computed in the prior systems selection and sizing process. The recomputed power consumption is propagated to the engine sizing domain and the overall masses are recomputed based on the systems' mass computed by the higher fidelity methods. The engine is sized with these power requirements and simulated, thus generating the propulsion performance maps which are successively propagated to the mission simulation domain. With the aerodynamic performance maps, aircraft parametric model and design masses from the initial sizing process, the propulsion performance maps from the engine sizing, the mission simulation domain calculates the required mission fuel. This is replaced with the fuel mass computed during the initial sizing process, thus changing the MTOM as well. This process continues till convergence of the MTOM within a specific tolerance is reached.

3.3. Subsystem models and assumptions

Flight control actuators, fuel tanks and anti-ice elements are the only subsystems considered within the scope of this thesis. These constitute most of the wing subsystems, together occupying nearly 80% [2] of the overall wing volume and 60% [3] of the wing mass.

The following assumptions are made to integrate the theory and develop the subsystems sizing domain as a part of the proposed framework.

1. Subsystems such as the wiring and ducting are not considered due to the complexity involved in the routing and their dependency on the power distribution centres located in the fuselage.

2. The geometrical sophistication will be minimal as the main requirement from geometry in this study is to estimate the volume, parametric model and to determine the volume allocation of the subsystems in the airframe. Analysis capability, manufacturability and assembly are not the requirements of the subsystems' parametric models at this stage and hence ignored.

3. The actuator configurations are fixed and hence independent of the control surface. In practice, actuator configurations are specific to the actuating control surface. For instance, the EHA of a horizontal stabiliser is different in configuration relative to the EHA of an aileron. In this thesis, the configurations are fixed as the focussed design stage is conceptual and early preliminary.

3.4. Development of the subsystems sizing domain

To transform the concept of subsystems parametric sizing presented in the previous sections to usable models, two major enablers have been utilised. Firstly, to integrate all the methods into a re-creatable framework in computer programs, a schema is selected. A schema is a data format that enables easy interpretation of data by computers and humans. This standardises the design process. All the data in this framework is wrapped with this schema, which is unique to aircraft design. The subsystem sizing methods have been developed into an executable computer program, which automates the parametric sizing process, based on the aircraft level and subsystem specific requirements. The schema and the framework of the sizing tool are presented in the following subsections. The parametrisation of the subsystem models and the theory for sizing the subsystems is presented in Chapter 4.

3.4.1. Common Parametric Aircraft Schema

Common Parametric Aircraft Configuration Schema (CPACS) ([31], [32]) is an open-source Extensible Mark-up Language (XML) schema developed by DLR to assist multidisciplinary conceptual and preliminary design of aircraft. CPACS can hold the product, process and analysis data and hence enables data exchange amongst various tools. CPACS is the chosen data format in this thesis due to its flexibility of holding parametric data and its compatibility with various complimentary in-house (DLR) tools implemented in this research. A part of the schema is presented in Figure 3.3.

The data of a specific component is stored in its respective ontology. For instance, all the geometric and parametric modelling data of the wing is stored as a "wing" ontology. Besides structuring the file, the use of ontologies also enables the reuse of these components at different locations in an easier way. This data can be interpreted or written with the help of supporting tools that wrap the data in the CPACS

[2] Estimated based on the volume allocation equations and product catalogues from literature ([29], [30]) .
[3] Estimated based on the mass breakdown equations from literature ([11], [16]).

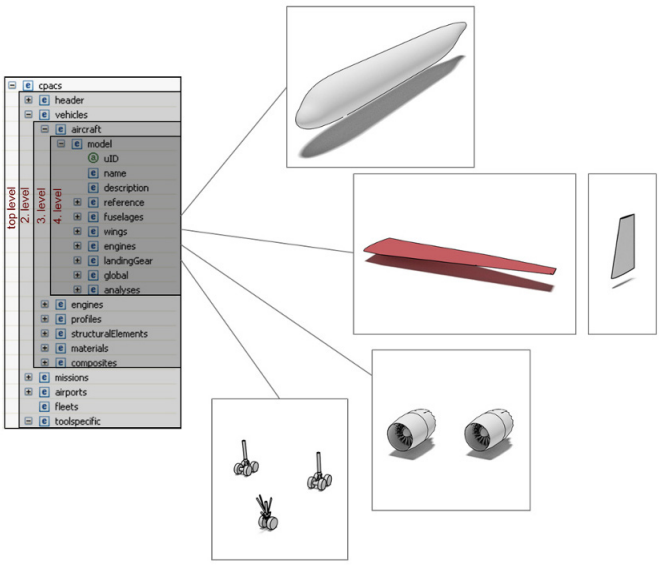

Figure 3.3: CPACS Schema

format. VAMPzero [33] and TIGL [34] are two such tools. TIGL enables visualisation of the geometry in the CPACS file. TIGL viewer is an open source geometry interpreter for CPACS files, developed by DLR. The geometry library developed in this tool uses the OpenCASCADE software, an open source 3D CAD development platform. The geometry generated can also be exported as IGES/STEP files from TIGL, which can then be interpreted in most of the CAD software. The parametric models of the aircraft and the generated subsystems are visualised in this thesis with TIGL viewer. A sample geometry generated by TIGL viewer by interpreting a CPACS file is presented in Figure 3.4.

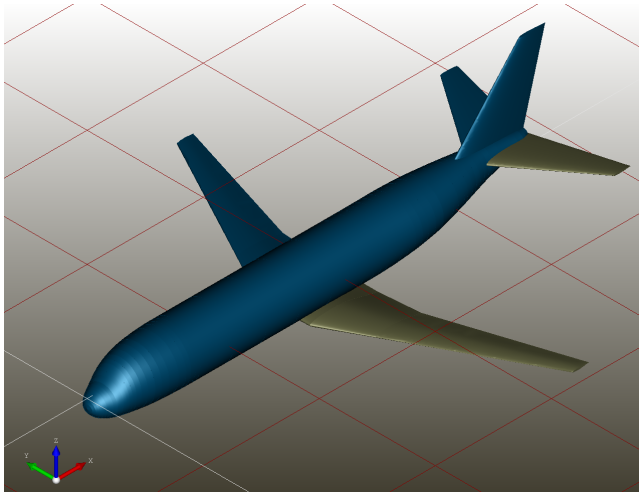

Figure 3.4: Geometry visualization of CPACS file in TIGL viewer

3.4.2. Framework of the sizing tool

Systems Model Generator (SMG) is the tool developed as a part of this thesis. The tool is developed in the programming language Python with an object-oriented methodology. The parametric data is

wrapped with the CPACS schema. The tool is developed such that the whole (selection and sizing) process is automated and the required tool settings can be changed through respective slots in the input file. The working of the tool can be split into five major stages, namely the input, subsystems architecture selection, subsystems sizing, intersection detection and output. The sizing process of the tool is presented in Figure 3.5.

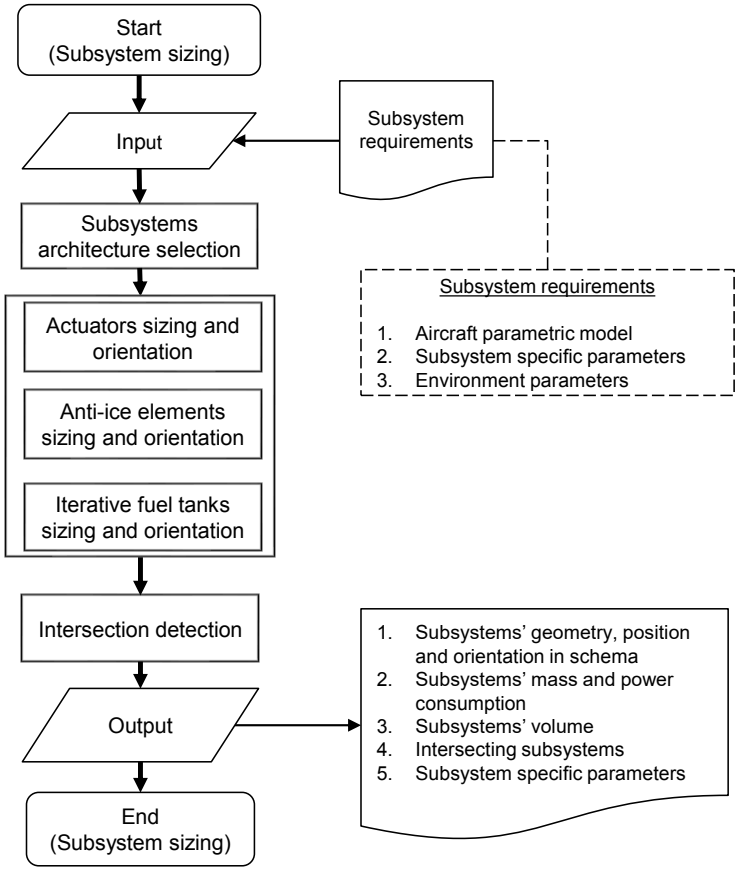

Figure 3.5: Algorithm of SMG

The **Inputs** consist of the subsystem specific parameters such as the architecture requirements, component efficiencies and the overall aircraft parameters computed in the initial design stage. The input file is in the CPACS format, with the system specific inputs in the toolspecifics slot of the file.

The **Subsystems architecture selection** is based on two inputs, aircraft type and technology level. This selection is done based on the "Knowledge Based System Selection (KBSS) and Knowledge Based Subsystem Selection (KBSUS)" concepts. The subsystems and the architectures can also be manually set by changing values for each subsystem individually in the input file, however this would result in a slightly higher setup time. The subsystems architecture is computed at this stage. This concept is further elaborated in Subsection 3.4.3.

In the **Subsystems sizing** process, each of the required subsystem from the architecture requirement list is sized to determine the mass, power consumption, parametric model and its orientation in the airframe. The current methods are capable of sizing the flight control actuators, anti-ice elements and the fuel tanks for the aircraft. This is further expanded in Subsection 3.4.4.

In the **Intersection detection** stage, all the parametric models, the subsystems models in the airframe and the aircraft parametric model are verified against each other to check for any intersections. The names of the subsystems with intersections are written to the output. This knowledge gives the designer an opportunity to resize, reposition or eliminate the intersecting components. This process is

elaborated in Subsection 3.4.6.

The **Output** constitutes all the outputs computed. These include the subsystem and architecture level parameters, which get written as an output XML file in the CPACS format. This file can be interpreted through supporting tools such as TIGL to observe the parametric models of the subsystems in the airframe and can be edited in parallel through an XML editor to make any modifications to geometry and/or orientation.

3.4.3. Knowledge based system and subsystem selection

Based on common terminology and knowledge from previous aircraft, rules have been derived and stored in the program as accessible dictionaries. With this availability, the required architecture is selected with the dictionary keys. The systems and subsystems that a specific aircraft requires depend on the functions the aircraft is required to perform. These functions are nearly similar for a specific type of aircraft. For instance, all civil transport aircraft systems need to facilitate flight control, communication, navigation, environmental control, protection of the wing surfaces against ice and rain and provision of emergency power. Hence, it is mandatory for civil transport type of aircraft to have the systems that perform these functions. Similarly, a Medium Altitude Long Endurance (MALE) Unmanned Aerial Vehicles (UAV) for surveillance needs defence related systems such as advanced radars and Infra Red (IR) cameras, besides the mandatory flight control and navigation systems, while not requiring an environmental control system. Hence, the required systems can be selected for a specific type of aircraft with a single input of "Aircraft Type". This is presented as a table in Table 3.1. However, as only three systems are considered in this thesis for the subsystems domain, the scope of KBSS is reduced as presented in Table 3.2. As seen from the table, there is no difference with incorporating KBSS but the functionality is incorporated so as to facilitate future developments of the tool when extended to more systems and aircraft configurations.

Based on the selected systems, the subsystems with the required quantity will be selected for each of the systems. This is done with the KBSUS process. The KBSUS in the scope of this thesis is presented in Table 3.3 and Table 3.4. Subsystems of the flight control system constitute the flight control actuators of every control surface. The presence of a control surface actuator is determined by the presence of the control surface. Typical MALE UAVs do not constitute secondary flight control surfaces, hence these actuators are assumed to be absent. Anti-ice elements of the wing are the subsystems of the anti-ice system. The anti-ice elements are present in most types of aircraft depending on the flight level and operating environment. The subsystems of the fuel system constitute the wing fuel tanks, the fuselage fuel tanks and the empennage fuel tanks. The fuel storage on MALE UAVs is only possible in the fuselage due to the thinner profiles of the wing and the empennage, thus explains their absence in the table.

Aircraft Type / System	Civil	UAV	Fighter
FCS	Yes	Yes	Yes
FUS	Yes	Yes	Yes
ECS	Yes	No	Yes
LGS	Yes	Yes	Yes
AIS	Yes	Yes	Yes
TRS	Yes	No	Yes
GALEQ	Yes	Yes	Yes

Table 3.1: Knowledge Based System Selection

The subsystems can be powered with different power sources. For example, the flight control actuators can be actuated with hydraulic power or electric power or a combination of both. This actuation is unique for each make and model. For instance the flight control system of an Airbus A320 uses hydraulic actuation [35] while that of a Boeing 777 uses hydraulic and electric actuation [36]. To ease the actuation selection for each component, predefined architectures are stored in the program, which are then selected with a single input called "Technology Level" (TL) . Six architectures

Aircraft Type / System	Civil	UAV	Fighter
FCS	Yes	Yes	Yes
FUS	Yes	Yes	Yes
AIS	Yes	Yes	Yes

Table 3.2: Scope of Knowledge Based System Selection in this thesis

Aircraft Type / Subsystem	Civil	UAV	Fighter
Aileron actuators	Yes	Yes	Yes
Elevator actuators	Yes	Yes	Yes
Rudder actuators	Yes	Yes	Yes
Spoiler actuators	Yes	No	Yes
THS actuators	Yes	No	Yes
Flap actuators	Yes	No	Yes
Slat actuators	Yes	No	Yes
Anti icing elements	Yes	Yes	Yes
Wing fuel tanks	Yes	No	Yes
Fuselage fuel tanks	Yes	Yes	Yes
Empennage fuel tanks	Yes	No	Yes

Table 3.3: Knowledge Based Subsystem Selection

Subsystem	Number	Basis
Aileron actuators	4	2 per control surface
Elevator actuators	4	2 per control surface
Rudder actuators	3	3 per control surface
Spoiler actuators	10	1 per control surface
THS actuators	1	1 per control surface
Flap actuators	8	2 per control surface
Slat actuators	8	2 per control surface
Anti icing elements	4	1 per slat
Wing fuel tanks	2	1 per wing
Fuselage fuel tanks	1	1
Empennage fuel tanks	2	1 per horizontal tail surface

Table 3.4: Number of subsystems

are stored, varying from technology levels 1-6 as presented in Table 3.5. In the table, "E" stands for electric power, "EH" is a combination of electric and hydraulic power, "H" is hydraulic power and "P" is pneumatic power. TL 1 is an all-electric subsystems architecture with total electrification of the flight control system, anti-ice system and the fuel system, while a TL 6 is a conventional subsystems architecture; with a hydraulic flight control system, pneumatic anti-ice system and electric fuel system. TL 2-5 are between conventional and all-electric subsystems architecture of TL 1. TL 2 constitutes all-electric subsystems architecture (similar to TL 1) with the flight control actuators replaced with EHAs. TL 3 is an MEA subsystems architecture with all-electric flight control system (EMAs) (elimination of hydraulic system) and retention of pneumatic system for bleed-air anti-ice. TL 4 is an MEA subsystems architecture as well, however the hydraulic system is retained for flight controls but the pneumatic system is eliminated as the anti-ice system is electrified. This is similar to the architecture of the Boeing 787. TL 5 is similar to TL 3 i.e. an electric flight control system and a pneumatic anti-ice system with an exception of the EMAs replaced with EHAs. With increasing the subsystems in the future or by defining different actuation for each flight control actuator, there is a possibility of a large number

of combinations for the technology levels (architectures), but in the scope of this thesis, only the 6 technology levels presented are defined for automatic selection. However, there is also a possibility to set the actuation of each subsystem manually to define the required architecture. The concept of technology level is introduced to standardise architectures and to enable the selection of the systems and the subsystems architectures for an aircraft just two inputs; "Aircraft Type" and "Technology Level". This concludes the subsystems architecture selection process.

Technology Level / Subsystem	1	2	3	4	5	6
Aileron actuators	E	EH	E	H	EH	H
Elevator actuators	E	EH	E	H	EH	H
Rudder actuators	E	EH	E	H	EH	H
Spoiler actuators	E	EH	E	H	EH	H
THS actuators	E	EH	E	H	EH	H
Flap actuators	E	EH	E	H	EH	H
Slat actuators	E	EH	E	H	EH	H
Anti icing elements	E	E	P	E	P	P
Fuel system	E	E	E	E	E	E

Table 3.5: Architecture based on technology level

3.4.4. Sizing individual subsystems

The sizing of each subsystem is independent of the other, thus is performed in parallel following the subsystems architecture selection process. Five sizing algorithms are defined, based on the unique parametric modelling requirement of each of the subsystems. Algorithms for actuator sizing, wing fuel tank sizing, fuselage fuel tank sizing, hot-air anti-ice element sizing and electro-thermal anti-ice element sizing are defined and elaborated in this subsection. All the parameters are computed based on rules, relating the required parameters to the inputs. Hence, the whole process is automated with the inputs defined in the input file. The parametrisation and the specific rules for sizing each subsystem are presented in Chapter 4.

The sizing process of the three actuators is similar and can be split into four sub-processes, as observed in Figure 3.6. With the actuator requirements defined parsed as input, first, the mass and power consumption of the actuator is computed. Successively, the geometry of the components and so of the subsystem is determined. Based on the control surface position, the orientation of the model is fixed. A generic geometry file for each actuator is already pre-defined as a schema in the tool. The tool, clones the generic geometry file of the specific actuator, replaces the dimensions of individual components to the computed dimensions and saves this data schema to the final output file. This generic geometry file serves as a blue-print, thus enabling to create any number of subsystems each, with its unique parameters. The whole process repeats for every single actuator required, specified in the requirement.

The wing fuel tanks are integral, and hence modelled from the parametric model of the wing. As seen in Figure 3.7, firstly, the wing parametric model is cloned and thus acts as a blueprint. The coordinates of all the airfoils that comprise the wing are extracted from the wing model. Each airfoil profile of the clone is then modified by slicing it from the leading edge and the trailing based on the front and rear spar positions as a fraction of the local chord, defined in the requirements[4]. The wing is then rebuilt with these replaced profiles, from the root to tip, defined as a fraction of the wing semi-span from the fuselage surface, defined in the requirements. The generated parametric model in the schema is saved to the final output file. The mass of the tank, occupying volume, material volume and fuel mass capable are computed as well based on the data from the parametric model generated. The process is similar for the empennage fuel tank as well, with the Horizontal Tail Plane (HTP) parametric model serving as a blue-print for it rather than the wing.

The fuselage fuel tank sizing is dependent on the parametric model of the aircraft for its size and position. As seen in Figure 3.8, the sizing process is similar to that of the actuators, where a generic

[4]The required profile is the central section.

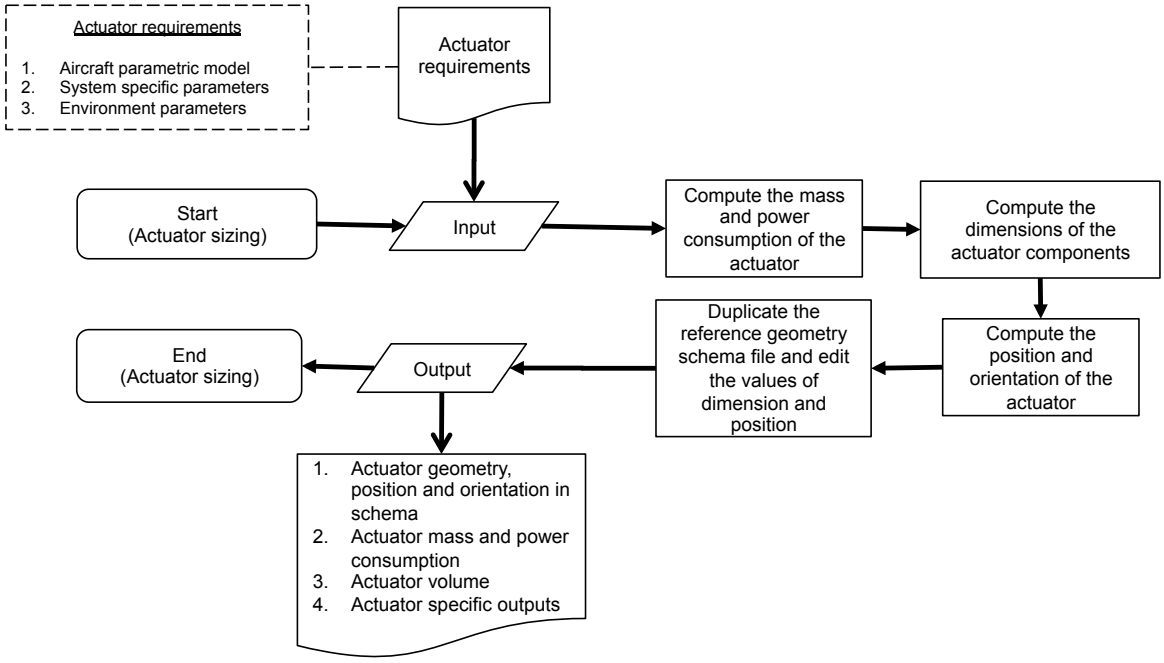

Figure 3.6: Sequence flowchart of the actuator sizing process

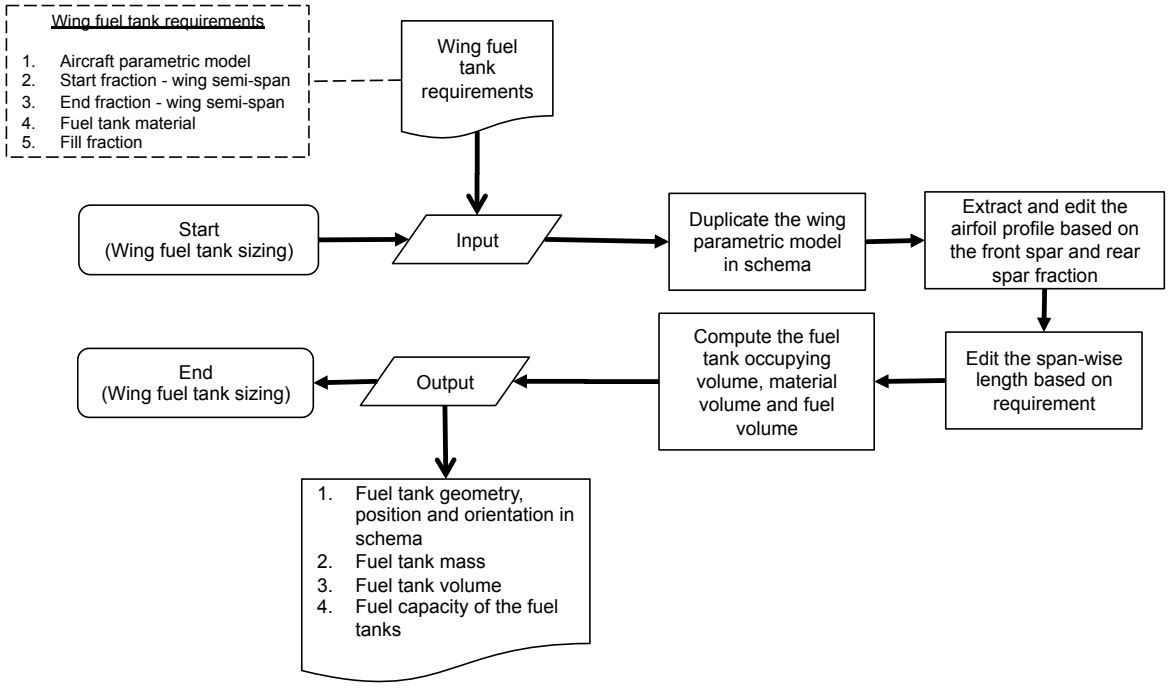

Figure 3.7: Sequence flowchart of the wing fuel tank sizing process

geometry file is cloned, edited and propagated to the output. If the fuselage fuel tank is a central tank, it is placed at the center of the wing. If the tank is an add-on, it is placed in the fuselage at the required fraction of the fuselage length, specified in the requirements. Parameters of mass and volume, similar to the wing fuel tank are computed based on the parametric model.

The hot-air anti-ice element is sized similar to the actuators with a generic geometry file cloned and edited, based on the computed geometry. This is evident from the flowchart is Figure 3.9. Based on the requirements, the power consumption is firstly computed. Successively, the geometric parameters

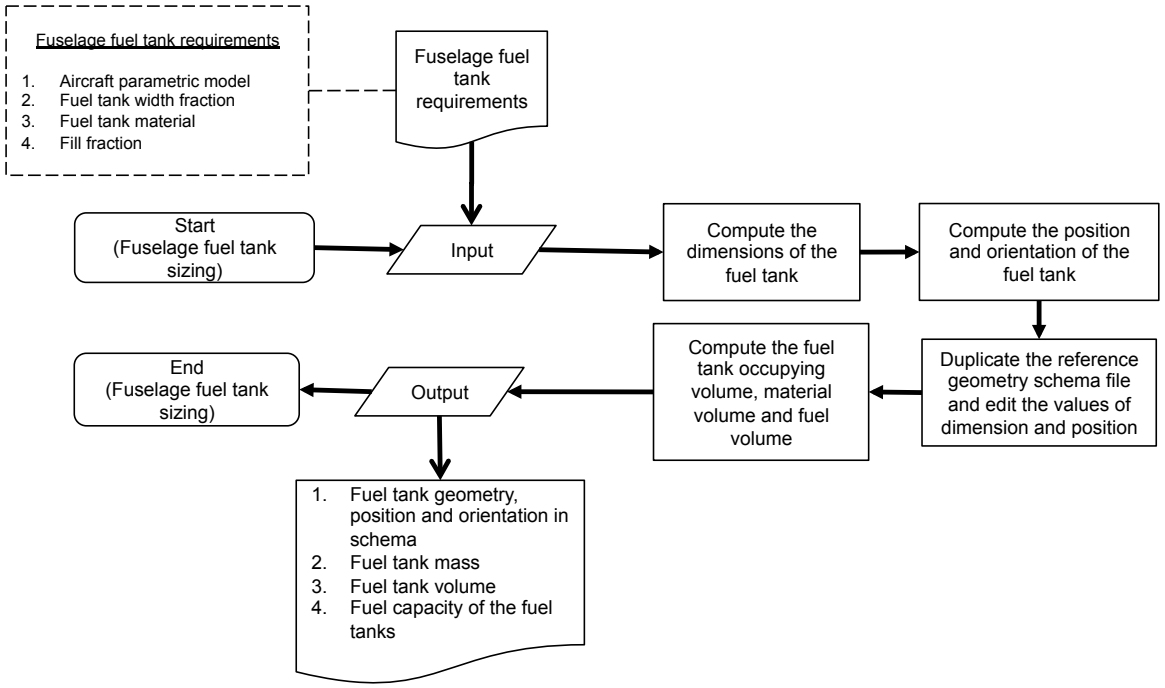

Figure 3.8: Sequence flowchart of the fuselage fuel tank sizing process

of the element are computed and based on the wing position from the aircraft parametric model, the subsystem position is determined. The data of the parametric model in schema is written to the output file. Based on the parametric model, the occupying volume, material volume and material mass are computed as well.

The electro-thermal anti-ice element is defined as a thin strip surrounding the leading edge of the wing. As the strip is placed on the wing leading edge, it is an aerodynamic design requirement for its profile to blend in. Hence, the wing parametric model is required to generate the parametric model of the electro-thermal anti-ice element. The process is presented in Figure 3.9. Similar to the sizing process of actuators and hot-air anti-ice element, the power consumption of the elements is first determined. The wing parametric model is then cloned, and similar to the wing fuel tank, the airfoil profiles are extracted and modified. The modifications are made such that the airfoil profile is sliced from the leading edge, with the chord as a fraction of the wing local chord, computed in the sizing process [5]. The volume and mass of the elements is determined based on the data from the parametric model and requirements of thickness and material density.

3.4.5. Automatic fuel tank sizing

In reality, while designing an airplane, the fuel tank limits nor the number of fuel tanks required are hardly known. With the required fuel mass known, it is usually an iterative process to fix the configuration and limits. This limits the use of the fuel tanks sizing process in an automated framework in the tool as sizing limits are not directly related to the requirements. To overcome this limitation, an automatic fuel tank sizing algorithm was developed which is presented in Figure 3.11. The only requirement is the required fuel mass. With this requirement, the wing fuel tank is first sized [6] by setting the start fraction to 0.1 and end fraction to 0.2. Iteratively, the end fraction is increased till 0.95, with 0.001 incremental with each run. At each iteration, the fuel mass capable is computed, based on the tank thickness, fuel density and fill fraction and the end fraction is only increased if the capable mass is lower than the required mass. Once the wing tank reaches its limit, an empennage tank is created with its start fraction at 0.1 and end fraction at 0.2. The iterative sizing process is similar to the wing fuel tank. Successively, a fuselage fuel tank is created and iteratively sized till it

[5] The required profile is the section from the leading edge to the chord fraction.
[6] The central tank is automatically created

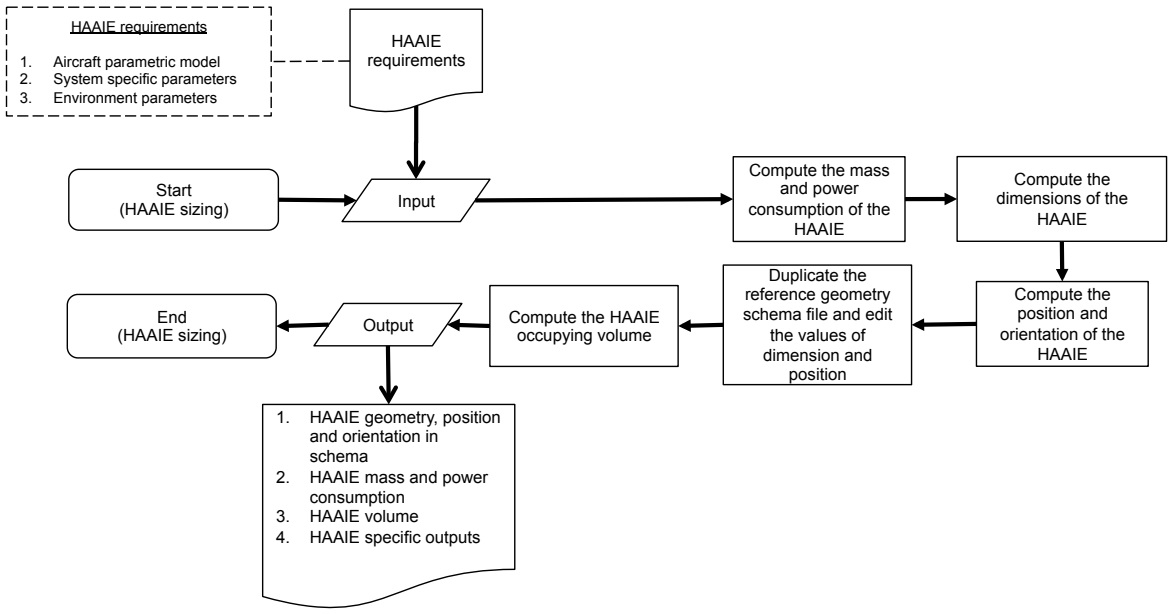

Figure 3.9: Sequence flowchart of the hot-air anti-ice element sizing process

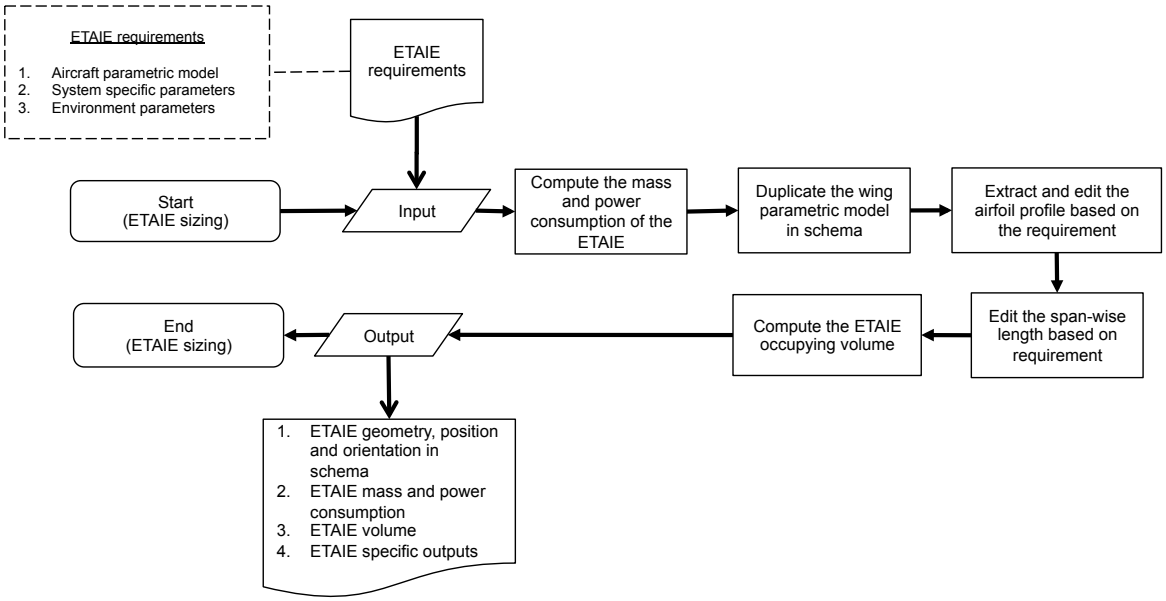

Figure 3.10: Sequence flowchart of the electro-thermal anti-ice element sizing process

reaches its limit. The sizing stops at this point as all the tank limits are reached. The status of the requirements fulfilment is written to the output. Though the core sizing algorithm stays the same, the automatic sizing algorithm overlooks the fuel tanks sizing process by manipulating the inputs, running the inner sizing algorithms, checking the requirements status and repeating this process till either the requirements meet or limits reach.

3.4.6. Intersection detection

With the presence of a large number of parametric models in close proximity, there is a high possibility that one or more of the models would intersect due to deviations in computed position, size or the number of subsystems. Besides, in reality, subsystems are positioned/designed around an object of obstruction. This level of detailed modelling in the conceptual and early preliminary design stages is

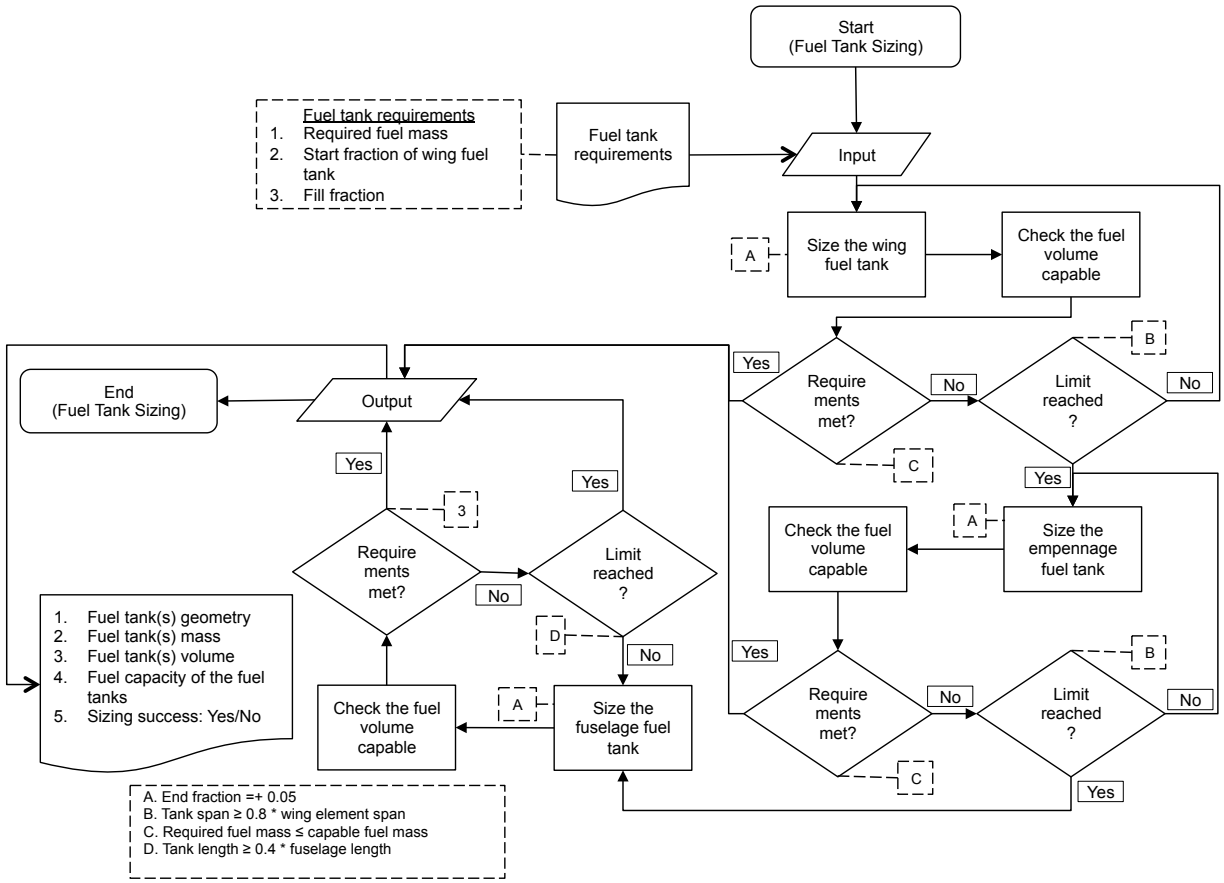

Figure 3.11: Sequence flowchart of the automatic fuel tank sizing process

quite complicated and beyond the scope of this research. In any case, it would be highly beneficial for the designer if the tool provides this knowledge of subsystems intersection, based on which, the subsystems could be resized, repositioned or eliminated, if required. An algorithm is developed for this specific purpose of intersection detection, which is presented in Figure A.1 of Appendix A. With all the parametric models in the CPACS file, the tool checks [7] all the parametric boundaries of the subsystems models against each other (and that of the aircraft parametric model) for intersections. If any, a dictionary is created with the names of the intersecting subsystems as seen from the flowchart in the figure and is propagated to the output. With this knowledge, the geometries or positions of the subsystems can be edited through the CPACS file or by changing the specific inputs and the tool can be re-run for a re-design.

[7] The check is performed with a check-intersect function from the TIGL library for CPACS parametric models.

3.5. Implementation of the framework

Within an aircraft design framework, it is required to identify the domains of interest and develop workflows to propagate the influence of that specific domain. In this thesis, workflows are developed to aid aircraft design with subsystems sizing, which is the proposed framework. To start developing any component for an aircraft, the geometry of the airframe and the design data such as the mass estimates are required. The mass estimates constitute the estimated masses of the groups such as structures, systems, fuel, passengers etc. from which an estimated maximum take of mass is computed. This initial design is usually generated by an aircraft design initiator. From this design data and other requirements, the systems are selected and the mass and power consumption of these systems are determined. This is done by an initial systems synthesis tool. The geometry of the subsystems is then computed after which they are oriented in the airframe. Besides, the mass and power consumption of these subsystems are computed as well. The computed power consumption is propagated to size and simulate the engine. The engine performance maps and the aircraft design data computed in the initial domain are propagated to the mission simulation tool which simulates the specific mission and computes the fuel consumption for the mission. This translates into the fuel mass for the mission which is a major driver for the aircraft performance, emissions, maintainability and the manufacturability.

The functions of each of the domains in the framework discussed in Section 3.2 can be performed by programs that can be executed with inputs and outputs exchange through files. The design initiator used in this research is VAMPzero, an open-source object-oriented conceptual aircraft design tool based on handbook methods ([37], [11], [12]). Initial system synthesis is performed by the Systems Synthesis Module (SSM), which aids in systems selection and computations of mass and power consumption of systems with semi-physics based methods ([15], [16]). The subsystems' geometry is computed by the Systems Model Generator (SMG), the tool developed as a part of this research, presented in the previous subsection. The engine is sized and simulated by the Engine Modelling Module (EMM), with thermodynamic relations ([38], [39]). The mission analysis is performed by the Fast and Simple Mission Simulation (FSMS) with standard equations of motion. All the tools are developed by DLR. The proposed framework is recreated as an executable workflow in the integration environment RCE [40], as presented in Figure 3.12. All the data exchange is through the CPACS format. The methods used in each of the tools are described in brief in the following subsections.

3.5.1. Design initialization

VAMPzero is an medium fidelity object oriented conceptual aircraft design tool developed in Python. It is an open-source tool developed by DLR and was validated with different Airbus and Boeing transport aircraft models [1]. With the TLAR defined in the CPACS format, VAMPzero generates the initial design. This consists of the aircraft mass breakdown, performance data and geometries of the fuselage, wing and the tail. The masses include the design masses, the payload masses, the fuel mass and the OEM. The design masses include the MTOM, Zero Fuel Mass (ZFM) and Zero Landing Mass (ZLM). The payload masses constitute the passenger and the cargo masses. The OEM constitutes the mass of the structures, power unit, systems and furnishing. VAMPzero can also be configured to compute only the desired parameters while keeping the rest constant. In this thesis, as the systems sizing would be performed by other tools (SSM and SMG), the systems mass requirement initially is configured such that it is unchanged by VAMPzero. The initial estimate would be made by empirical relations and successively, it would be replaced by computation from SSM and SMG. VAMPzero, in this thesis will also be used for design initialization and successive iterations to recompute all the parameters. This process loops till convergence is reached.

3.5.2. Systems selection and sizing

In this thesis, SSM is implemented for the initial systems selection and sizing. SSM models the power consuming, power producing and the power distributing aircraft systems with semi-physics based methods [16]. The power consuming systems constitute the on-board systems which consume hydraulic power, electric power or bleed air. The power producing systems are the generators which produce electrical power and hydraulic power from shaft power of the engine. The power distributing systems constitute the pneumatic ducting, hydraulic piping and the electrical wiring from the power generators to the consumers. The subsystems are categorised into seven groups and include a vast majority of the on-board systems. The seven systems that are modelled with SSM are the flight control system

(FCS), environmental control system (ECS), landing gear system (LGS), anti-ice system (AIS), galley equipment (GALEQ) and the power generation and distribution system (PGDS). The mass and power consumption of the remaining systems (Misc) are considered as miscellaneous additions. Besides the conventional hydraulic and pneumatic actuation, the systems can also be modelled with electric actuation. The parameters are computed by a combination of energy equivalence, component break down and regression based methods from literature. The output of SSM constitutes the systems architecture, the total mass of the systems, the total shaft power consumption and the bleed-air consumption at system and architecture level. The modelling basis for each of the systems is described in brief and the cited literature can be referred for a deeper understanding.

Flight control system

The flight control system constitutes actuators of primary and secondary flight control surfaces. The aileron, elevator, rudder, spoiler, trimmable horizontal stabilizer and the high lift devices are included in the FCS. The power required to actuate a control surface is computed based on the required actuation velocity and the hinge moment of the control surface. It is a function of the control surface dimensions, the ambient conditions and the hinge moments of the control surfaces [41].

Environmental control system

The mass of ECS is a function of the mass of the air conditioning equipment. The power consumption is computed based on the required power to maintain the cabin temperature and pressure for the duration of the flight. The heat load is the heat generated from the passengers, the galley equipment and the hat transfer from the atmosphere through the skin of the aircraft into the cabin. It is a function of the fuselage geometry, the number of passengers and the required cabin temperature and pressure ([42] , [15]).

Landing gear system

The LGS constitutes the landing gear extraction/retraction system, the nose wheel steering system (NWSS) and the wheel braking system (WBS). The landing gear extraction.retraction system is further divided into nose landing gear and main landing gear. The mass of the landing gear is a function of the structural mass of the landing gear. The power consumption for extension and retraction is the power required to lower the mass of the whole landing gear to a certain angle with a certain velocity, for a specific period of time. It is a function of the landing gear mass and dimensions ([43], [16]). The mass of the NWSS is a function of the structural mass of the landing gear. The power required is the power consumed by the landing gear to turn at a certain angle, with a specific velocity, supporting the mass of the aircraft. It is a function of the MTOM ([46], [47], [16]). The mass of the WBS is a function of the structural mass of the landing gear. The power consumption is the power required to bring the aircraft to a stop during after landing. It is computed based on the MTOM and the thrust of the aircraft ([16], [43]).

Anti-ice system

The AIS system is further divided into wing ice protection system and cowl ice protection system. The mass of the ice protection systems is a function of the mass of the anti icing and de icing equipment. The power consumption of the wing ice protection system is the power required by the bleed air or the electric heaters to maintain the wing at a certain temperature to avoid icing, for a specific period of time. It is a function of the wing geometry, amongst many. Similarly, the power consumption of the cowl ice protection system is the power required to maintain the engine cowl at a temperature. It is a function of the cowl dimensions, besides the surface temperature and duration requirements. ([44], [45], [16]).

Galley equipment

The galley equipment constitutes the in-flight entertainment system (IFE) and the furnishings. These systems are modelled from component level. The number of IFE equipment and the food and beverage machines such as the coffee machines, the hot water machines and the ovens are specified, along with the mass and power consumption of each of the system from literature. The total mass and power consumption is hence, the summation of the masses and power consumption of all the listed systems. The furnishing constitutes the seats and the additional equipment such as the over-head compartments

and lavatories. The seat mass is calculated based on the number of classes, seat mass of each class, and the number of seats per class. The overhead compartment and lavatory mass is estimated based on empirical relations which are a function of the number of passengers and crew [11].

Power generation and distribution Systems

The power generation systems are further divided into pneumatic power generation system, electric power generation system, hydraulic power generation system and mechanical power generation system. The mass and power consumption of these systems are a function of the MTOM of the aircraft and the total power requirements of the respective power consuming systems [16]. The power distribution systems constitute the pneumatic ducts, hydraulic pipes and the electrical wires. The mass of the power distribution systems are a function of the aircraft geometry and the power requirement of each of the respective power consuming systems [16].

Miscellaneous systems

The miscellaneous systems (Misc) constitute the remaining systems such as the avionics, lights etc. that are not included in the systems categorised above. The mass and power consumption of each of these systems is computed based on low fidelity empirical methods [11].

3.5.3. Subsystems selection and sizing

SMG firstly sets systems and subsystems architecture with KBSS and KBSUS (Subsection 3.4.3). The tool then computes the geometric parameters, orientation parameters and the performance parameters (mass, power consumption) of each of the subsystems. These subsystems include the flight control actuators, anti-ice elements and fuel tanks. The flight control actuators are modelled for all the primary and secondary flight control surfaces of a civil transport aircraft. The tool then performs checks to determine intersections amongst the subsystems and the aircraft parametric model. All the results including the names of the intersecting subsystems are wrapped as per the required CPACS ontology to the output. The framework of this tool is presented in Subsection 3.4.2 and the sizing rules of the subsystems are presented in Chapter 4.

3.5.4. Engine sizing

EMM is a medium fidelity tool that sizes the engines based on design requirements such as bypass ratio, turbine inlet temperature, overall pressure ratio, component efficiencies, etc. and two performance requirements, namely maximum thrust and off-takes (shaft power and bleed air). Thermodynamic relations are used with ideal gas assumptions for simulating this sized engine. Parameters such as the temperature, pressure, mass flow rate of air at every section are determined with energy equivalence relations. The mass flow rate of fuel is determined as well, at each mission point for every thrust setting. This constitutes the performance map of fuel consumption which is propagated to the mission simulation for computation of the mission fuel mass.

3.5.5. Mission simulation

In this thesis, an in-house tool, FSMS is used for simulation of the aircraft for the mission defined in the requirements. FSMS assumes the aircraft as a point mass body and determines the performance of the aircraft based on standard equations of motion for a 2-dimensional mission. The aerodynamic and propulsion parameters at each mission point are interpolated from the performance maps computed in the previous domains. One of the performance parameters computed by FSMS is the fuel consumption. Based on this, the mass of fuel for the mission is calculated.

3.5.6. Integration

RCE is an integration environment to facilitate automated data exchange between various tools [48]. In this research, it is implemented to exchange data between VAMPzero, SSM, SMG, EMM and FSMS through the CPACS file. The tools are integrated into RCE, to not only facilitate multidisciplinary design but to also store the knowledge so as to facilitate usage and development of the tools by peers and successors [49].

From the workflow presented in Figure 3.12, it can be observed that the tools are denoted as boxes with abbreviations. The initial input file with TLAR is passed to VAMPzero, where the workflow starts. The tool-specific parameters are input through the tool specific input provider below each of the tool.

The arrows specify the direction of information flow. All the data exchanges through CPACS and the tool outputs are written into tool-specifics of the CPACS file as well. Adapting this schema enables the whole design and performance knowledge of the aircraft to be stored and propagated with a single file.

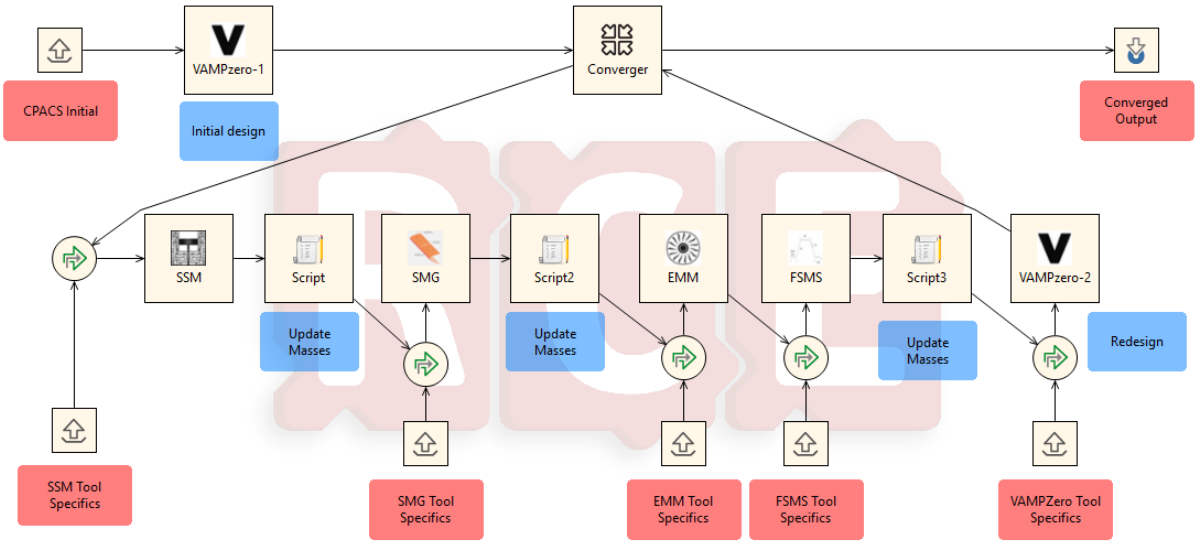

Figure 3.12: Recreation of the framework in RCE

The design is initiated with the inputs of wing dimensions, fuselage dimensions and other top level requirements. An estimated value of the systems mass is also an input. Based on the design and performance parameters computed by VAMPzero and other tool-specific parameters, SSM computes the systems architecture, masses and power consumption. This calculated systems mass is updated to the OEM and MTOM. Subsequently, the parameters are propagated to SMG which generates the wing subsystems parametric models and orients them in the airframe. The mass and power consumption values of the wing subsystems are recomputed and updated to the systems mass, OEM and MTOM. With the maximum thrust (computed by VAMPZero), shaft power and bleed-air off-takes (computed by SSM and SMG), EMM sizes the engine and generates the performance maps which constitute the fuel consumption at each mach-number and altitude specified in the design mission. All the computed parameters are propagated to FSMS which computes the fuel consumption at every mission point and calculates the total fuel mass for the mission and updates the MTOM as well. These new values are propagated back to VAMPzero for redesign. The design is iterated till the specified convergence tolerance is reached. The final output file is stored in the directory specified in the output tool. This file can be interpreted with any XML viewer to find the computed parameters or can be exported to TIGL viewer to visualise the geometries. The workflow can be modified to facilitate Design Of Experiments (DOE) and optimisation studies as well.

3.6. Chapter summary

In this chapter, a framework for integrated parametric subsystem sizing with the aircraft is presented along with the implementation. Different domains of the multidisciplinary framework, which contribute to the overall aircraft design and sizing are introduced and described. With the aid of enablers, it is evident that the process can be standardised and integrated with ease. This ensures that certain processes such as the parametric sizing and design generation can be automated based on a few top level and system specific requirements. Moreover, once the workflow is integrated, it is possible to run a large number of case studies within in a certain period. The supporting domains are already developed into pre-existing tools which can be plugged in into these workflows. SMG, is one such domain, which is developed as a part of this research. The structure of the program and the algorithms implemented to enable parametric sizing of different subsystems are presented in this chapter as

well. The parametric models of the individual subsystems generated, and the sizing rules which relate the parametric dimensions of the subsystems to the aircraft and subsystem specific parameters are presented in the following chapter.

4

Subsystems parametrisation and sizing

4.1. Introduction

In Chapter 3, the framework developed as a part of this research to enable integrated parametric sizing of the aircraft subsystems with the aircraft is presented. The domain of subsystems selection and sizing along with the sizing algorithms implemented is presented. The parametrisation and the sizing rules of these subsystems are described in this chapter to provide an insight into the rule-based sizing processes, which relate the aircraft and subsystem specific parameters to subsystems' geometry, mass, power consumption and orientation in the airframe. Each of the subsystem is introduced with its function and the parametric model is described with the number of parameters required for sizing. These constitute the required number of dimensions for sizing a parametric model. The sizing of the flight control actuators is presented in Section 4.2, fuel tanks in Section 4.3 and anti-ice elements is Section 4.4. Two major sizing processes are implemented based on the subsystems. The flight control actuators, fuselage fuel tank and hot-air anti-ice element are sized by changing the dimensions of the components of a predefined model. The wing fuel tank, empennage fuel tank and the electro thermal anti-ice element are sized by duplicating the parametric model of the wing and manipulating the profile as per the requirements. These subsystems are highly sensitive and dependent to the profile of the wing parametric model and hence this approach results in the least deviation with low modelling steps. The chapter is concluded with a brief summary in Section 4.5.

4.2. Flight control actuators

The flight control system provides the means to control the aircraft's direction and orientation. This is achieved by means of flight control surfaces, which can be deflected by the pilot by means of a control stick. Modern aircraft translate the input force of the pilot into electrical signals which are processed by a computer and propagated to the flight control actuators. Flight control actuators are devices that translate these control signals into mechanical force to the control surface for deflection. This translation is done by means of a power source such as hydraulic fluid or electrical power. Flight control actuators can be divided into three main categories based on the source of power. Electro hydraulic actuators, also known as fly-by-wire actuators derive the necessary power from the hydraulic source of the aircraft. Electro hydrostatic actuators have an inbuilt hydraulic reservoir, thus derive electrical power from the generators to pump this fluid to provide the required actuation. Electro mechanical actuator works solely on electrical power for actuation. It consist of an electric motor, geared to a screw. The motor provides rotation to turn the engaged screw, which provides the required actuation. More actuators exist but are not considered in the scope of this research as they are not widely used nor expected in the near future in modern civil transport aircraft. The parametrisation and the sizing of the flight control actors is presented in this section.

4.2.1. Electro hydraulic actuator

The electro hydraulic actuator is idealised as an assembly of five components, namely the cylinder, rod, head, base and valve block. These components can be seen in Figure 4.1. The cylinder, the rod and the valve block are defined with two parameters each, length and diameter. The head and the base, similarly are defined with parameters of diameter and thickness. All the components are modelled as cylinders. A simplified parameter dependency for sizing is presented in Figure 4.2. The control surface is idealized as a thin panel [50]. With the dimensions of the control surface, the conditions at cruise, the maximum angle of attack (α) and the maximum deflection (δ), the hinge moment of the control surface can be determined with methods proposed by Truckenbrodt [51].

$$M_{hinge} = \frac{1}{2} \cdot \rho \cdot v^2 \cdot C_{hinge}(\alpha, \delta) \cdot S^2{}_{ref,cs} \tag{4.1}$$

Here, ρ and v are the density and the velocity at cruise conditions and $S_{ref,cs}$ is the reference area of the control surface. The hinge coefficient is given by

$$C_{hinge} = C_{h,\alpha} \cdot \alpha + C_{h,\delta} \cdot \delta + C_{h,0} \tag{4.2}$$

The hinge moment for zero deflection ($C_{h,0}$) equal to zero as it is assumed that no hinge moment is generated at zero deflection. The coefficients relating to the angle of attack ($C_{h,\alpha}$) and control surface deflection ($C_{h,\delta}$) can be determined with the control surface width to depth ratio (λ_{cs}) [51].

$$\lambda_{cs} = \frac{c_{cs}}{c_{mean\ chord}} \tag{4.3}$$

c_{cs} is the mean control surface width and $c_{mean\ chord}$ is the mean chord length.

$$C_{h,\alpha} = -\frac{1}{\lambda_{cs}^2} \cdot [(3 - 2\lambda_{cs}) \cdot \sqrt{\lambda_{cs} - \lambda_{cs}^2} - (3 - 4\lambda_{cs}^2) \cdot asin\sqrt{\lambda_{cs}}] \tag{4.4}$$

$$C_{h,\delta} = -\frac{4}{\pi}\left(\frac{1 - \lambda_{cs}}{\lambda_{cs}}\right)^{\left(\frac{3}{2}\right)} \cdot [asin\sqrt{\lambda_{cs}} - asin\sqrt{\lambda_{cs} - \lambda_{cs}^2}] \tag{4.5}$$

This method was also implemented by Lammering [15] for determining maximum required power for control. The actuation force for the control surface can be determined based on the hinge moment. The critical conditions of control are checked by varying the control surface deflection and the angle of attack. The actuation force and the required number of actuators per control surface lead to the actuation force required per actuator. With the system pressure and the required force per actuator, the piston diameter can be determined with pascals law. Based on the control surface dimensions, maximum deflection and the hinge fraction, the stroke of the actuator can be determined with basic trigonometry. The diameter and lengths of the rod, cylinder, base, head and valve block are determined based on relations derived from existing actuator models [30] relating the piston diameter and actuator stroke to these parameters. Similar methods are proposed by Frischemeier [21], relating geometric parameters to physical parameters. The actuator mass is determined based on the force to mass ratio of the actuator also known as the ”figure of merit”. With certain subsystem specific parameters such as the output velocity, the peak and maximum deflection rates, the actuator efficiencies and the usage fractions, the actuator power consumption is also determined with energy equivalence methods proposed by Chakraborty [16].

4.2.2. Electro hydrostatic actuator

The EHA is idealised an assembly of nine components constituting the cylinder, rod, head, base, accumulator, valve block, electric motor, pump and power electronics module. These components can be seen in Figure 4.3. The hydraulic cylinder, rod, head and base are parametrised similar to the hydraulic actuator presented in the previous subsection. The accumulator, valve block, pump and electric motor are parametrised with two dimensions each, length and diameter. The power electronics module is idealised as a cuboid, parametrised by length, width and thickness. Similarly, all the components, besides the power electronics will be modelled as cylinders. Similar to the electro hydraulic actuator, first the piston diameter and the actuator stroke are determined with physics based methods relating the control requirements, system pressure and control surface parameters to the piston area and actuator

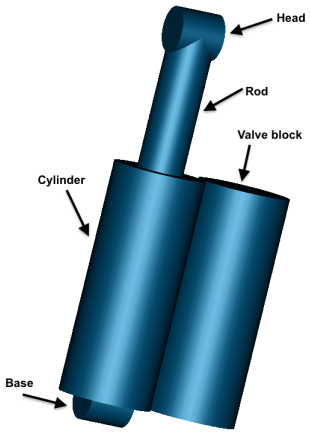

Figure 4.1: Electro hydraulic actuator parametric model

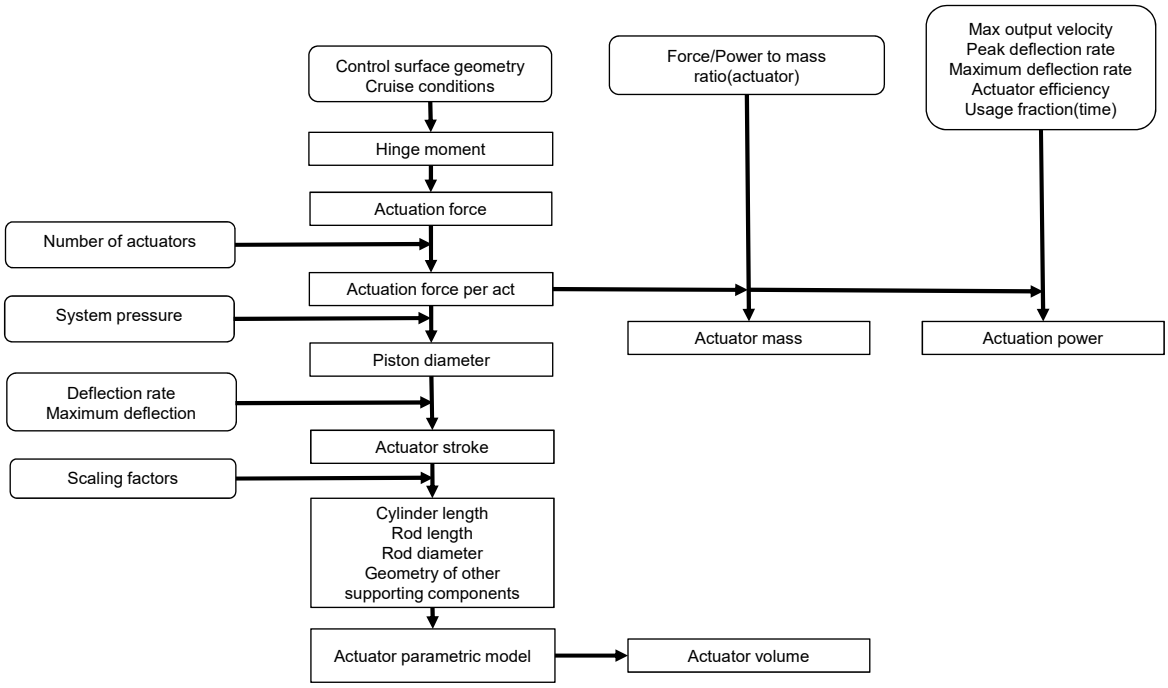

Figure 4.2: Electro hydraulic actuator and EHA sizing

stroke. Successively, the parameters of the remaining components are sized as a functions of these two parameters with empirical relations derived from literature. A similar EHA model was considered by Manjulury et.al [4] for sizing the flight control actuators with a KBE methodology. The sizing methods are similar to those proposed by Frischemeier [21].

4.2.3. Electro mechanical actuator

The EMA constitutes five components, namely, the cylinder, rod, head, base and electric motor. The assembly is presented in Figure 4.4. All the components are parametrised as cylinders with diameter and length (or thickness), similar to the components of the subsystems discussed in the previous sections. The sizing of EMA is slightly different from the electro hydraulic actuator and EHA sizing in a way that scaling factors are used from an early stage. The dependency is presented in Figure 4.5. The difference in the approach is due to the elimination of hydraulics for EMA. With the required force and the actuator stroke determined, the parameters of the components are determined with scaling factors relating the physical parameters to the component dimensions. Firstly, a scaling ratio (x^*) is defined for

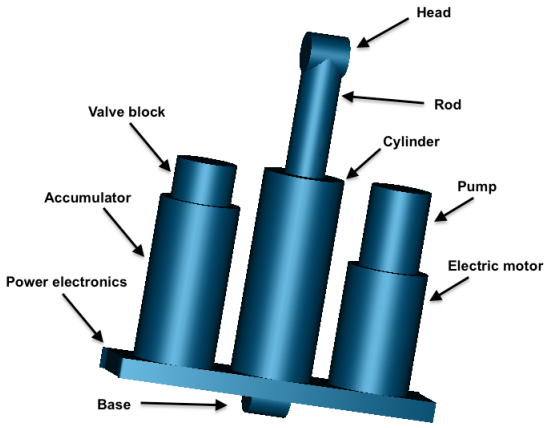

Figure 4.3: Electro hydraulic actuator parametric model

each parameter which relates the required parameter (x) to a reference value of the parameter (x_{ref}). Similar methods were implemented by Munjulury et. al [4] for the EMA sizing with a KBE methodology.

$$x^* = \frac{x}{x_{ref}} \tag{4.6}$$

To attain geometric similarity when scaling, the geometric proportions are kept constant. The dimension variations of all the parameters can be determined with the generic length variation parameter l^*. The variation of a cylinder radius can be given by

$$r^* = l^* \tag{4.7}$$

Mechanical components designed with a fixed constraint such as the maximum allowable stress (σ_{max}) enable relating the transmitted force scaling fraction (F^*) to the length scaling fraction (l^*)

$$F^* = l^{*3} \tag{4.8}$$

With this method, various estimation models proposed by Budinger et. al [52] were implemented to determine the dimensions of each of the components of the EMA. The mass and power consumption of the actuator are determined with semi-physics based methods which are functions of various subsystem specific parameters such as the mechanical efficiencies, actuation velocities, state of the art, etc. proposed by Chakraborty [16].

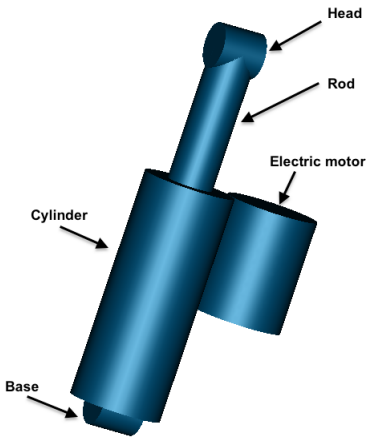

Figure 4.4: Electro mechanical actuator parametric model

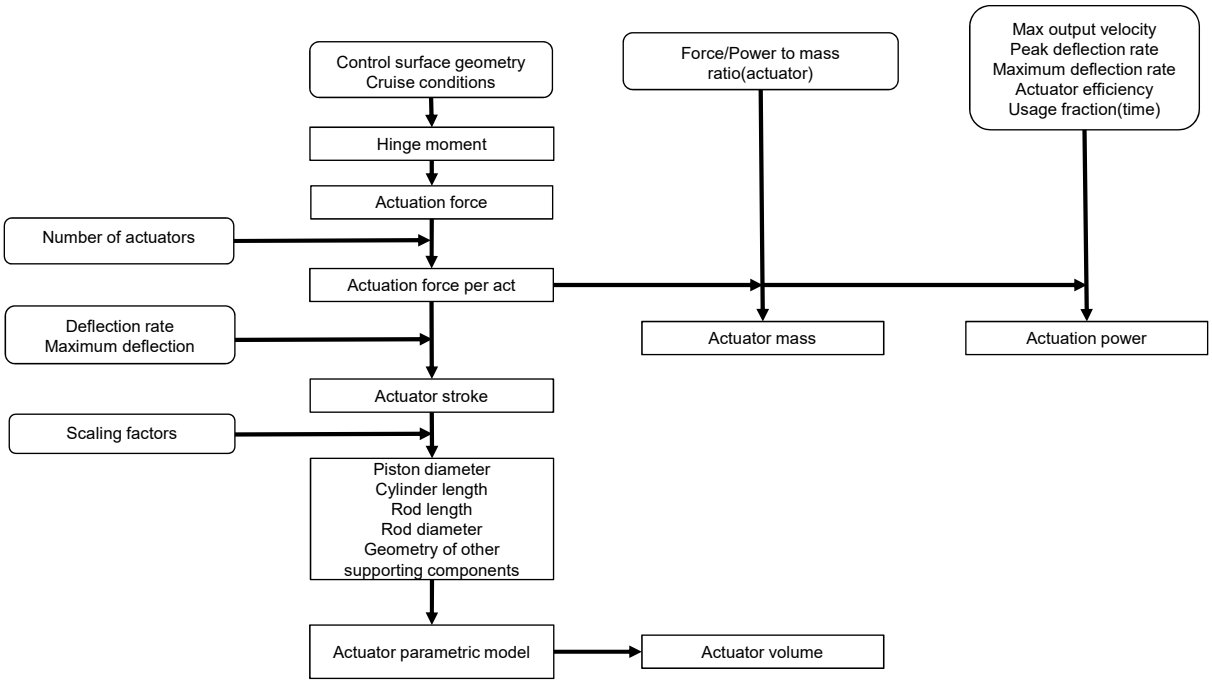

Figure 4.5: EMA sizing dependency

4.2.4. Actuator positioning

The actuators are positioned in the airframe based on the data extracted from the parametric model of the aircraft. A diagram which represents in brief, the parameter dependency for actuator positioning is presented in Figure 4.6. The control surfaces include the ailerons, elevators, rudder, spoilers, flaps, slats and the horizontal stabilizer. With the control surface dimensions along with their position and orientation in the airframe [1], the actuators are positioned and oriented for each of the control surface in the airframe based on the positioning architecture. Two positioning architectures are implemented, based on the number of actuators required per control surface. If a control surface requires a single actuator, the actuator would be positioned at the center of the control surface. However, for a higher number of actuators, the actuators would be placed at equidistant points along the span of the control surface.

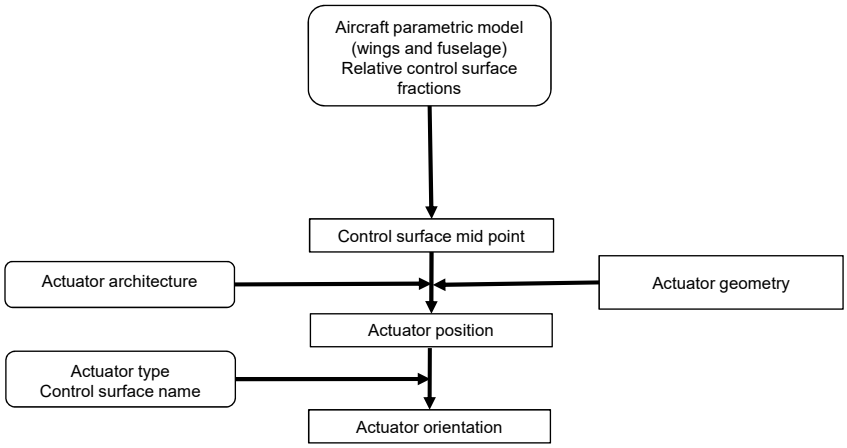

Figure 4.6: Actuators positioning

[1]This data is available in the CPACS file with the aircraft parametric model

4.3. Fuel tanks

Modern medium and long range transport aircraft store their fuel in the wing between the structure (wet wings) and in tanks inside the fuselage. These constitute the wing fuel tanks, fuselage fuel tanks and the empennage fuel tanks [53]. The sizing process of the fuel tanks has already been presented in Chapter 3. The parametrisation of each of these tanks and the binding limits for sizing are presented in the following subsections.

4.3.1. Wing and empennage fuel tanks

The wing fuel tanks tanks are bound by the front spar, rear spar, tank end ribs , upper skin and lower skin. Hence, only four parameters are required a to generate a wing fuel tank, namely, start fraction, end fraction , front spar fraction and rear spar fraction. The start and end fractions are the fractions relative to the wing semi-span [2] from the fuselage surface. The front spar and rear spar fractions are fractions of the front spar and rear spar positions relative to the local wing chord from the leading edge of the wing. These bounds are presented in Figure 4.7.

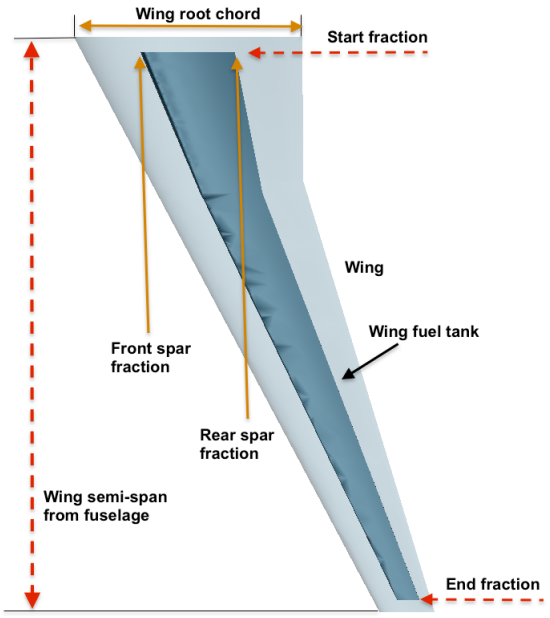

Figure 4.7: Wing fuel tank parametrisation

4.3.2. Fuselage fuel tanks

The fuselage fuel tank is modelled as a cuboid and hence parametrised by length, breadth and height as presented is Figure 4.8. This fuel tank can be positioned anywhere along the length of the fuselage with the input defined by the fraction of the fuselage length, from the nose of the fuselage. The width, height and length of the fuselage tank are determined based on the width to diameter fraction, height to diameter fraction and the length to length fraction. The width to diameter fraction is the fraction of the tank width relative to the fuselage diameter, similarly the with to length fraction is the maximum length of the tank as a fraction of the fuselage length.

4.3.3. Fuel tanks sizing

The overall sizing rules of the fuel tanks are summarised with parameter dependencies in Figure 4.9. With the wing and fuselage parametric models and the required fuel mass, the fuel tanks are first sized in an iterative manner and oriented in the airframe. The fuel tanks are parametrised as hollow models, hence thickness is specified as well. With the parametric models, volumes such as the fuel tank occupying volume and fuel tank material volume are determined. This leads to calculating the the fuel

[2] HTP semi-span for empennage fuel tank

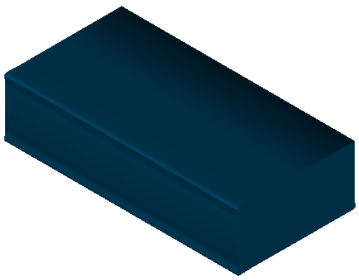

Figure 4.8: Fuselage fuel tank parametric model

volume capable based on the required fuel fill fraction; which is a fraction of the tank overall volume that needs to be filled with fuel with considerations for inerting, internal structure and component volumes. With the fuel density, the fuel mass capable is determined. Similarly, the fuel tank mass is determined based on the fuel tank material density.

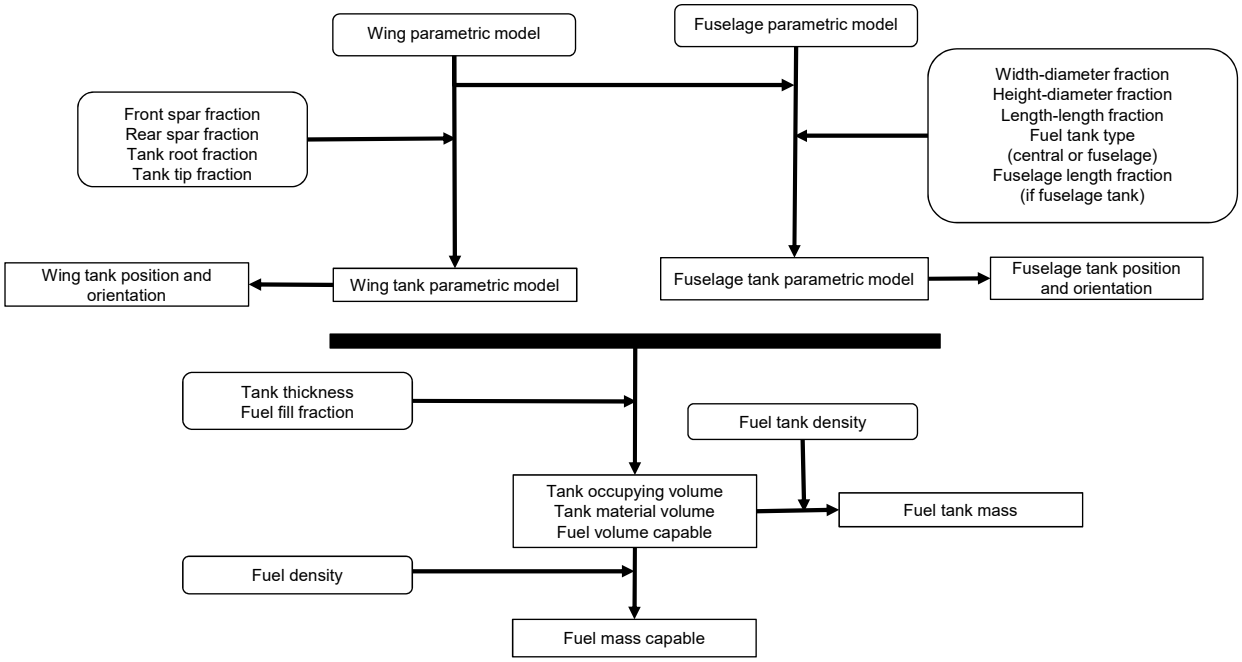

Figure 4.9: Fuel tanks sizing

4.4. Anti-ice elements

Ice accumulation on the lifting surfaces not only leads to an increase in the mass but also changes the wing profile due to its presence. This results in an increase in mass and flow separation on the wing, leading to an overall decrease in lift. The dangers of this effect vary from slight performance decrease to wing stall, leading to fatal accidents. Anti-ice elements are responsible for preventing the ice accumulation on the aircraft wing. Thermal anti-ice elements heat the wing to a certain temperature to prevent the formation of ice. This heat is generated by different means. A conventional hot-air anti-ice system consists of tubes called ”piccolo tubes” running along the leading edge of the wing. The high temperature bleed-air from the engine is diverted to the piccolo tubes which results in heating the wing surface through conduction (or convection) and radiation. In recent years, electro-thermal anti-ice elements have been introduced which generate this heat by electricity, thus eliminating the necessity for bleed-air extraction from engines. These constitute thin strips placed on the leading edge of the wing, thus form an integral part of the wing. However, electro thermal anti-ice elements lead

to an increase in wing drag due to the interference between the wing surface and the element. The parametrisation and sizing rules of the hot-air anti-ice element and the electro-thermal heating strip are presented in the following subsections.

4.4.1. Hot-air anti-ice elements

The piccolo tubes for ice elimination are modelled as tubes. Hence, they are parametrised with outer diameter, thickness and length. The sizing methodology is similar to actuators, relating subsystem specific and top level parameters to the geometry. The parameters dependency for sizing is presented in Figure 4.10. With the wing parametric model and the conditions at cruise, the required area of protection, length of protection and the start and end fractions of the element as a function of the wing semi-span are determined based on energy equivalence methods [16]. The span-wise extent of the protection is most influenced by the mean aerodynamic chord (c_{mac}) of the wing, according to a study carried out by Airbus, cited by Chakraborty [16] and Liscout-Hanke [54]. A linear relationship between the c_{mac} and the extent of protection was derived by Liscout-Hanke based on the study. This study included different civil transport aircraft, ranging from short-medium range aircraft such as the Airbus A320, Boeing 737, to medium-long range aircraft such as the Boeing 767, Airbus A330, Boeing 757, Boeing 777, Boeing 787 and the Airbus A380. Chakraborty [16] however, derived the following equation; a linear and a quadratic relationship between the variables based on the same study.

$$EOP = k_0 + k_1 \cdot c_{mac} + k_2 \cdot {c_{mac}}^2 \tag{4.9}$$

"EOP" is the fraction of the wing semi-span to be protected, and "k_0", "k_2" and "k_3" are constants. Successively, with the chord of the slat and scaling factors derived from literature ([22],[23],[24]), relating diameter of the piccolo tube to the slat chord, the root diameter of the tube is determined by the scaling factor method. The diameter of the tube (dia_{pic}) is proportional to the area of protection ($Area_{protection}$) as the wing is heated by the tube, which is in turn heated by convection with the bleed-air.

$$dia_{pic} \propto Area_{protection} \tag{4.10}$$

The area of protection, is a function of the local chord of the slat (C_{slat}). Hence, it can be assumed that the diameter of the tube is proportional to the local chord of the slat and that their ratio is a constant (k^*). With these relations, the diameter of the piccolo tube can be determined based on the local chord of the slat, and the slat chord and reference diameter of the reference model. The diameter of the tube tip is determined based on the wing taper ratio. The cross-section of the tube in the slat in presented in Figure 4.12. In a similar way, the position of the element from the leading edge (d_{pic}) of the slat is determined as well.

$$Area_{protection} \propto C_{slat} \tag{4.11}$$

$$dia_{pic} \propto C_{slat} \tag{4.12}$$

$$\frac{dia_{pic}}{C_{slat}} = k^* \tag{4.13}$$

$$\frac{dia_{pic\ ref}}{C_{slat\ ref}} = k^* \tag{4.14}$$

$$dia_{pic} = \frac{dia_{pic\ ref}}{C_{slat\ ref}} \cdot C_{slat} \tag{4.15}$$

The presented sizing methodology is similar to the scaling fractions methodology presented in the actuators sizing subsection. With the parametric model, thickness and material density, the occupying volume and the mass of the piccolo tubes are determined. With the subsystem specific parameters such as the available supply temperature, time fraction of usage and overall efficiencies, the power consumption of the anti-ice system can be determined with semi-physics based methods [16]. The parametric model of the piccolo tubes in the airframe is presented in Figure 4.11. Due to the method's

high dependency on the reference parameters, the diameter and position of the piccolo tube are highly sensitive to the scaling ratios. A sensitivity analysis with these parameters is presented in Chapter 5. In spite of the limitations, this method can be considered as a starting point for the hot-air anti ice element parametric sizing in the absence of a practical physics-based method for the initial design stages.

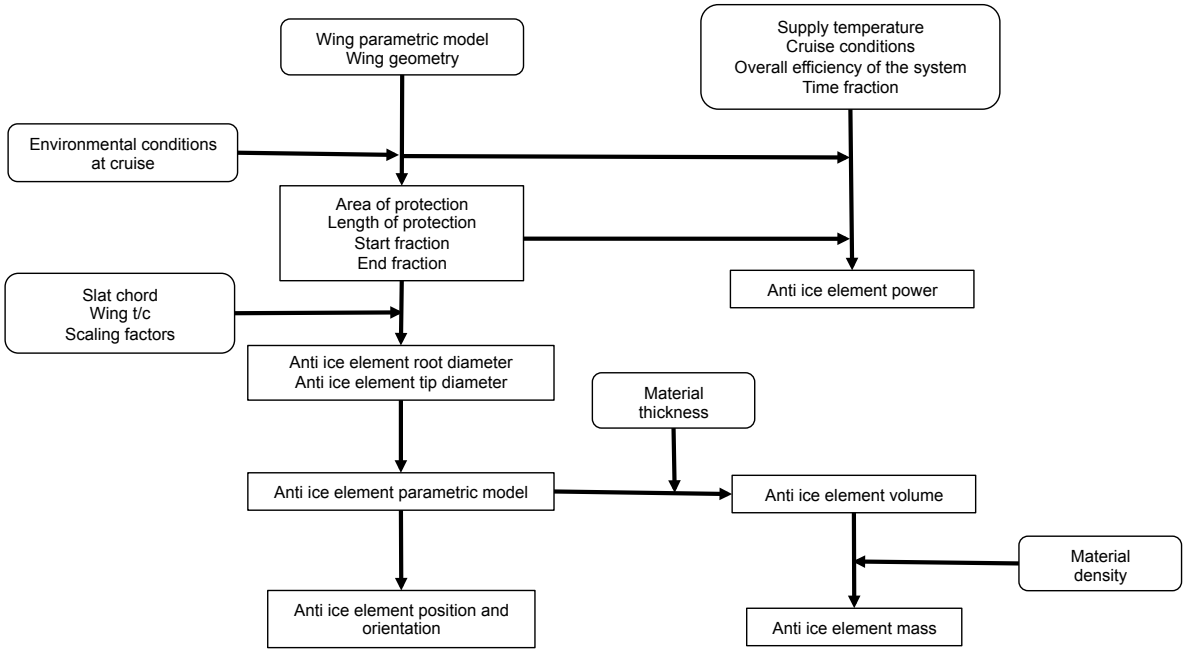

Figure 4.10: Hot-air anti-ice element sizing

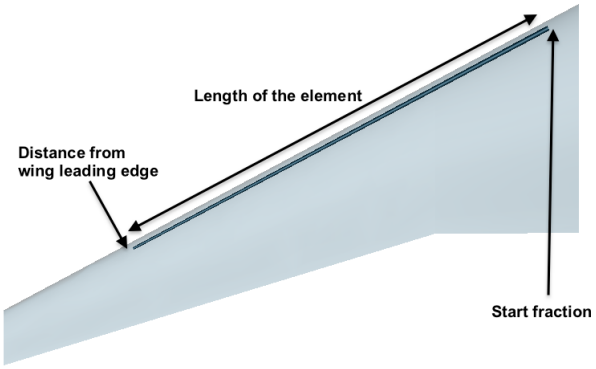

Figure 4.11: Hot-air anti-ice element parametric model

4.4.2. Electro-thermal anti-ice elements

Electro-thermal anti-ice elements are parametrised as thin strips running along the leading edge of the wing. As the profile of these strips needs to be similar to the wing leading edge, they are sized in a similar fashion to the wing fuel tanks, by duplicating the wing parametric model and manipulating the airfoil profile as per the requirements of start fraction, end fraction, upper surface fraction and lower surface fraction. These parameters are determined in a way similar to the hot-air anti ice elements, presented in the previous subsection. The parametric model of the electro-thermal anti-ice element in the airframe is presented in Figure 4.13. Similarly, the mass of the models is determined with the parametric model, thickness and the material density. The power consumption is determined with similar semi-physics based methods from literature [16] with a focus on electrification of the subsystem.

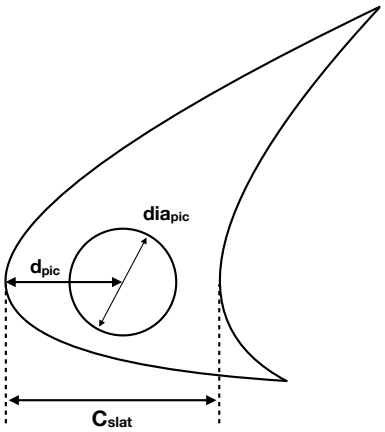

Figure 4.12: Cross-section of the hot-air anti-ice element in the slat

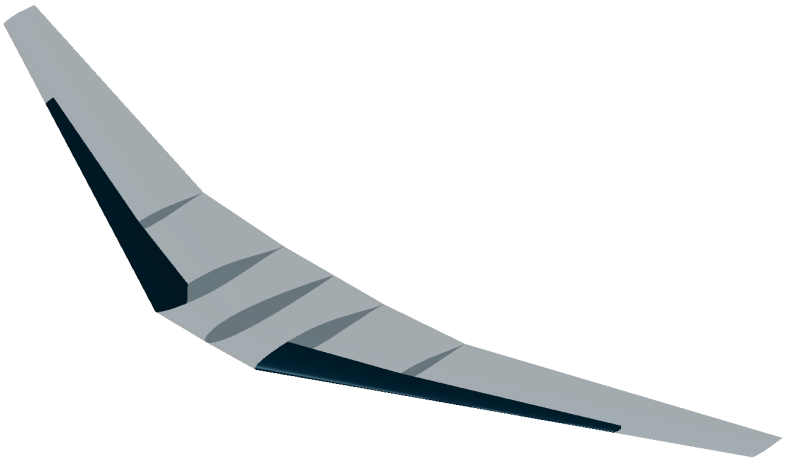

Figure 4.13: Electro-thermal anti-ice element parametric model

4.5. Chapter summary

In this chapter, the parametrisation of the subsystems along with the rules which enable sizing of these subsystems from the aircraft and subsystem level parameters are presented and explained in detail. The subsystem models enable the creation and analysis of different architectures such as an MEA subsystems architecture or different fuel tank configurations. With the fuel tanks and anti-ice elements, due to the inclusion of material density and thickness, impact of different materials can be assessed as well on an overall aircraft level from perspectives of mass and volume. Most of the methods used are semi-physic based methods which are relatively more accurate than the empirical methods. The scaling factor methodology is partly empirical as well, leading to inaccuracies of predictions. One such parameter is the hinge moment, which in reality is highly sensitive to the mission segment, usage fraction and the three dimensional control surface data. The assumptions made to simplify these co-relations is a result of in-availability of other parameters of design at the initial stages [3]. However, this limitation can be worked around by determining exactly how much the result would deviate for an estimated deviation in the input, i.e. with a sensitivity analysis. Moreover, the results can also be validated against literature to determine if the theory supports the results. The validation and sensitivity analysis of the models for this purpose, from a subsystem, system and aircraft level are presented in the following chapter.

[3] An input slot for hinge moment is also defined where the user can specify the hinge moment of the control surface from literature or by implementing higher fidelity methods.

5

Validation and sensitivity analyses

5.1. Introduction

The sizing rules and the parametrisation of the subsystems are presented in the previous chapter with a focus on the methods implemented. The possibilities of errors due to the implemented methods was also addressed. Validating the subsystem models ensures that the results are in strong agreement with the theory and literature. Sensitivity analysis serves a two fold purpose. Firstly, the methods can be verified by observing the trends in the results and any anomalies found can be tracked to the root cause to determine if it is an error in translation of theory or an effect that is observed at the extremes. Secondly, the sensitivities of the results, such as the volume, mass and power consumption against the input parameters can be assessed. This provides knowledge on the estimated deviation of the results for an estimated range of the input parameter, thus enabling to determine the parameters that cause the highest influence on the design. The sensitivity analysis as a part of this thesis is performed at the subsystem (Section 5.2), system (Section 5.3) and aircraft level (Section 5.4). At the subsystem and system level, subsystem specific parameters are varied and at the aircraft level, wing and fuselage geometric parameters are varied and the trends against the results are observed. A configuration similar to the Airbus A320-200 was chosen for the validation and sensitivity analysis studies. The reference actuator models at subsystem level are of the aileron.

5.2. Subsystem level

The sensitivity analysis of the electro hydraulic actuator volume, with certain subsystem specific parameters is presented in Figure 5.1. The varied input parameters are the hinge fraction[1], control surface deflection angle, system pressure, gearing ratio, hinge moment and the control surface chord. Ever parameter specified above is kept constant besides the parameter that is varied. The parameters are varied to the extremes to determine the variation in the result and validate it with the considered theory or literature. Hinge moment in the tool is calculated by the method presented in Section 4.2.1. However, as the fidelity of this methodology is low, for the sensitivity analysis, the hinge moment is assumed as an input and is varied about a certain range. This approach is considered with an outlook to replace the current hinge moment calculation method by higher fidelity methods with external tools in successive research. It is observed from the figure that an increase in any of the parameters besides the system pressure leads to an increase in the overall volume. A higher hinge fraction requires a longer rod, while higher deflection angle, gearing ratio and hinge moment would result in a higher force requirement. To achieve this higher force with at a constant system pressure, a higher diameter of the piston and cylinder is required (area based on pascals law). This reasons the higher increase in volume. However, increasing the system pressure would generate the same force at a lower diameter, which explains the inverse proportionality. The trends are in well agreement with the theory presented in Chapter 4 and with literature [30]. The quantitative changes are tabulated in Table 5.1. The hinge fraction has the highest influence, with every 1% variation, the volume varies by 1%. Gearing ratio has the least influence. Increasing the system pressure by 1% would decrease the actuator volume

[1] Fraction of the control surface chord where the actuator hinge would be placed.

by nearly 0.5%. Thus, a low gearing ratio and high system pressure are ideal for a minimal actuator volume.

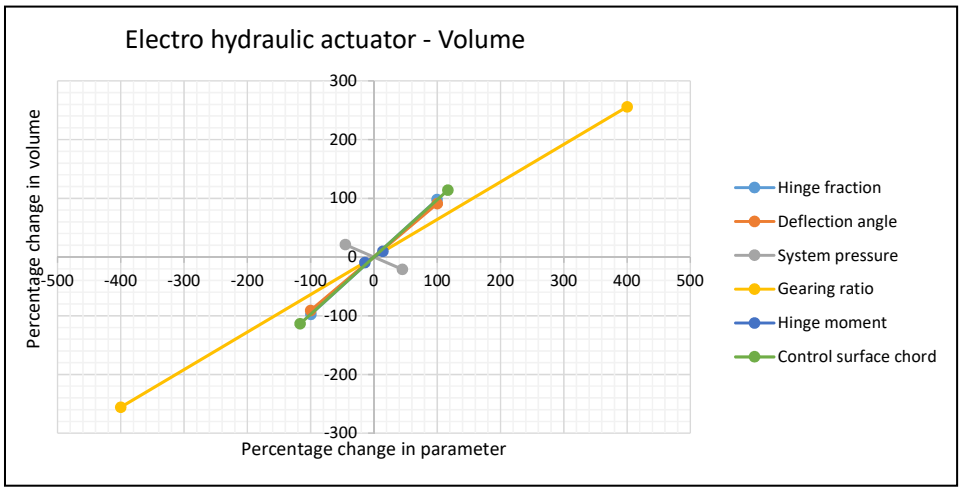

Figure 5.1: Sensitivity of the electro hydraulic actuator volume with the subsystem level parameters

Variable	Variation in variable	Variation in volume
Hinge fraction	0.1 (20%)	20%
Gearing ratio	0.5 (16.6%)	10.6%
System pressure	1 MPa (4.8%)	-2.2%
Deflection angle	1° (3.3%)	3%
Hinge moment	100 Nm (2.85%)	2%
Control surface chord	0.1 m (16.6%)	16.2%

Table 5.1: Percentage variation of the electro hydraulic actuator volume with the subsystem level parameters

The parameters of the wing fuel tank are varied as well to assess the overall influence. The start fraction, end fraction, fill fraction, front spar fraction and rear spar fraction are varied and the influence on the fuel tank occupying volume is studied from the observations presented in Figure 5.2. The quantitative values are presented in Table 5.2. It is observed that the volume of tank decreases by 3.7% with increase in start fraction by 0.001, which is nearly 10%. Similarly, the volume of tank increases by 0.63% with an end fraction increase of 0.001, around 1%. This is in well agreement with theory as the wing has higher volume at the root relative to the tip. Similarly the Front spar fraction has a higher influence relative to the rear spar fraction. Though the trends are quite straight forward, the ability to generate this quantified knowledge would aid in fuel tank sizing decisions while designing novel aircraft configurations. Similar sensitivity studies were performed for other parameters such as the fuel tank mass and fuel mass capable (Appendix B) and the results enabled the tool verification, besides validation.

Variable	Variation in variable	Variation in volume
Start fraction	0.01 (10%)	-3.7%
End fraction	0.01 (1.17%)	0.63%
Front spar fraction	0.01 (3%)	-3.2%
Rear spar fraction	0.01 (1.43%)	2%

Table 5.2: Percentage variation of the wing fuel tank volume with the subsystem level parameters

The sizing of the hot-air anti ice element is based on the sizing factors determined with the reference parameters considered for the tube diameter. These constitute the reference tube diameter and

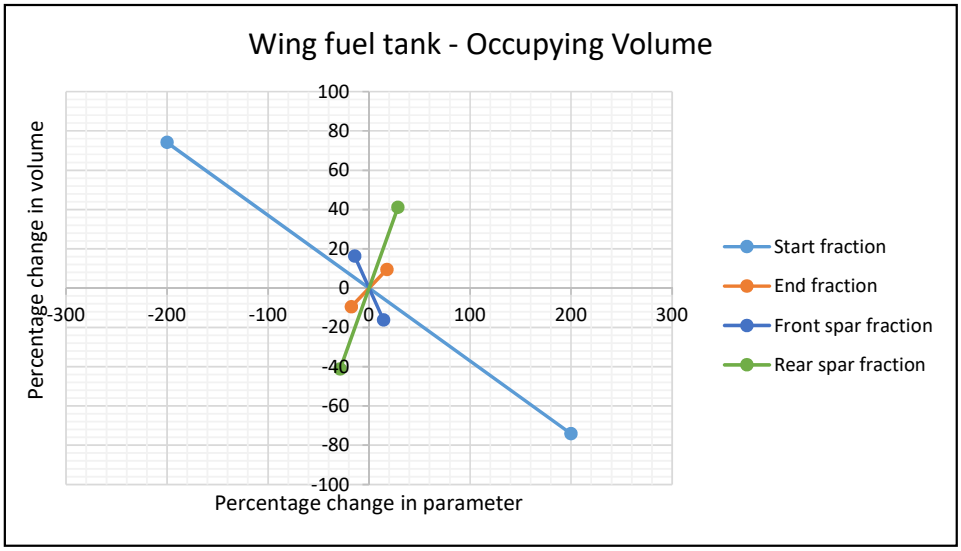

Figure 5.2: Sensitivity of the wing fuel tank volume with the subsystem level parameters

the reference slat chord. The variation of volume with variation of these parameters is presented in Figure 5.3 and the percentage change in values are represented in Table 5.3. It is observed that the volume of the elements is highly sensitive to the reference parameters, with nearly 44% variation of the volume with 0.5cm (12.5%) variation in reference tube diameter. Similarly, the volume decreases by 25% with a 0.5cm (36%) increase in the reference slat chord. Due to the high sensitivity of the parameters and the use of empirical methods. This method can be replaced by physics based methods in successive research, depending on higher number of variables and physics-based functions, thus leading in a more accurate result.

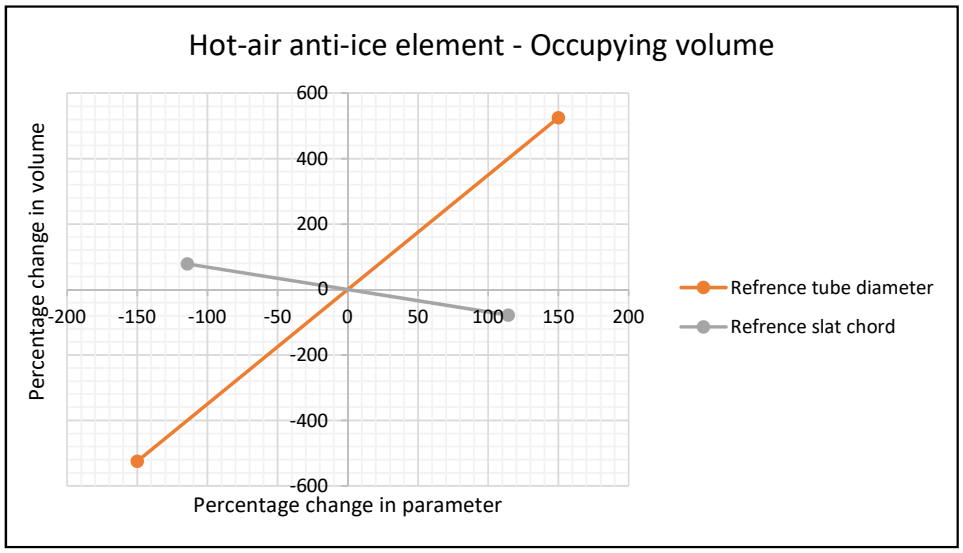

Figure 5.3: Sensitivity of the hot-air anti-ice element volume with the subsystem level parameters

Variable	Variation in variable	Variation in volume
Reference slat chord	0.5 cm (35.7%)	-24.5%
Reference tube diameter	0.5 cm (12.5%)	43.7%

Table 5.3: Percentage variation of the wing fuel tank volume with the subsystem level parameters

5.3. System level

The fuel tanks and the hot-air anti-ice elements are validated against literature for an A320-200 equivalent configuration. The fuel system consists of a central tank and two wing tanks [55], as observed in Figure 5.4a. A similar configuration recreated with SMG is presented in Figure 5.4b. Comparing both the configurations, presented in Table 5.4 it was observed that the fuel mass capability of the wing fuel tanks deviated the maximum by around 6%, though the overall deviation of the fuel mass capable with all the fuel tanks mounted to nearly 4.4%. This deviation is owed to the estimation of the fill fraction, based on the internal volume occupied by the structure, inerting gas and other supporting components.

The anti-ice elements were validated in a similar method with literature [55] and a deviation of around 9% in the occupying volume was observed. The absolute values are presented in Table 5.5. The comparison of the configurations is presented in Figure 5.5. The error is attributed to the sensitivity of the scaling factor methodology implemented for the anti-ice element sizing discussed in the previous section.

The iterative sizing capability of the fuel tanks is verified with a sensitivity analysis by gradually increasing the fuel mass capability requirement. As seen in Figure 5.6, from points 1-2, the tank size initially remains constant in spite of increasing the required capable fuel mass. This is due to minimum requirement of the tank size being larger than the volume required by the capable fuel. The central tank is pre-modelled and hence, the requirements are met for very low values of fuel mass. After a certain limit, it is observed that the fuel tanks' size increase with increasing the required fuel mass, which is a consequence of the iterative sizing. The change in slope of the plot signifies the addition of a fuel tank. At point 2, the wing fuel tank is added and its size is increased in the span-wise direction, till the limit is reached, at point 3. The empennage tank is added at this point and its size, similar to the wing fuel tank is increased till the limit, which is reached at point 4. At this point, the fuselage fuel tank is added and it's length is increased in the direction of the empennage till the limit is reached, as observed at point 5. As all the limits are reached at point 5, the fuel tanks' size no longer increases in spite of increasing the fuel requirement. This is the plateau observed in the plot from points 5-6. The change in the parametric models of the tanks during this sizing process is presented in Appendix A.

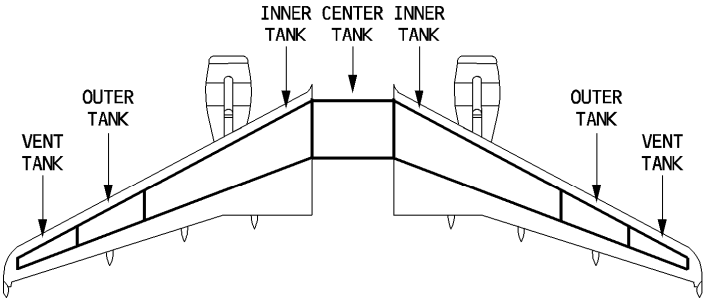

(a) Fuel tanks configuration from literature [55]

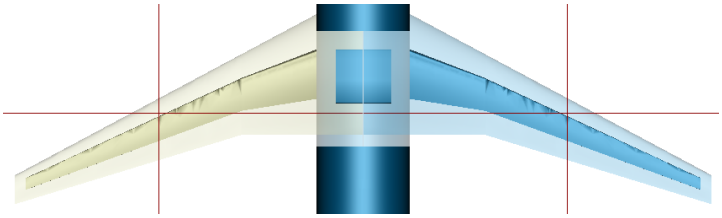

(b) Fuel tanks configuration from SMG

Figure 5.4: Fuel tanks validation

Fuel mass capable (kg)	A320	A320-SMG	Deviation (%)
Central tank	6476	6581	1.62
Wing tanks	12250	12970	5.87
Total	18728	19551	5.39

Table 5.4: Deviation of the fuel tanks' parameters relative to literature

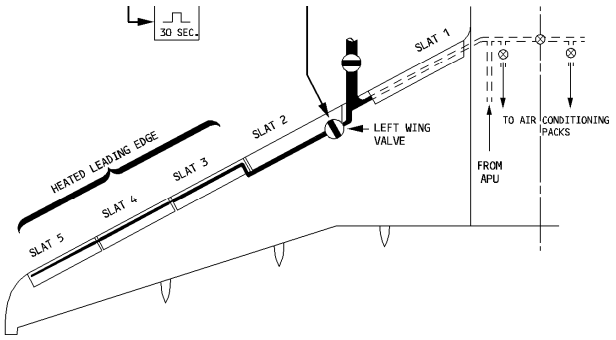

(a) Anti-ice elements configuration from literature [55]

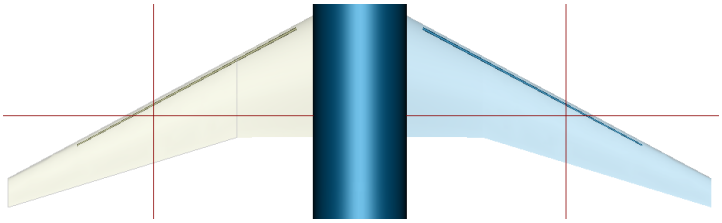

(b) Anti-ice elements configuration from SMG

Figure 5.5: Anti-ice elements validation

Occupying volume (m^3)	A320	A320-SMG	Deviation (%)
Anti-ice element	0.1788	0.1952	9.17

Table 5.5: Deviation of the anti-ice elements' parameters relative to literature

5.4. Aircraft level

At the aircraft level, the wing geometric parameters such as the wing aspect ratio, taper ratio, wing span and fuselage geometric parameters such as the fuselage diameter and the fuselage length are varied. All the stated parameters are kept constant besides the varied parameter for the sensitivity analysis. In the first study, the aspect ratio of the wing is varied from -2.6% to 2.6% from the initial value of 10.3 with the span fixed. The variation of the outputs is presented in Figure 5.7 and tabulated in Table 5.6. The increase of wing aspect ratio with constant span leads to a decrease in the wing reference area and consequently the wing volume decreases as well. This results in an overall airframe volume decrease by 0.5% for every 1% increase in aspect ratio. Due to the decrease in the wing area, the control surface areas decrease as the control surfaces are sized as a fraction of the wing dimensions. This leads to a lower dynamic pressure on the control surfaces, causing a decrease in the hinge moment (Section 4.2.1). The lower hinge moment leads to a decrease in the required actuation forces. The related decrease in actuator volume is 5%, mass and power consumption is 3% per percentage increase of the aspect ratio. The decrease in the wing volume also leads to a decrease in the properties of the anti-ice elements due to the reduced area of protection and of the fuel tanks due to the direct co-relation with the wing volume.

A similar study is conducted by varying the fuselage diameter from -25% to 25% with the baseline at 4.5 m. With every 0.5 m (11%) increase in fuselage diameter, it is observed from Figure 5.8 that the actuator volume increases by 300%, actuator mass and actuator power consumption by nearly

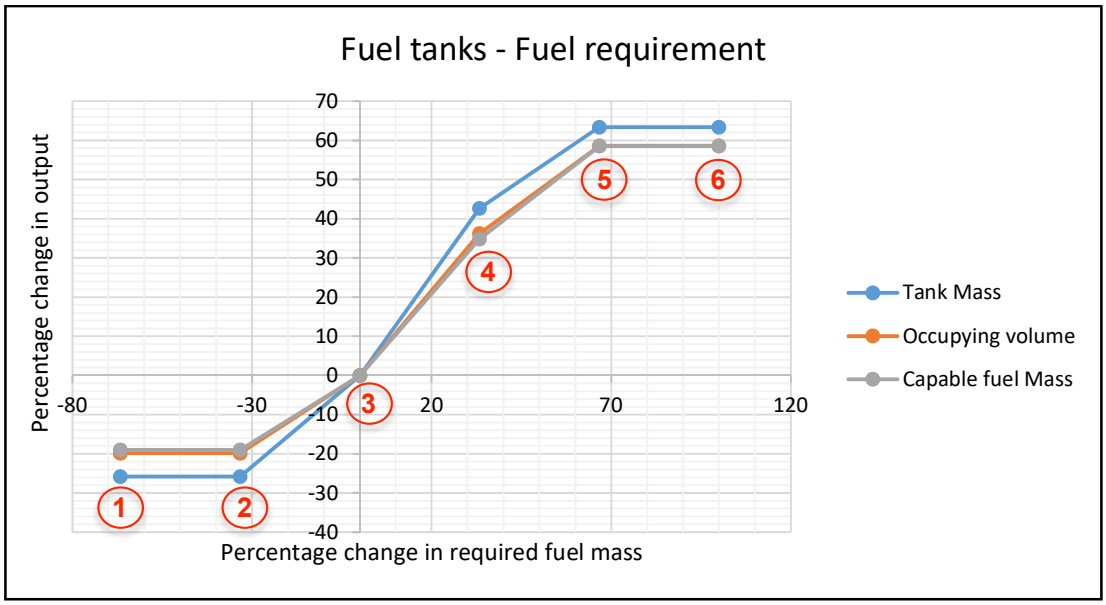

Figure 5.6: Sensitivity analysis of the fuel tank sizing

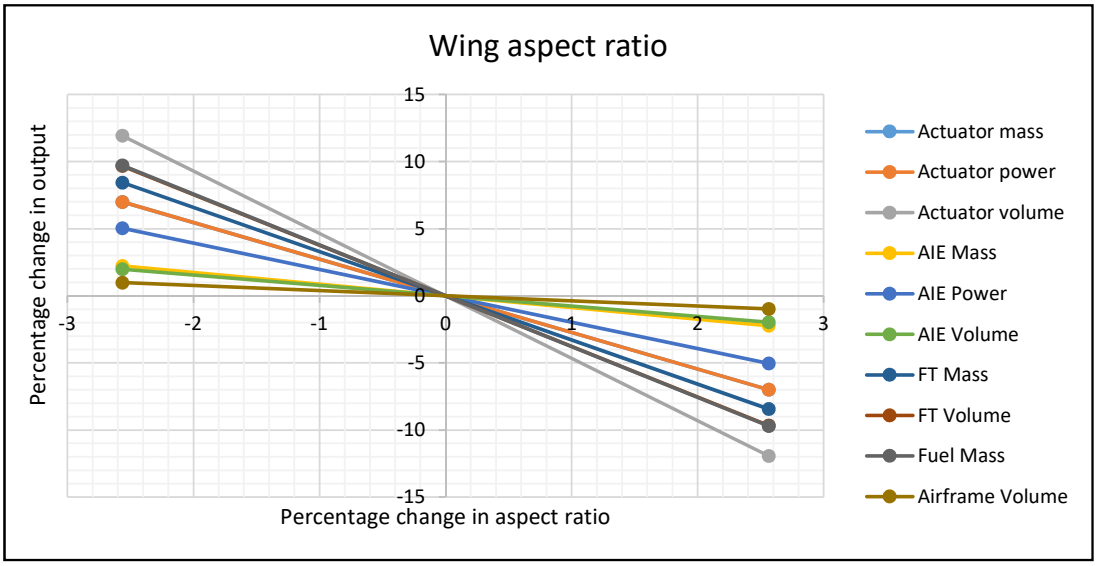

Figure 5.7: Variation of results with wing aspect ratio

90%. The percentage variations of results are presented in Table 5.7. An increase in fuselage diameter leads to an increase in the HTP and Vertical Tail Plane (VTP) geometries, which results in larger control surfaces and so larger actuators. The airframe volume increases by 53% for 11% increase in the fuselage diameter. This is a contribution of the fuselage volume and the increased HTP and VTP volumes. The higher fuselage diameter leads to an increase in the central fuel tank dimensions, thus increasing the capable fuel mass by nearly 9% and the fuel tanks overall volume by 6%. The wing however remains unchanged due to the fixed dimensions, resulting in the constant anti-ice element parameters. It is observed that the actuators are highly sensitive to the change in dimensions of the fuselage due to the snowball effect on the lifting surfaces as a result of the higher structural mass.

Variable	Variation
Actuators mass	-3%
Actuators power	-3%
Actuators volume	-5%
Anti-ice elements mass	-1%
Anti-ice elements power	-2%
Anti-ice elements volume	-1%
Fuel tanks mass	-3.5%
Fuel tanks volume	-4%
Fuel mass capable	-4%
Airframe volume	-0.5%

Table 5.6: Percentage variation of the parameters with 1% (0.1) variation of the aspect ratio

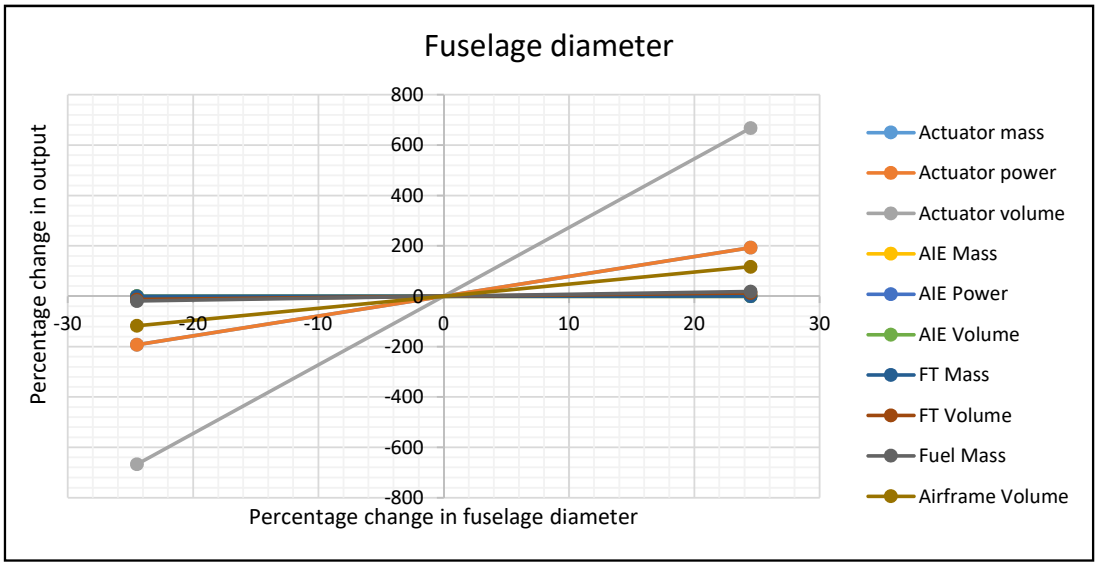

Figure 5.8: Variation of results with fuselage diameter

Variable	Variation
Actuators mass	87%
Actuators power	87%
Actuators volume	300%
Anti-ice elements mass	0%
Anti-ice elements power	0%
Anti-ice elements volume	0%
Fuel tanks mass	0.20%
Fuel tanks volume	6%
Fuel mass capable	9%
Airframe volume	53%

Table 5.7: Percentage variation of the parameters with 11% (0.5m) variation of the fuselage diameter

5.5. Chapter summary

In this chapter, validation and sensitivity analysis of the models at the subsystem, system and aircraft level are presented. The most and the least sensitive parameters at each stage for a specific system or the subsystem and the quantitative influence on the overall parameters is assessed as well. Though only a few models were presented, the sensitivity analysis was performed on all the subsystem models

and the results are presented in Appendix B. The results are observed to be in well agreement with the theory as well. The sensitivity analysis provides an insight into the effects of the input parameters on the results at the subsystem, system and aircraft scale. However, propagating the design knowledge to generate and influence a new design requires integration of supporting domains. This must be initiated by generating a design from scratch with certain top level parameters. This integrated aircraft design process is demonstrated with a case study in the following chapter.

6

Case study

6.1. Introduction

In the previous chapter, the validation and the sensitivity analysis of the subsystem models is presented. In this chapter, a case study with the proposed framework of integrated subsystems sizing with the aircraft, presented in Chapter 3 is demonstrated. TLAR similar to the Airbus A320-200 [56] are considered for the design case as it is one of the most widely used aircraft and literature exists for validation of the results. Two architectures, a conventional systems architecture and an MEA systems architecture are generated for this design with the framework. The description of the case is described in detail in Section 6.2. The design framework and the results at each of the domain are focussed in Section 6.3. To conclude, the chapter is summarised in Section 6.5.

6.2. Case description

The reference aircraft for the case study is a 150 passenger single-class aircraft with a payload of 13,550 kg, equivalent to the Airbus A320-200. For the design mission a range of 2780 NM is considered and the fuselage length and diameter are fixed as 37.57 m and 4.14 m respectively. The wing span of 36.5 m is fixed as well. The systems mass is initially fixed as 12,000 kg, which is later recomputed by supporting higher fidelity tools. The TLAR are specified in Table 6.1. For this aircraft, the following two systems architectures are generated and compared.

1. A conventional systems architecture , all the possible systems are actuated with hydraulic and pneumatic power.
2. An MEA systems architecture in which all the systems are electrified, thus working primarily on only electric power.

6.3. Design framework and results

Overview

The proposed design framework in Chapter 3 is represented as a Design Structure Matrix (DSM) presented in Figure 6.1 with the specific inputs and outputs of each domain. With the TLAR specified in Table 6.1, an initial design is generated by VAMPZero. This design is propagated to SSM for the subsystems selection and sizing. In this domain, the subsystems are selected and sized based on the subsystem specific requirements. The major outputs from this domain include the systems' mass, systems' power consumption. This updates the OEM and the MTOM of the design. The updated design is propagated to SMG for parametric sizing of the subsystems. The subsystems are resized based on the volume allocation requirements. The mass and power consumption of the subsystems are also computed besides the parametric models and their volumes. The systems mass, systems power consumption, OEM and MTOM are updated based on these computations. The design is propagated to EMM which sizes and simulates the engine to provide thrust and enable required power off-takes. The sized engine is simulated to determine the performance maps at each mach number, altitude and thrust

Parameter	Value
Performance	
Range (NM)	2,780
Masses	
Payload (kg)	13,550
Systems (kg)	12,000
Fuselage	
Length (m)	37.57
Diameter (m)	4.14
Wing	
Span (m)	36.5
Aspect ratio ($-$)	10.3
Taper ratio ($-$)	0.24
Sweep (qc) (deg)	25

Table 6.1: TLAR of the design aircraft

level for the mission. This design is propagated to FSMS. Based on the overall masses, aerodynamic parameters and the engine performance maps, FSMS simulates the aircraft for the mission and determines the fuel mass. Thus, the MTOM is updated. This design is not yet converged as the first mass of systems provided to VAMPZero is a guess value. Thus, the design is propagated to the converger which stores the MTOM. The systems mass computed by SSM and SMG is propagated to VAMPZero to restart the sizing process once again. The cycle continues till two consecutive values of MTOM received by the converger differ within the specified tolerance. In this thesis, the specified tolerance is 0.1. The normalised convergence of certain major parameters of the conventional architecture are presented in Table 6.2 and Figure 6.2. Due to the high tolerance value specified, the design converges within five iterations. The convergence data of the major parameters for the MEA systems architecture is presented in Table C.1 and Figure C.1. For a clear understanding of the generation and propagation of the parameters through the domains the parameters of the pre-final iteration (iteration-4) through different domains are discussed from this point on throughout this chapter.

Iteration	Msys	OEM	Mfuel	MTOM	Unit
1	12,111	40,628	19,527	73,705	kg
2	12,132	40,643	19,538	73,731	kg
3	12,147	40,654	19,547	73,751	kg
4	12,155	40,660	19,551	73,761	kg
5	12,155	40,660	19,551	73,761	kg

Table 6.2: Change in parameters of conventional systems architecture with iteration

VAMPZero

In the initial run, based on the Top Level Aircraft Requirements (TLAR) (Table 6.1), the design is initialized by VAMPZero. At this stage, the methods are not sensitive to the systems architecture, hence the same geometry is generated for both the architectures as observed in Table 6.3. This updates the aircraft parametric model (Figure 6.3), geometric parameters (Table 6.3), aircraft masses , propulsion and aerodynamic parameters to the CPACS file. In successive iterations, the systems mass is replaced by the values computed by higher fidelity methods; SSM and SMG in the preceding iteration. Hence, the masses are sensitive to the systems architecture from the second iteration. In the fourth iteration (after which the design converges), the OEM is computed as 40,654 kg, capable fuel mass as 19,547 kg and MTOM as 73,751 kg for the conventional systems architecture. Similarly, the OEM is computed as 42,110 kg, capable fuel mass as 19,096 kg and MTOM as 74,756 kg for the MEA systems architecture. The parameters and the relative deviations are presented in Table 6.4. All the parameters are propagated to the SSM, SMG and FSMS, while only the required thrust is propagated to EMM for engine sizing and simulation.

Converger					
	VAMPZero	➢ Aircraft parametric model ➢ Aircraft geometry ➢ Masses- (MTOM, MOEM, Mfuel) ➢ Maximum thrust	➢ Aircraft parametric model ➢ Aircraft geometry ➢ Masses- (MTOM, MOEM, Mfuel)	➢ Maximum thrust	➢ Aircraft parametric model ➢ Aerodynamic performance map – CL vs Alpha, CD vs Alpha ➢ Masses- (MTOM, MOEM, Mfuel)
		SSM	➢ Systems' masses (Msys) ➢ Systems' power consumption (Psys)		
➢ MOEM* (Msys*)			SMG	➢ Subsystems' masses ➢ Subsystems' power consumption ➢ Msys* ➢ Psys*	➢ MOEM* (Msys*)
				EMM	➢ Engine performance map – Fuel flow rate – Mission point
➢ MTOM* (Mfuel*)					FSMS

Figure 6.1: DSM of the framework with propagation of parameters to different disciplines

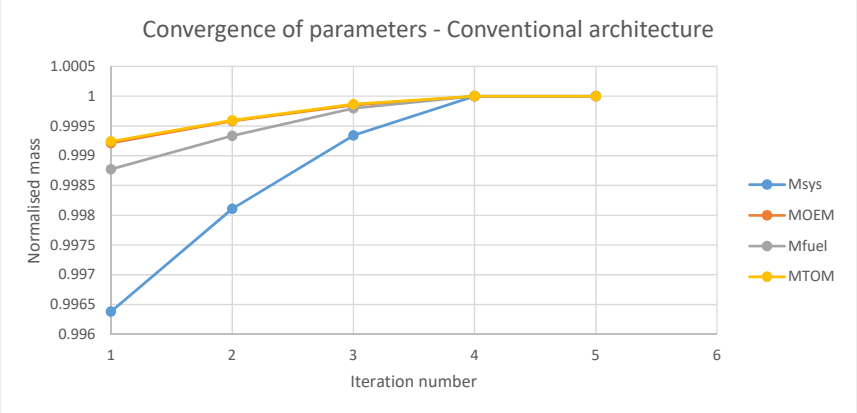

Figure 6.2: Normalised convergence of the major parameters of the conventional systems architecture

SSM

With the parameters from VAMPZero, systems architecture requirements and system specific parameters from the input, the systems architecture is set and the respective mass and power consumption of the systems is computed by SSM. A brief introduction to SSM and the sizing dependencies of each system are presented in Subsection 3.5.2. The higher fidelity methods at this stage are sensitive to the systems architecture. In the conventional systems architecture, the Flight Control System (FCS) and the Landing Gear System (LGS) are actuated with hydraulic power while the Environmental Control System (ECS) and Anti-Ice System (AIS) are actuated with bleed-air from the engines. In the MEA systems architecture, all the systems are electrified. The relative differences of the MEA systems' mass

[1]Percentage change of MEA systems architecture, relative to conventional systems architecture with SSM

Parameter	Conventional and MEA (VAMPZero)	Conventional (Literature [56])
Fuselage		
Length (m)	37.57	37.57
Diameter (m)	4.14	3.95
Wing		
Span (m)	36.50	35.80
Aspect ratio $(-)$	10.30	10.30
Taper ratio $(-)$	0.24	0.24
Sweep (qc) (deg)	25	25
Area (m^2)	129	124
VTP		
Height (m)	6.64	6.26
Aspect ratio $(-)$	1.71	1.82
Taper ratio $(-)$	0.35	0.26
Sweep (qc) (deg)	30	34
Area (m^2)	26	21.5
HTP		
Span (m)	14.21	12.40
Aspect ratio $(-)$	5.15	5
Taper ratio $(-)$	0.30	0.26
Sweep (qc) (deg)	30	29
Area (m^2)	39	31

Table 6.3: Key parameters of the aircraft, common to aircraft with either MEA or conventional systems architectures

Parameter	Conventional (VAMPZero)	Conventional (Literature [56])	MEA (VAMPZero)	% Change [1]
Masses				
Systems mass (kg)	12,147	12,000	13,603	12
OEM (kg)	40,654	42,600	42,110	3.6
Fuel mass (kg)	19,547	21,252	19,096	-2.3
MTOM (kg)	73,751	73,500	74,756	1.35
Propulsion				
Max thrust (N)	202,650	240,000	203,437	0.4

Table 6.4: Initial design parameters of the aircraft with MEA systems architecture, relative to the conventional systems architecture from VAMPZero (iteration-4) and literature (conventional)

relative to the conventional systems' are presented in Figure 6.4. The highest negative deviation is the mass of the power generation and distribution system (PGDS) as the hydraulic system which includes the hydraulic piping and hydraulic power unit is eliminated in the MEA systems architecture. Mass of the environmental control system contributes to the highest mass increase due to the higher mass contribution of the on-board compressor units which replace the bleed-air for air conditioning. A similar increase in the systems mass is observed in complementary systems as well due to the higher mass of the electric alternatives. This increases the overall mass of the MEA architecture by 9% (1094 kg) and the power consumption by 8.1% (14.6 kW) relative to the conventional systems architecture as seen in Table 6.5. As the systems' mass is recomputed, the OEM and MTOM as well are recomputed and updated in the CPACS file. The miscellaneous systems (Misc) constitute the remaining systems such as the avionics, lights etc. that are not included in the systems categorised above. However, they are not influenced directly by the systems architecture directly as the methods are not sensitive to the degree of electrification. However, the overall systems mass influences the parameters of these systems through the empirical relations, which are functions of the OEM and the number of passengers.

[2]Percentage change of MEA systems architecture, relative to conventional systems architecture with SSM

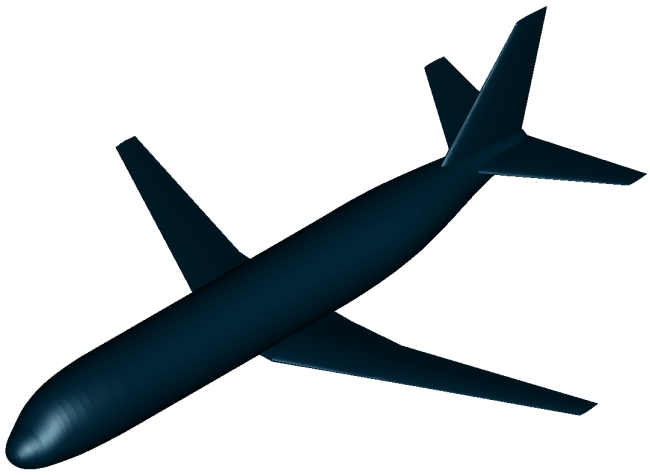

Figure 6.3: Parametric model of the aircraft

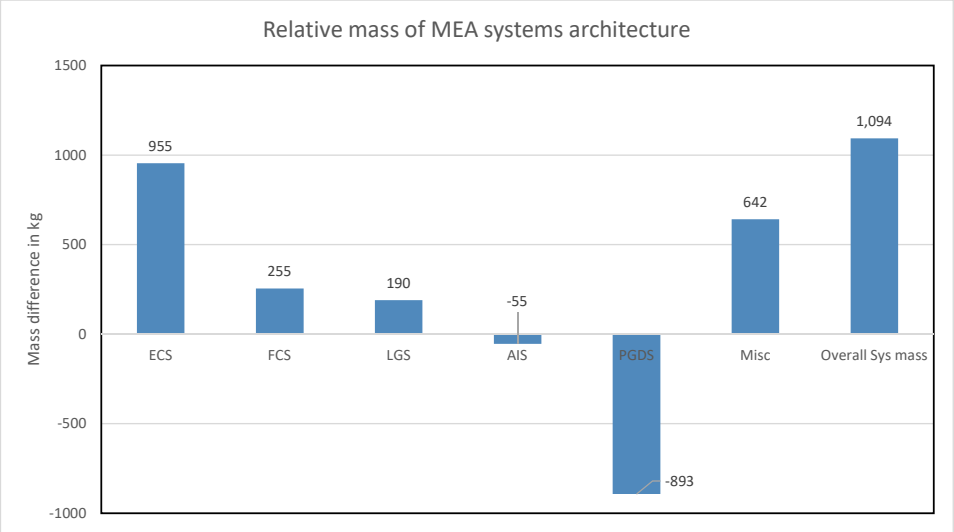

Figure 6.4: Relative differences of masses of the MEA systems to the conventional systems

Parameter	Conventional (SSM)	Conventional (Literature [15])	MEA (SSM)	% Change [2]
Systems mass (kg)	12,155	12,000	13,249	9
Systems power consumption (kW)	180	175	194.6	8
Systems bleed-air consumption (kg/s)	2.5	2.5	0	100
OEM (kg)	40,660	41,863	41,754	2.7
MTOM (kg)	73,867	73,413	74,961	1.5

Table 6.5: Key parameters computed by SSM and their change for MEA systems architecture relative to conventional systems architecture (iteration-4)

SMG

Consequently, the subsystems architecture is selected and the parametric models along with the mass and power consumption at the subsystem level are computed with SMG. The methodology of subsystems sizing by SMG is presented in Section 3.4 and the underlying sizing rules of the subsystems are presented in Chapter 4. One of the main objectives of this stage is that all the subsystems fit in the airframe, provide the required function and do not intersect with the other subsystems. This usually

leads to changing the subsystem parameters by iteration to meet the requirements. In this case study, the parameters of the actuators had to be iterated to find the design that fits into the airframe. This results in the increase increase of the MEA actuators' overall mass by 620 kg (41%), power consumption by nearly 2 kW (-2%) and volume by 0.1 m^3 (58%) relative to the conventional systems architecture. This is due to the higher actuator density due to the lower volume requirement. The systems' mass is recomputed due to this change, leading to a re-computation of the OEM as 42,118 kg and the MTOM as 75,352 kg. The updated parameters are presented in Table 6.6. This leads to more accurate results of the systems as higher number of requirements are fulfilled, relative to the previous stage. With this update, the systems mass of MEA systems architecture is higher by 12%, power consumption by 8.6% , OEM by 2.3% relative to the conventional systems architecture. The parametric models of the subsystems generated with the airframe are presented in Figure 6.5 for a conventional subsystems architecture and in Figure 6.6 for an MEA subsystems architecture. The updated power consumption is propagated to the engine sizing domain, the functions of which are performed by EMM.

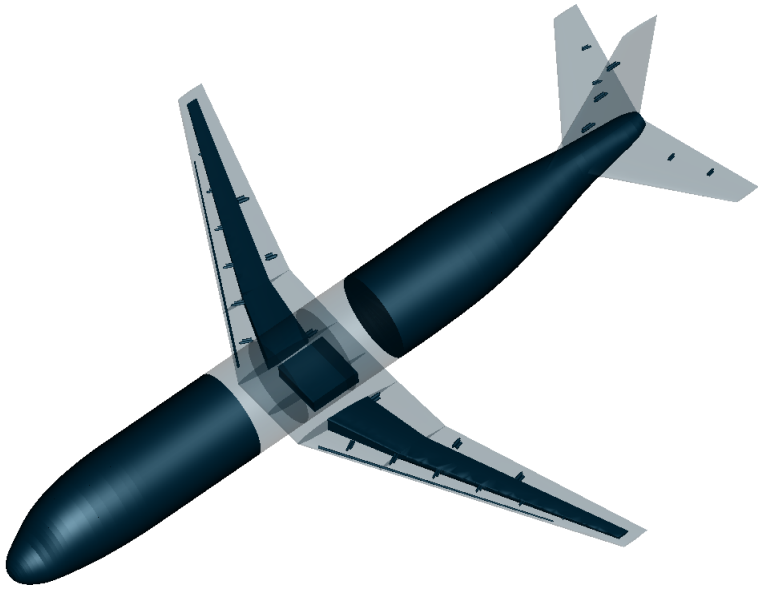

Figure 6.5: Parametric models of the conventional systems

Parameter	**Conventional (SMG)**	**Conventional (Literature [15])**	**MEA (SMG)**	**% Change** [3]
Actuators volume (m^3)	0.145	-	0.230	58
Actuators mass (kg)	1,510	1,500	2,130	41
Actuators power consumption (kW)	73	70	72	-2
Subsystems volume (m^3)	19.6	-	19.7	0.6
Systems mass (kg)	12,155	12,000	13,613	12
Systems power consumption (kW)	180	175	196	8.6
Systems bleed-air consumption (kg/s)	2.5	2.5	0	100
OEM (kg)	40,660	41,863	42,118	3.3
MTOM (kg)	73,867	73,413	75,325	2

Table 6.6: Key parameters computed by SMG and their change for MEA systems architecture relative to conventional systems architecture (iteration-4)

EMM

A turbofan engine with the requirements equivalent to the CFM56-5B [57] is considered for the engine sizing. A bypass ratio of 6, a burner temperature of 1450 K and an overall pressure ratio 32.6 are fixed.

[3]Percentage change of MEA systems architecture, relative to conventional systems architecture with SMG

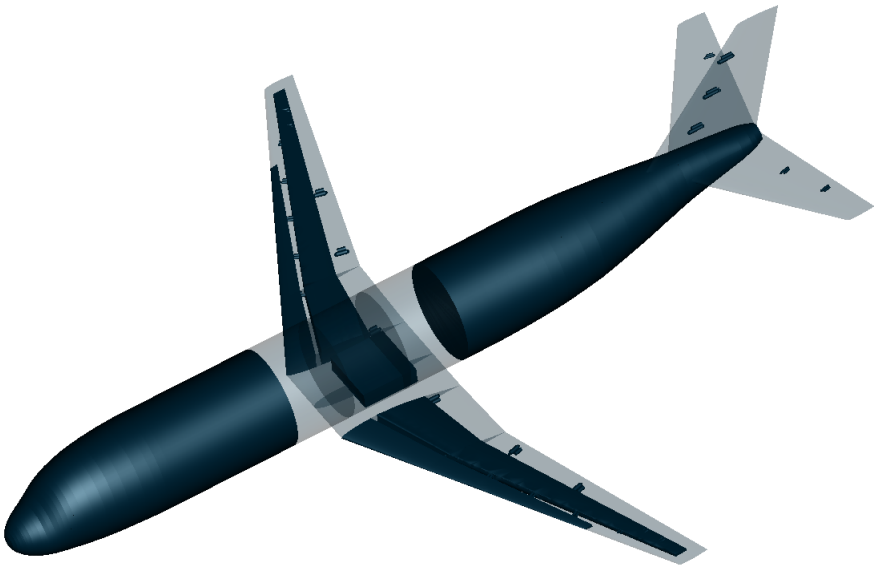

Figure 6.6: Parametric models of the MEA systems

Parameter	Value
Name (−)	CFM56-5B
Type (−)	Turbofan
Bypass ratio (−)	6
Burner temperature (K)	1450

Table 6.7: Engine specifications (iteration-4)

The main requirements for the engine sizing are a maximum thrust of 101,325 N at sea level, computed by VAMPZero, shaft power consumption and bleed-air consumptions of 180 kW and 1.25 kg/s for the conventional systems architecture and shaft power consumption of 194.6 kW for the MEA systems architecture with elimination of bleed-air requirement. These requirements are computed by SMG and SSM. The engine specifications are presented in Table 6.7 .With the engine specific parameters, thrust requirement, shaft power and bleed air off-takes, the engine is sized to fulfil the power and thrust demands of the aircraft. The sized engine is simulated for each thrust setting at every mach number and altitude, specified in the design mission. The fuel consumption at each of these mission points is determined based on the requirements. The SFC of the engine in the cruise condition is presented in Table 6.8. A decrease of 11% is observed in the SFC of the engine for the MEA systems architecture relative to the the conventional systems architecture. The higher SFC is a consequence of the bleed-air extraction from the engines in the conventional systems architecture relative to the total elimination of bleed-air in the MEA systems architecture. The influence of bleed-air extraction in the conventional systems architecture is higher than the influence of higher shaft power (and thrust) requirement of the MEA systems architecture. This was indeed the observation in prior research ([15], [16])

Parameter	Conventional	MEA	% Difference
Max thrust (N)	101,325	101,719	0.4
SFC ($\frac{kg}{N \bullet h}$)	0.054	0.048	-11%

Table 6.8: SFC of the engine for the aircraft with the MEA systems architecture relative to the conventional systems architecture (iteration-4)

FSMS

With the engine performance map, aerodynamic performance parameters and aircraft masses, the aircraft is simulated by FSMS for the design mission presented in Figure 6.7. The aircraft is assumed as a point mass and the mission fuel mass is computed based on standard equations of motion. This computed fuel mass is updated, thus changing the MTOM. The whole framework is iterated till MTOM converges. The overall decrease in mission fuel mass is 2.3% for the MEA systems architecture, relative to the conventional systems architecture. The final results are tabulated in Table 6.9. The fuel consumption benefit by the elimination of bleed-air extraction is superior to the fuel consumption penalty due to the higher shaft power, systems mass and engine thrust of the MEA systems architecture. These results are presented in Figure 6.8.

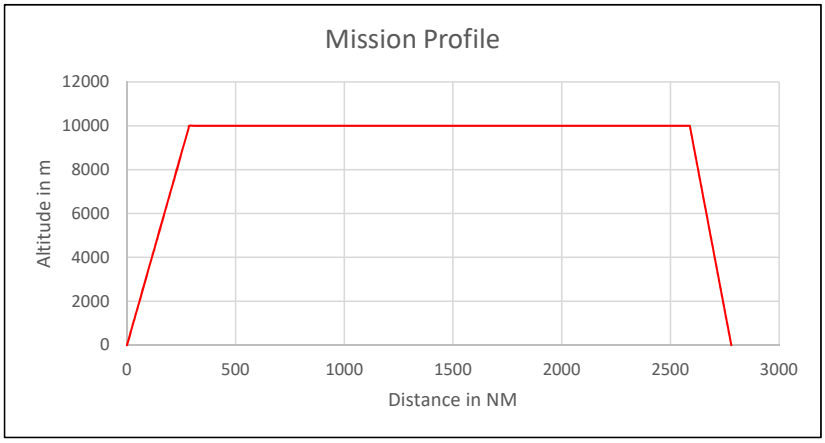

Figure 6.7: Design mission for the aircraft

Parameter	Conventional	Conventional (Literature [15])	MEA	% Change [4]
Actuators volume (m^3)	0.145	-	0.230	58
Actuators mass (kg)	1,510	1,500	2,130	41
Actuators power consumption (kW)	73	70	72	-2
Subsystems volume (m^3)	19.6	-	19.7	0.6
Systems mass (kg)	12,155	12,000	13,613	12
Systems power consumption (kW)	180	175	196	8.6
Systems bleed-air consumption (kg/s)	2.5	2.5	0	100
OEM (kg)	40,660	41,863	42,118	3.3
Fuel mass (kg)	19,551	21,252	19,101	-2.3
MTOM (kg)	73,761	73,413	74,769	1.3

Table 6.9: Final results (iteration-4) of the MEA systems architecture and the conventional systems architecture

[4]Percentage change of MEA systems architecture, relative to conventional systems architecture with SMG

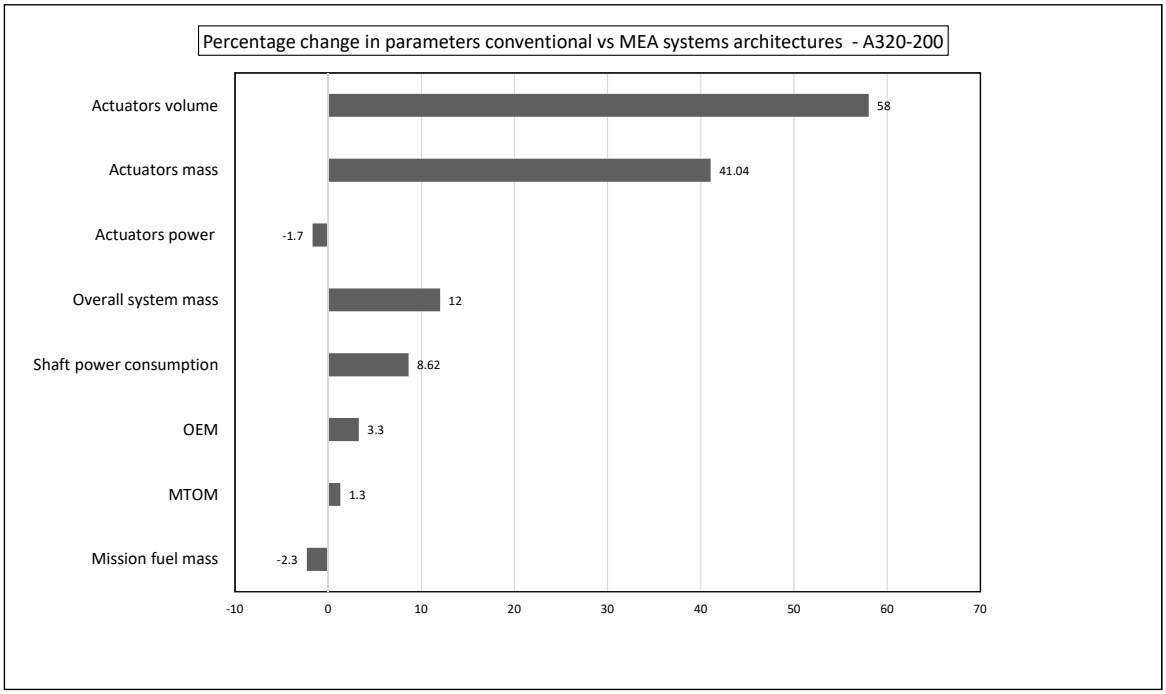

Figure 6.8: Percentage change of the parameters for the MEA systems architecture relative to the conventional systems architecture

6.4. Comparison with related studies

The benefits of MEA systems architecture is a well researched topic through out the past decades. This is attributed to the ever growing technologies in electronics and computation. Jones [58] presented findings of the expected benefits of the MEA systems architectures for civil transport aircraft in his research by comparing different studies over the decades. The main focus of his research was the estimated benefits of electrification of the systems. He presented the Integrated Digital Electric Aircraft (IDEA) study [59] conducted by Lockheed and Boeing which estimated a fuel consumption reduction of 3% for an MEA systems architecture relative to a conventional systems architecture for a 200 passenger Boeing 757. Similarly, the Collaborative Research Initiative into Secondary Power Systems (CRISPS) study [60] estimated a fuel saving around 3-5% for an Airbus A320 aircraft based on the degree of electrification. The methods used for these estimations were mostly empirical and based on the estimation of technological progress of the MEA systems. In relatively recent times, Jomier [61] conducted a similar study and observed an OEM increase around the same range as the result in this thesis. However, all the above studies were only based on projected estimations and did not implement multidisciplinary design methodologies. Chakraborty [16] conducted a similar study by implementing semi-physics based methodologies similar to the ones implemented in this thesis for sizing the aircraft systems simultaneous with the aircraft. The relative mission fuel mass benefit for the MEA systems architecture was computed as 3.13%, which is nearly 1% higher relative to the 2.3% computed in the current research. This deviation is attributed to the higher systems mass and power consumption calculated in this research due to the additional volumetric requirements implemented in the subsystems sizing domain, the domain developed as a part of this research. The presented conclusions are briefly summarised in Table 6.10.

6.5. Chapter summary

In this chapter, the proposed framework was demonstrated with a case study by comparing a conventional systems architecture to an MEA systems architecture for an aircraft configuration equivalent to the Airbus A320-200. The generation and propagation of the parameters at each domain was described in detail as well. The contribution of the parametric systems modelling domain is the added knowledge of the parametric models of the subsystems in the airframe. This knowledge of volume allocation

	IDEA [59]	CRISPS [60]	Jomier [61]	Chakraborty [16]	Current research
Estimated benefit	3%	3%-5%	2%	3.13%	2.3%
Analysis type	Empirical Estimation	Empirical Estimation	Based on current developments of individual technologies	Integrated sizing of systems with the aircraft	Integrated parametric sizing of subsystems with the aircraft
Use case	Boeing B757	Airbus A320	Airbus A320, Dassault Falcon 2000, Alenia ATR-72	Small, medium and very large civil transport aircraft	Short-medium range civil transport aircraft

Table 6.10: Summary of the case study conclusions

aided the redesign of the subsystems based on the restrictions of intersections and confinement within the airframe. This redesign contributed to accurate mass and power consumption parameters of the systems in this case study. It was assessed that the MEA systems architecture reduces the mission fuel mass by nearly 2.5%. The results were within acceptable range relative to literature. Though the relative variation of the mission fuel mass seems low, the framework assists to compute the absolute values of parameters and enable multidisciplinary design of the overall aircraft. The aim of this case study is to validate the framework with literature, thus designing novel configurations with this framework would generate new knowledge about the design in the initial stages. This would enable to assess different systems and subsystems architectures and make certain design decisions that would channel the design into the most feasible path. The conclusions of this research and the recommendations for future development of the framework are proposed in the following chapter.

7

Conclusions and recommendations

7.1. Conclusions

In the scope of this research, a framework to size the subsystems with the aircraft in an integrated multidisciplinary process from a volumetric perspective is presented. The contributions and the conclusions of this research are as follows.

1. **Integrated sizing** framework developed in this research served the objective of enabling automated parametric sizing of the subsystems in an integrated aircraft design process, within a multidisciplinary environment. The disciplines included aircraft design generation, systems selection and sizing, subsystems selection and sizing, engine sizing and mission simulation. Medium fidelity methods were implemented in these domains for sizing. The subsystem selection and sizing domain which enables parametric sizing of the subsystems was developed as a part of this research. It was possible to generate and propagate the knowledge of the parametric models of the subsystems such that the influence and the snowball effects are captured. The whole framework was recreated in an integration environment to carry-out design studies. The methods were verified and validated with literature and the framework is demonstrated with a case study. In the case study, a short-medium transport aircraft with a conventional systems architecture and an MEA systems architecture were generated and the results were assessed with respect to literature. A 2.3% in fuel benefit was observed for the aircraft with the MEA systems architecture, relative to the conventional systems architecture. Excluding high fidelity methods for major domains such as aerodynamics, structures and flight control would indeed lead to certain inaccuracies. However, it was considered acceptable in the scope of this research as the main objective of this thesis was to demonstrate the methodology for automatic integrated parametric sizing of the subsystems with the aircraft.

2. **Subsystems selection and sizing** domain developed as a part of this research is capable of selecting and sizing the parametric models of subsystems. The flight control actuators, fuel tanks and anti-ice elements which constitute the majority of the wing subsystems were modelled. Different design techniques were implemented, such as sizing the subsystems from predefined geometric templates or from the parametric model of the aircraft so as to blend-in the subsystem model with the aircraft profile. The sizing rules were implemented to enable modelling conventional subsystems and the all-electric equivalents of these subsystems. The methods implemented for sizing however were a combination of empirical and physics based methods. The limitations with the empirical methods is the high uncertainty of the result due to the dependency of the results on a few parameters and the relations based on statistic regressions. The implemented physics based methodology were medium fidelity as well due to the limited knowledge of the design in the early stage.

3. **Design automation** methodologies developed for sizing include the automatic fuel tanks sizing and the intersection detection. The automatic fuel tanks sizing enables sizing of the fuel tanks automatically in an iterative manner based on just the required fuel mass. New tanks are added

and the dimensions are increased till the requirements are met. The intersection detection capability provides the designer with the knowledge regarding intersection of any on-board parametric subsystem models or the airframe. This enables the designer to redesign the subsystems/aircraft or re-allocate the positions to the subsystems to avoid this pitfall. Such processes lower the design time and enable the designer to allocate his time to innovative tasks such as carrying out different case studies.

4. **Integration** of the proposed framework in an integration environment enabled to carry-out different design studies within a short period. Each domain of the framework was replaced by an executable computer program and a workflow was created to simulate the framework. This is an example of model-based engineering which enables easy integration and implementation of different domains. This eliminates the task of re-inventing the wheel as each domain would be developed by the respective specialists but can still be used by peers by simply plugging the tool into their multidisciplinary workflow. The SMG tool developed as a part of this research will serve the same purpose. Data parsing complications might occur when integrating tools developed by different specialists. The implementation of a standardised data schema lowers the required interpretation time by both human and computer alike.

5. **Verification and validation** for such high number of cases was possible within such a short time only with the integration and automation methodologies described in the prior paragraphs. These techniques demand high setup time but the ease of carrying out a large number of studies within the short period outweigh the initial delay. The verification and validation added credibility to the design methods to a certain extent and also served in verifying the tool over a wide range of inputs with the sensitivity analysis.

6. **Case study** enabled the demonstration of the overall framework in a quantitative manner. This served as a test for assessing the capabilities of all the developed methodologies as the results were validated at each step. Generating and assessing the parameters of the conventional systems architecture against an MEA systems architecture and validating the results with literature not only added credibility to the framework and the modelling methods but also enabled to quantify the added benefit of the novel domain developed. The higher design knowledge provided by the parametric models and the intersection detection functionality enabled to redesign the actuators such that they would fit in the airframe and avoid intersections. This lead to a higher energy density of the actuators due to the decreased size, thus leading to a lower fuel benefit relative to literature. It is also slightly distressing that most of the current research predict the added fuel benefit for total electrification of the aircraft as less than 5%. However, it is evident from our past that it is such challenges that empower humans to seek out revolutionary technologies.

7. **Knowledge** of the design is increased in the initial design stage with this methodology. Though a case study with a low fuel benefit was demonstrated with this framework, it is vital to acknowledge that this result was derived based on more knowledge of the design. This case study also serves as a validation for the proposed design methodology. The knowledge of the design generated by this framework is in the form of parametric models and volume allocation of the models in the airframe, in a quantified manner . This vast design knowledge is generated in the initial design stages, however due to a lot of assumptions and estimations the absolute values might differ from that of a detailed design. Till this gap is bridged to an acceptable range, this method can only be used to estimate the trends of the effects of integration of certain technologies. With this knowledge, the vital parameters can be identified and manipulated to drive the trends in the desired direction.

7.2. Recommendations for future work

Based on the above discussion, it is evident that further development of the framework is vital to fully exploit the benefits of increasing design knowledge, integrated sizing and design automation. For this purpose, the following domains are recommended to carry-out future developments.

1. The developed framework enables orientation of the components in the airframe and identification of intersections amongst the components and the airframe. However, it is the responsibility

of the designer to reposition or redesign the subsystems to avoid these intersections in the successive designs. This is often time consuming as the designer needs to deal with a large number of volume allocation possibilities to determine the most appropriate solution. Automating this process would not only overcome the above limitations but would also lead to determining the most optimal solution for this problem of space allocation for optimal packaging of subsystems. Similar challenges have been dealt in the past in the naval engineering domain with optimising the storage of containers on-board a container vessel ([62], [63], [64]). These methods are based on heuristics and can be developed with the tool such that optimal packaging of the subsystems can be done in an automated process.

The framework can be further developed in different perspectives.

2. The framework can be extended by introducing medium - high fidelity methods for major domains such as aerodynamics, structures and flight control. This introduction would indeed reveal a high number of snowball effects due to the interdependencies. For instance, an actuator that doesn't fit in the wing can be protected by an external cowling. The added fuel penalty for the drag generated by this cowling and the structural mass can be assessed against the fuel penalty due to higher mass of the smaller actuators that fit completely inside the airframe.

3. The subsystems discipline can be extended to include more number of subsystems such as instrumentation, galley equipment and power distribution units which occupy high volume. This would provide a large amount of knowledge regarding the possible systems architectures. Design studies such as assessing the combined influence of fuselage and wing subsystems on the overall design and performance can be performed.

4. The fidelity of the sizing methods can be improved, which would result in more accurate results. For instance, the current semi-physics based methods for actuators sizing can be replaced with recreated modelica [65] models which would simulate the control laws with respect to the design mission and assess the power consumption. With the ever increasing computational power, this integration would not substantially increase the overall design time, in-spite of demanding a higher setup time.

5. The framework can be extended to different aircraft configurations such as a Blended-wing body (BWB) or an Unmanned Aerial Vehicle (UAV). The UAV design, in specific would be highly beneficial as a UAV design is solely driven on the systems that are required. As such, the knowledge of parametric models and space allocation would add value to the design as the designer could generate higher number of possible configurations based on the optimum packaging of the subsystems as per the requirements. Developing the overall framework to include flight controls domain, a UAV could be designed for instance, for higher manoeuvrability or low fuel consumption. As such, a large number of design possibilities can be generated and assessed effectively in a shorter duration. Moreover, the framework can be extended to assess the cg effects of the subsystems on the aircraft.

In this way, the proposed framework can be developed to carry out design studies by generating and propagating the knowledge of the parametric subsystem models. The possibility in also extended to different domains, aircraft configurations, and different subsystems, which in the past, could have only been possible in the late preliminary or detailed design stages. With this research, we are one step closer to increasing the design knowledge in the initial design stages.

A

Design methods

A.1. Flow charts

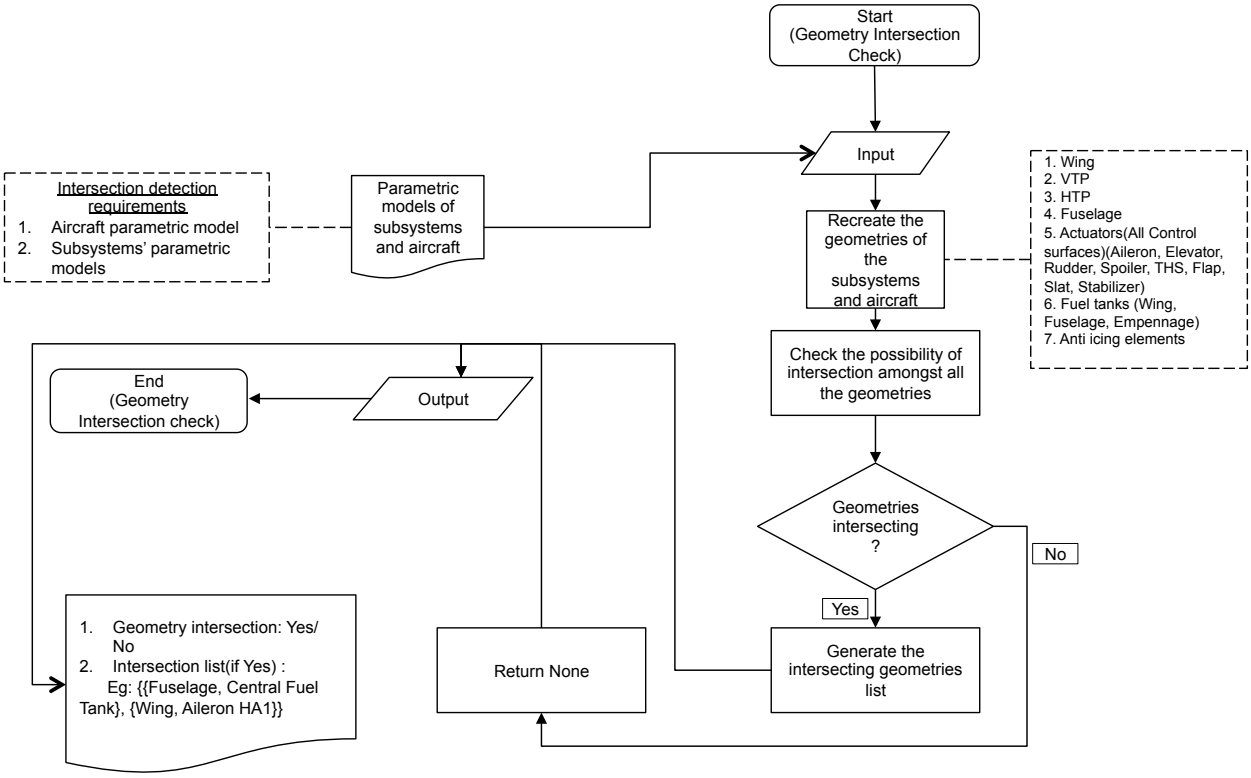

Figure A.1: Flowchart of intersection detection

A.2. Automatic fuel tanks sizing

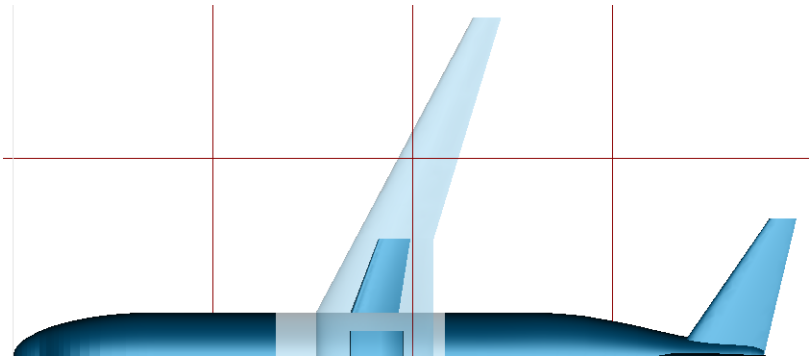

(a) Initial configuration of the fuel tanks

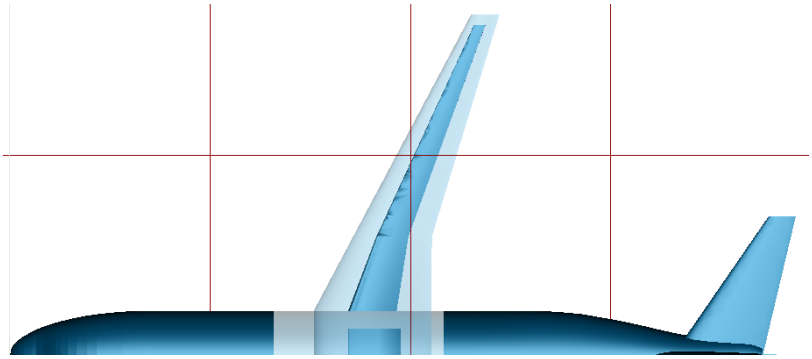

(b) Increases the end fraction of the wing fuel tanks till maximum limit is reached

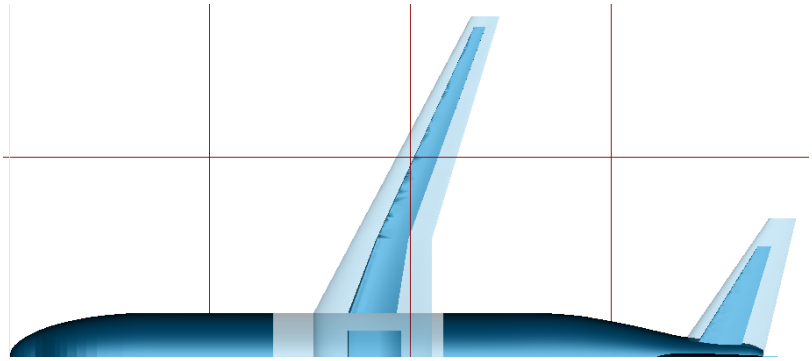

(c) Introduces the empennage fuel tank and increases the end fraction till limits reached

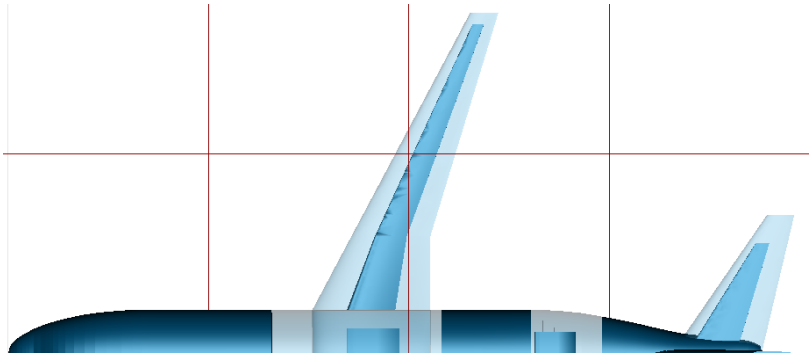

(d) Introduces the fuselage fuel tank and increases the end fraction till limits reached

Figure A.2: Automatic sizing of fuel tanks

B

Sensitivity analysis

B.1. Sensitivity analysis - Subsystem level

B.1.1. EHA

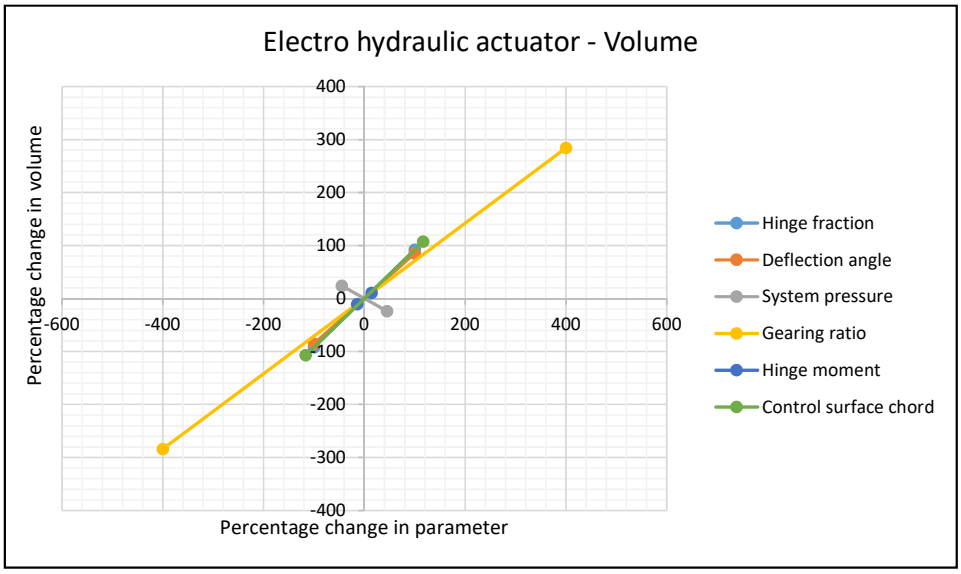

Figure B.1: Sensitivity of the EHA volume with the subsystem level parameters

Variable	Variation in variable	Variation in volume (Baseline = 1441 cm^3)
Hinge fraction	0.1 (20%)	18.5%
Gearing ratio	0.5 (16.6%)	11.8%
System pressure	1 MPa (4.8%)	-2.5%
Deflection angle	1° (3.3%)	3%
Hinge moment	100 Nm (2.85%)	2%
Control surface chord	0.1 m (16.6%)	15.3%

Table B.1: Percentage variation of the EHA volume with the subsystem level parameters

B.1.2. EMA

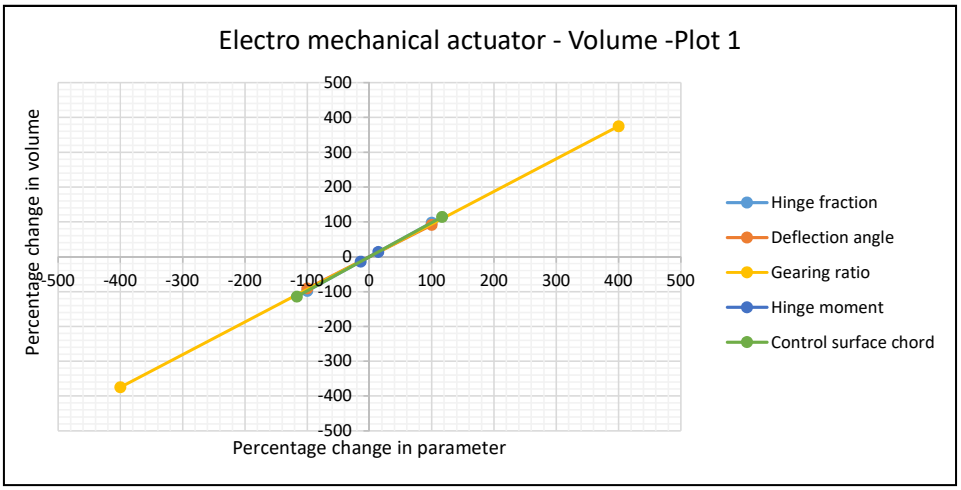

Figure B.2: Sensitivity of the EMA volume with the subsystem level parameters - Plot 1

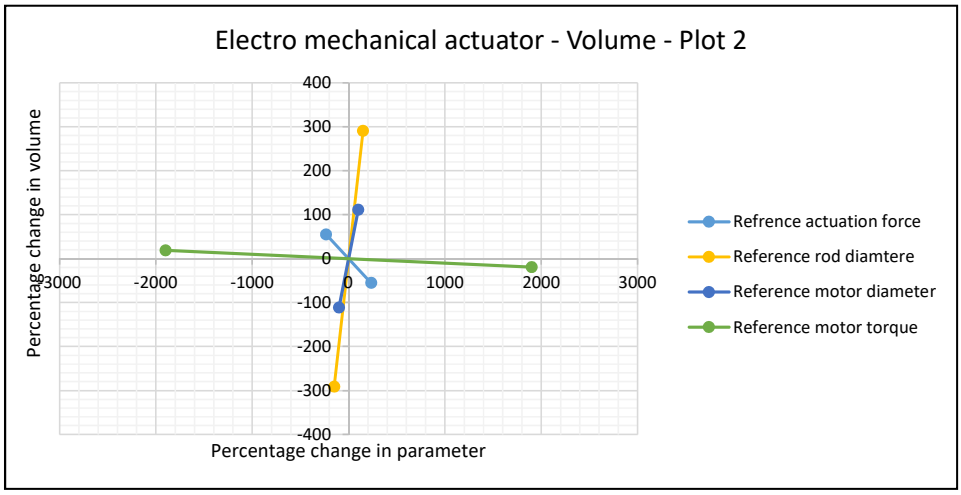

Figure B.3: Sensitivity of the EMA volume with the subsystem level parameters - Plot 2

Variable	Variation in variable	Variation in volume (Baseline = 4200 cm^3)
Hinge fraction	0.1 (20%)	19.5%
Gearing ratio	0.5 (16.6%)	15.6%
Deflection angle	1° (3.3%)	3%
Hinge moment	100 Nm (2.85%)	2.7%
Control surface chord	0.1 m (16.6%)	16.3%
Reference cylinder diameter	1 cm (12.5%)	24%
Reference torque	100 Nm (100%)	-1%
Reference rod diameter	1 cm (33.33%)	51.8%
Reference output force	1 kN (16.6%)	-4%
Reference motor diameter	1 cm (10%)	11%

Table B.2: Percentage variation of the EMA volume with the subsystem level parameters

B.1.3. Wing fuel tank

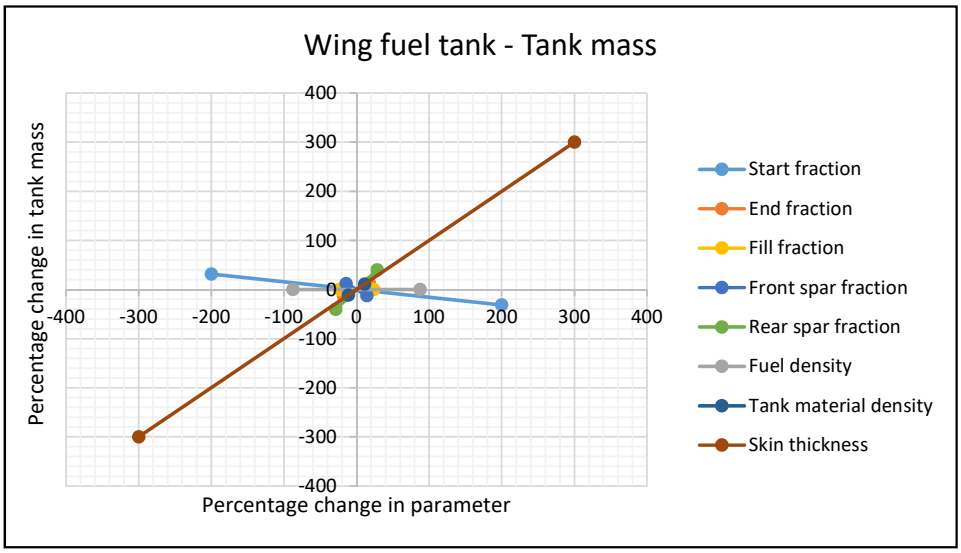

Figure B.4: Sensitivity of the wing fuel tank - tank mass with the subsystem level parameters

Variable	Variation in variable	Variation in tank mass
Start fraction	0.01 (10%)	-4%
End fraction	0.05 (6%)	3.1%
Front spar fraction	0.02 (6%)	-6.5%
Rear spar fraction	0.02 (3%)	4%
Tank material density	100 kg/m^3 (4%)	4%
Tank skin thickness	0.5 cm (100%)	100%

Table B.3: Percentage variation of the wing fuel tank - tank mass with the subsystem level parameters

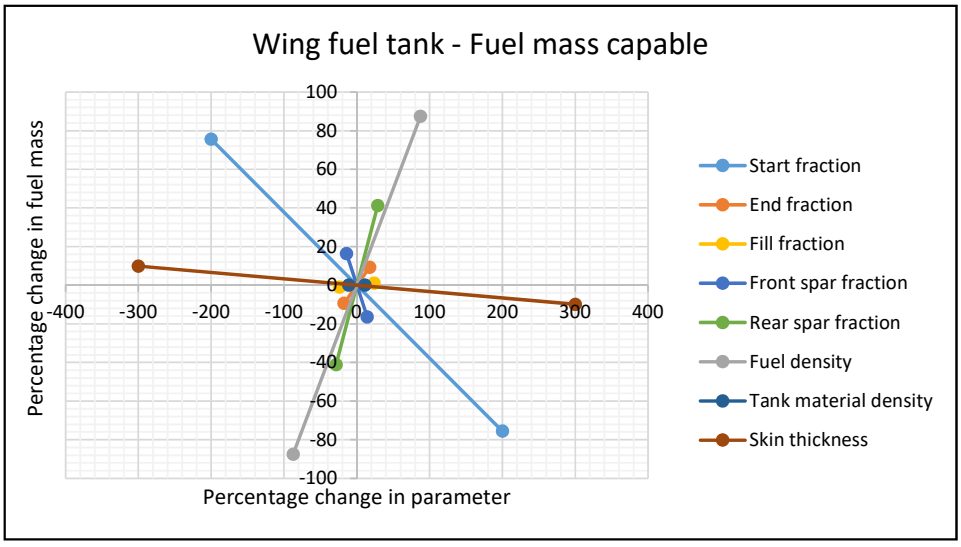

Figure B.5: Sensitivity of the wing fuel tank - fuel mass capable with the subsystem level parameters

Variable	Variation in variable	Variation in fuel mass capable (Baseline = 12,970 kg)
Start fraction	0.01 (10%)	-4%
End fraction	0.05 (6%)	3.1%
Front spar fraction	0.02 (6%)	-6.5%
Rear spar fraction	0.02 (3%)	4%
Fill fraction	0.1 (12.5%)	12.5%
Fuel density	0.1 kg/l (12.5%)	12.5%
Tank skin thickness	0.5 cm (100%)	-3%

Table B.4: Percentage variation of the wing fuel tank - fuel mass capable with the subsystem level parameters

B.1.4. Hot-air anti-ice element

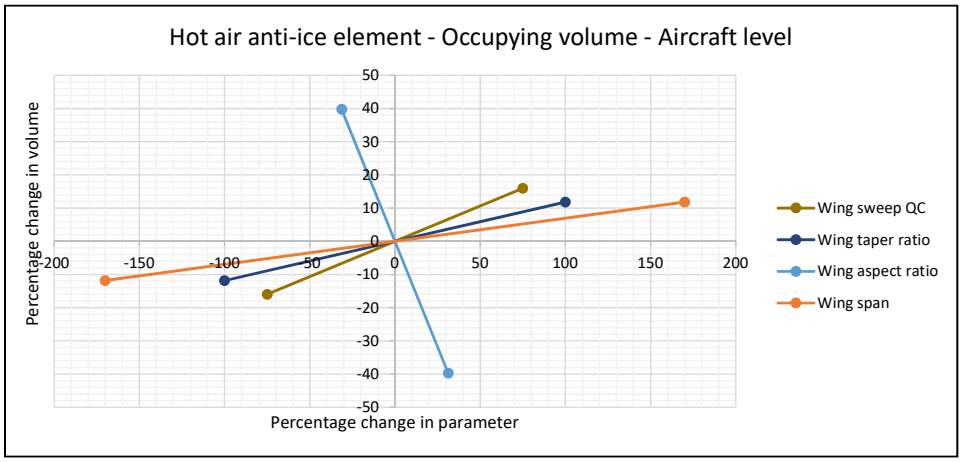

Figure B.6: Sensitivity of the hot-air anti-ice element occupying volume with the aircraft level parameters

Variable	Variation in variable	Variation in volume
Quarter chord wing sweep	1° (5%)	1%
Wing taper ratio	0.1 (50%)	6%
Wing aspect ratio	1 (12.5%)	-16%
Wing span	1 m (3.33%)	0.23%

Table B.5: Percentage variation of the hot-air anti-ice element occupying volume with the aircraft level parameters

B.1.5. Electro-thermal anti-ice element

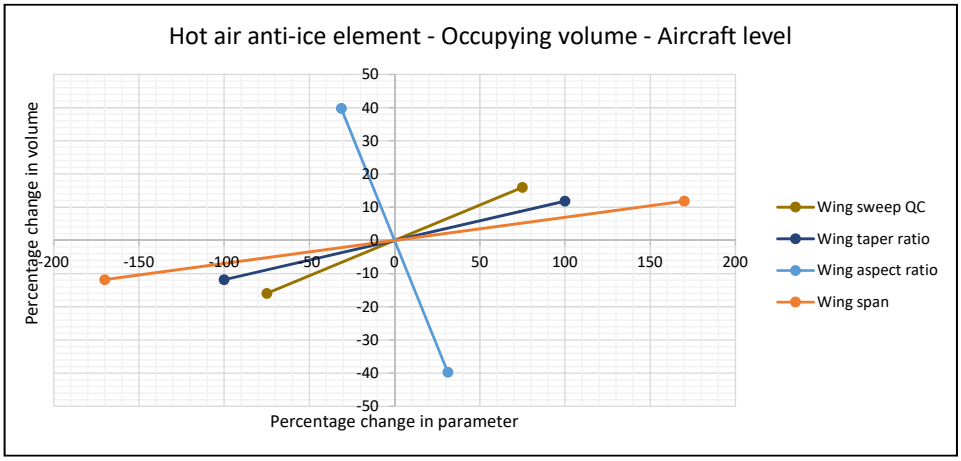

Figure B.7: Sensitivity of the electro-thermal anti-ice element occupying volume with the aircraft level parameters

Variable	Variation in variable	Variation in volume
Quarter chord wing sweep	1° (5%)	0.4%
Wing taper ratio	0.1 (50%)	-1%
Wing aspect ratio	1 (12.5%)	-12.4%
Wing span	1 m (3.33%)	-0.65%

Table B.6: Percentage variation of the electro-thermal anti-ice element occupying volume with the aircraft level parameters

B.2. Sensitivity analysis - Aircraft level

B.2.1. Wing taper ratio

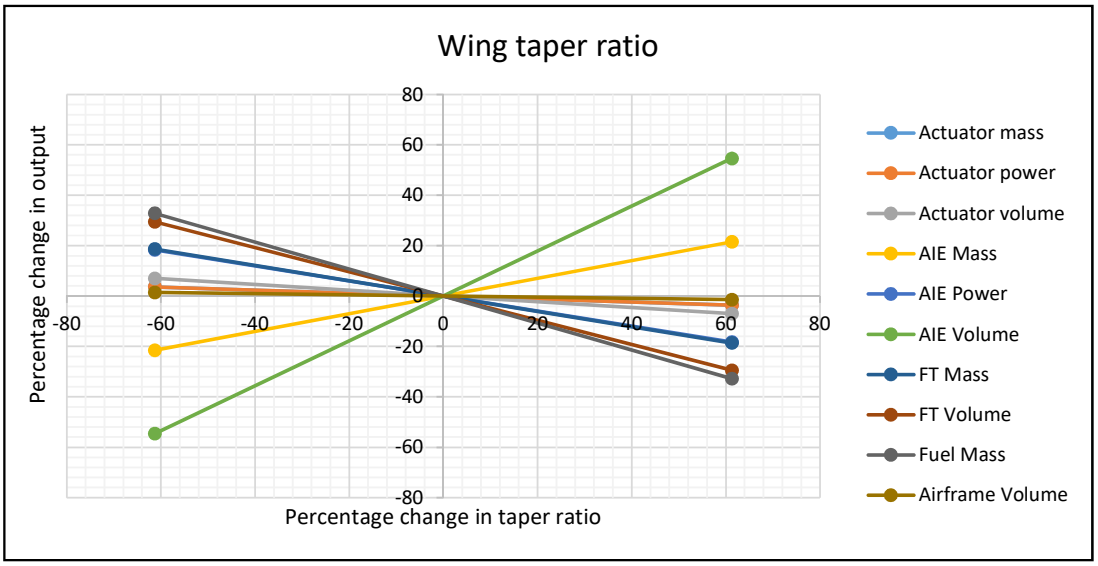

Figure B.8: Variation of results with wing taper ratio

Variable	Variation
Actuators mass	-2.7%
Actuators power	-2.7%
Actuators volume	-4.6%
Anti-ice elements mass	14.63%
Anti-ice elements power	-12.45%
Anti-ice elements volume	37.13%
Fuel tanks mass	-12.70%
Fuel tanks volume	-20%
Fuel mass capable	-22.3%
Airframe volume	-1%

Table B.7: Percentage variation of the parameters with 0.1 (41%) variation of the wing taper ratio

B.2.2. Wing span

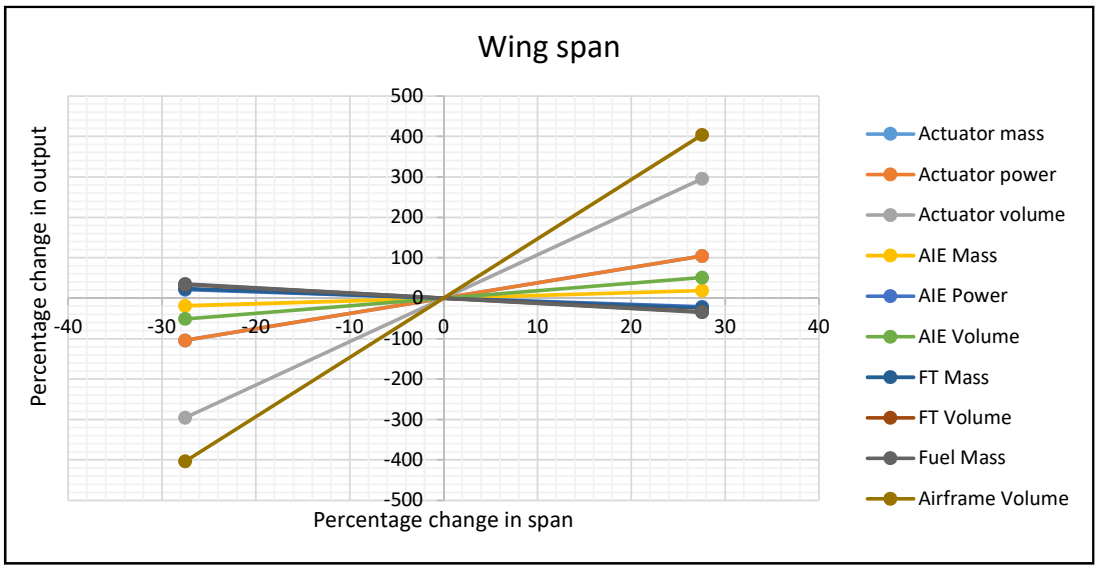

Figure B.9: Variation of results with wing span

Variable	Variation
Actuators mass	12.3%
Actuators power	12.3%
Actuators volume	16.4%
Anti-ice elements mass	4.6%
Anti-ice elements power	8.3%
Anti-ice elements volume	4.6%
Fuel tanks mass	13.3%
Fuel tanks volume	13.9%
Fuel mass capable	13.4%
Airframe volume	43%

Table B.8: Percentage variation of the parameters with 1 m (3%) variation of the wing span

B.2.3. Wing quarter chord sweep angle

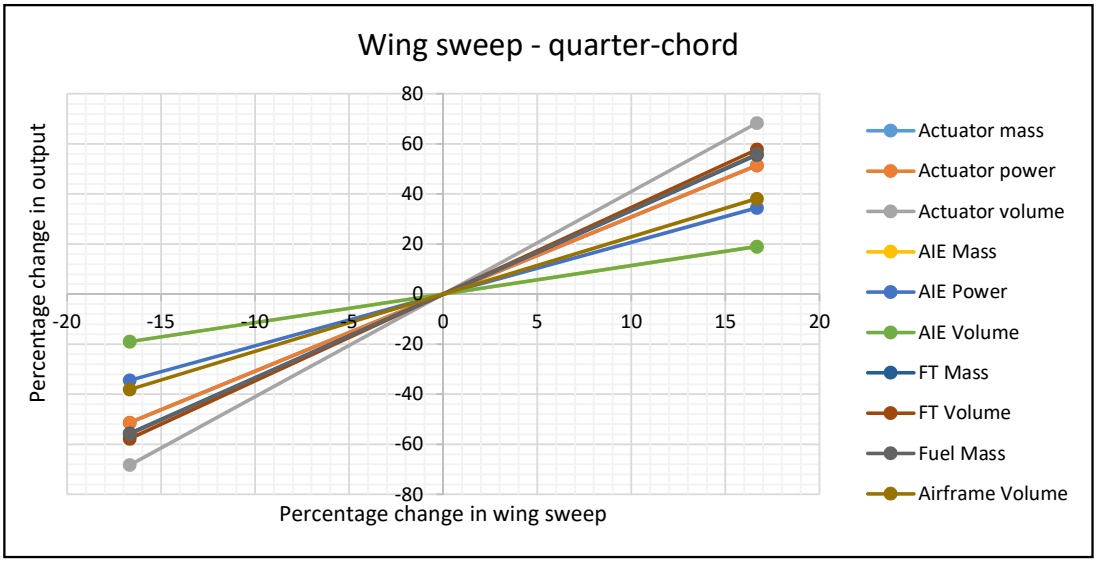

Figure B.10: Variation of results with wing quarter chord sweep angle

Variable	Variation
Actuators mass	0.35%
Actuators power	0.35%
Actuators volume	0.6%
Anti-ice elements mass	2.7%
Anti-ice elements power	4.5%
Anti-ice elements volume	2.7%
Fuel tanks mass	1%
Fuel tanks volume	0.85%
Fuel mass capable	0.8%
Airframe volume	0.32%

Table B.9: Percentage variation of the parameters with 1° (4%) variation of the wing quarter chord sweep angle

B.2.4. Fuselage length

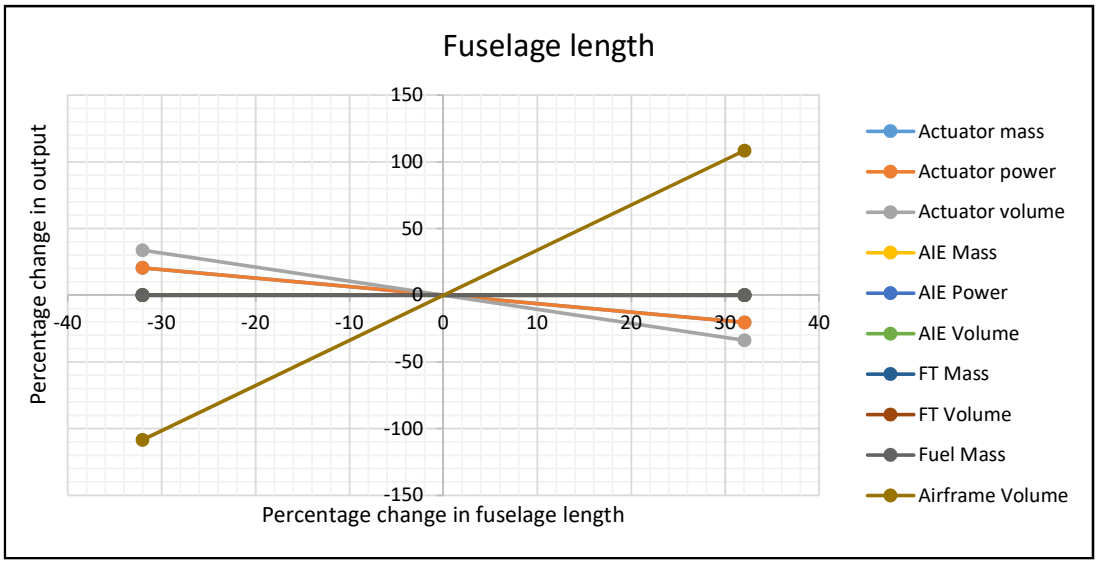

Figure B.11: Variation of results with fuselage length

Variable	Variation
Actuators mass	-1.7%
Actuators power	-1.7%
Actuators volume	-3%
Anti-ice elements mass	0%
Anti-ice elements power	0%
Anti-ice elements volume	0%
Fuel tanks mass	0%
Fuel tanks volume	0%
Fuel mass capable	0%
Airframe volume	9%

Table B.10: Percentage variation of the parameters with 1° (4%) variation of the fuselage length

C

Case study data

C.1. Case study - MEA systems architecture

Iteration	Msys	OEM	Mfuel	MTOM	Unit
1	13,563	42,078	19,072	74,700	kg
2	13,578	42,098	19,087	74,735	kg
3	13,603	42,110	19,096	74,756	kg
4	13,613	42,118	19,101	74,769	kg
5	13,613	42,118	19,101	74,769	kg

Table C.1: Change in parameters of MEA systems architecture with iteration

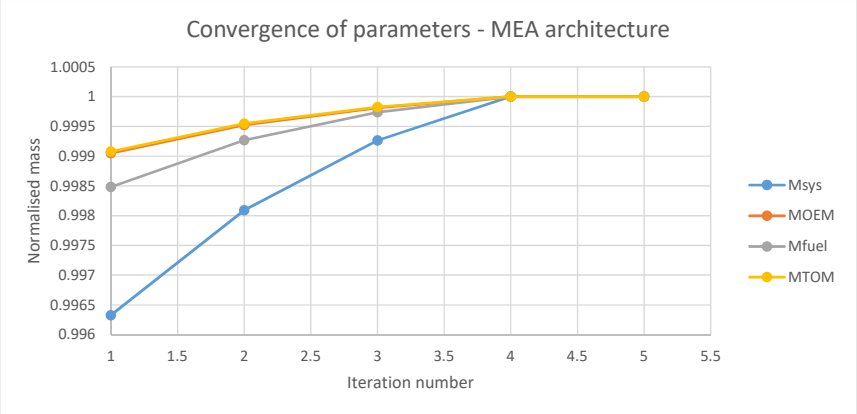

Figure C.1: Normalised convergence of the major parameters of the MEA systems architecture

Bibliography

[1] D. Böhnke, *A multi-fidelity workflow to derive physics-based conceptual design methods,* Ph.D.Technischen Universität Hamburg-Harburg (2015).

[2] V. R. C. Munjulury, M. Tarkian, and C. Jouannet, *Model based aircraft control system design and simulation,* In:ICAS, 27th International Congress Of The Aeronautical Sciences.Nice, France, 19-24 September 2010. Edingburgh:Optimage Ltd. (2013).

[3] E. A. Inés, *Knowledge-Based Flight Control System Integration in RAPID,* Bachelor Thesis.Linköping University (2015).

[4] R. C. Munjulury, E. A. Inés, A. Diaz Puebla, and P. Krus, *Knowledge-based flight control system and control surfaces integration in rapid,* In:Aerospace Technology Congress.Stockholm, Sweden, 11-12 October 2016. USA:Aerospace Technology Congress (2016).

[5] A. Sabaté López and R. C. Munjulury, *Parametric modeling of aircraft fuel systems integration in rapid,* Linköping University. [online] Available at: http://liu.diva-portal.org/smash/get/diva2:847028/FULLTEXT01.pdf (2015), [Accessed March, 2017].

[6] J. Fuchte, B. Nagel, and V. Gollnick, *Automatic fuselage system layout using knowledge based design rules,* In:Deutscher Luft- und Raumfahrtkongress, Deutscher Luft- und Raumfahrtkongress 2012. Berlin, Germany, 10-12 September 2012. Berlin:DGLR (2012).

[7] G. La Rocca and M. Van Tooren, *Enabling distributed multi-disciplinary design of complex products: a knowledge based engineering approach.* Journal of Design Research , pp.333 (2007).

[8] D. Scholz, *Aircraft systems – reliability, mass, power and costs,* Hamburg University of Applied Sciences. [online] Available at: http://www.fzt.haw-hamburg.de/pers/Scholz/ewade/2002/Scholz.pdf (2002), [Accessed May, 2017].

[9] IATA, *Iata technology roadmap,* International Air Transport Association (IATA). [online] Available at: http://www.iata.org/whatwedo/environment/Documents/technology-roadmap-2013.pdf (2013), [Accessed Dec, 2017].

[10] N. Foster, R., *Innovarion: The attacker's advantage, 1st ed.,,* Summit Books (April 1986).

[11] D. P. Raymer, *Aircraft Design: A Conceptual Approach,* Washington, D.C.:AIAA Education Series (1992).

[12] E. Torenbeek, *Synthesis of Subsonic Airplane Design,* Delft: Springer (1982).

[13] G. La Rocca, *Knowledge based engineering techniques to support aircraft design and optimization,* Ph.D.Delft University of Technology (2011).

[14] G. La Rocca and M. van Tooren, *Development of design and engineering engines to support multi-disciplinary design and analysis of aircraft,* Delft Science in Design–A Congress on Interdisciplinary Design , 107 (2005).

[15] T. Lammering, *Integration of Aircraft Systems into Conceptual Design Synthesis,* Ph.D.Institut für Luft-und Raumfahrtsysteme (ILR), RWTH Aachen University (2014).

[16] I. Chakraborty, *Subsystem architecture sizing and analysis for aircraft conceptual design,* Ph.D.Georgia Institute of Technology (2015).

[17] Dassault systems, *CATIA,* [online] Available at: https://www.3ds.com/products-services/catia/ (2017), [Accessed May, 2017].

[18] V. R. C. Munjulury, P. Berry, and P. Krus, *Rapid–robust aircraft parametric interactive design: A knowledge based aircraft conceptual design tool,* In:CEAS, CEAS 2013-International Conference of the European Aerospace Societies.Linköping, Sweden, 16-19 September 2013. Wien:Springer (2013).

[19] Tornado, *Tornado,* [online] Available at: http://tornado.redhammer.se/index.php/theory (2017), [Accessed May, 2017].

[20] Dassault systems, *CATIA SYSTEMS ENGINEERING – DYMOLA,* [online] Available at: https://www.3ds.com/products-services/catia/products/dymola/ (2017), [Accessed May, 2017].

[21] S. Frischemeier, *Electrohydrostatic actuators for aircraft primary flight control-types, modelling and evaluation,* In:SICFP, 5th Scandinavian International Conference on Fluid Power, SICFP '97.Linköping, Sweden, 28-30 May 1997. Linköping:SICFP (1997).

[22] R. Hannat and F. Morency, *Numerical Validation of Conjugate Heat Transfer Method for Anti-/de-Icing Piccolo system,* Journal of Aircraft **51**, pp.104 (2014).

[23] C. Sreedharan, Q. Nagpurwala, and S. Subbaramu, *Effect of Hot Air Jets from a Piccolo Tube in Aircraft Wing Anti-Icing Unit,* MSRUAS-SASTech Journal **13**, pp.1 (2014).

[24] R. Stolte, U. Wollrab, and Airbus Operations Gmbh, *De-icing system for an aircraft,* US Patent 12/988,142 (2011).

[25] P. Stoner, D. Christy, D. Sweet, and Goodrich Coporation, *Low power, pulsed, electro-thermal ice protection system,* US Patent 7,246,773 (2007).

[26] H. W. F. G. J. LeDoux, S. and R. Ratcliff, *Mdopt - a multidisciplinary design optimization system using higher order analysis codes,* In:AIAA/ISSMO Multidisciplinary Analysis and Optimization Conference 2004. New York, USA, 30 August - 01 September 2004. USA:AIAA (2004).

[27] I. Kroo and V. Manning, *Collaborative optimization: Status and directions,* In:8th AIAA/NASA/ISSMO Symposium on Multidisciplinary Analysis and Optimization 2008. California, USA, 06-08 September 2000. USA:AIAA (2004).

[28] G. La Rocca and M. J. L. Van Tooren, *Knowledge-Based Engineering Approach to Support Aircraft Multidisciplinary Design and Optimization,* Journal of aircraft **46**, pp.1875 (2009).

[29] A. Filippone, *Advanced Aircraft Flight Performance,* Cambridge, UK:Cambridge University Press (2012).

[30] Parker Hannifin Corp, *HYDRAULIC CYLINDERS, ELECTROHYDRAULIC – PARKER SERIES 2HX/3HX FAMILY,* [online] Available at: http:http://ph.parker.com/us/en/heavy-duty-industrial-tie-rod-construction-electrohydraulic-cylinders-series-2hx (2017), [Accessed November, 2017].

[31] DLR, *CPACS - A Common Language for Aircraft Design,* [online] Available at: http://www.cpacs.de/ (2017), [Accessed March, 2017].

[32] B. Nagel, D. Böhnke, V. Gollnick, P. Schmollgruber, A. Rizzi, G. La Rocca, and J. J. Alonso, *Communication in aircraft design:can we establish a common language?* In:ICAS, 28th International Congress Of The Aeronautical Sciences.Brisbane, Australia, 23-28 September 2012. Edingburgh:Optimage Ltd. (2012).

[33] DLR, *VAMPzero - Conceptual Design for the Needs of MDO,* [online] Available at: https://software.dlr.de/p/vampzero/home/ (2017), [Accessed March, 2017].

[34] DLR, *TIGL,* [online] Available at: https://software.dlr.de/p/tigl/home/ (2017), [Accessed March, 2017].

[35] I. Moir and A. Seabridge, *Aircraft Systems: Mechanical, electrical and avionics subsystems integration.3rd ed.* Chichester, England:John Wiley & Sons (2011).

[36] C. R. Spitzer, *The Avionics Handbook,* Boca Raton, USA:CRC press (2001).

[37] J. Roskam, *Airplane Design,* Ottawa, Kansas:Roskam Aviation & Engineering Corporation (1985).

[38] H. I. H. Saravanamuttoo, G. F. C. Rogers, and H. Cohen, *Gas turbine theory,* London, United Kingdom:Pearson Education (2001).

[39] J. D. Mattingly, *Elements of gas turbine propulsion,* New York, USA:McGraw-Hill Science, Engineering & Mathematics (1996).

[40] DLR, *RCE - Remote Component Environment,* [online] Available at: https://software.dlr.de/p/rcenvironment/home/ (2017), [Accessed March, 2017].

[41] I. Chakraborty, D. N. Mavris, M. Emeneth, and A. Schneegans, *A methodology for vehicle and mission level comparison of more electric aircraft subsystem solution: Application to the flight control actuation system,* Proceedings of the Institution of Mechanical Engineers, Part G: Journal of Aerospace Engineering , 1088 (2014).

[42] C. Müller, D. Scholz, and T. Giese, *Dynamic simulation of innovative aircraft air conditioning,* DGLR: Deutscher Luft-und Raumfahrtskongress. Bonn: Deutsche Gesellschaft für Luft-und Raumfahrt (2007).

[43] N. S. Currey, *Aircraft landing gear design: principles and practices,* Washington, D.C.:AIAA Education Series (1988).

[44] W. B. Wright, *An evaluation of jet impingement heat transfer correlations for piccolo tube application,* 42nd AIAA Aerospace Science Meeting and Exhibit (2004).

[45] O. Meier and D. Scholz, *A handbook method for the estimation of power requirements for electrical de-icing systems,* DLRK, Hamburg (2010).

[46] I. Chakraborty, M. J. LeVine, M. Hassan, and D. N. Mavris, *Assessing taxiing trade spaces from aircraft, airport, and airline perspectives,* in *AIAA AVIATION 2015 Conference, No. AIAA-2015-2386, American Institute of Aeronautics and Astronautics, Dallas, TX* (2015).

[47] A. Cameron Johnson, *Some aspects of the design of aircraft steering systems,* Aircraft Engineering and Aerospace Technology **43**, 7 (1971).

[48] D. Seider, S. Zur, J. Flink, R. Mischke, and O. Seebach, *Rce–distributed, workflow-driven integration environment,* (2013).

[49] S. Zur and A. Tröltzsch, *Optimization of the dlr spaceliner inside the integration environment rce,* Engineering Optimization 2014 **1**, 757 (2014).

[50] D. Scholz, *Entwicklung eines cae-werkzeuges zum entwurf von flugsteuerungs- und hydrauliksystemen, vol. 262 of fortschritt-berichte vdi,* VDI, Duesseldorf, Germany (1997).

[51] E. Truckenbrodt, *Fluidmechanik, vol. 2, 4th ed.„* Springer, Berlin, Germany (1996).

[52] M. Budinger, J. Liscouët, F. Hospital, and J. Maré, *Estimation models for the preliminary design of electromechanical actuators,* Proceedings of the Institution of Mechanical Engineers, Part G: Journal of Aerospace Engineering **226**, pp.243 (2012).

[53] R. Langton, C. Clark, M. Hewitt, and L. Richards, *Aircraft Fuel Systems,* Chichester, England:John Wiley & Sons (2009).

[54] S. Liscouet-Hanke, *A Model Based Methodology for Integrated Preliminary Sizing and Analysis of Aircraft Power System Architectures,* Ph.D.Universite' de Toulouse (2008).

[55] Airbus, *Airbus a320 flight crew operating manual,* Airbus (2008).

[56] Airbus, *Airbus a320 - dimesnions and key data,* [online] Available at: http://www.aircraft.airbus.com/aircraftfamilies/passengeraircraft/a320family/a320/ (2017), [Accessed November, 2017].

[57] CFM International, *Cfm56-5b technology,* [online] Available at: https://web.archive.org/web/20100307035338/http://www.cfm56.com/products/cfm56-5b (2017), [Accessed November, 2017].

[58] I. Jones, R, *The more electric aircraft—assessing the benefits,* Proceedings of the Institution of Mechanical Engineers, Part G: Journal of Aerospace Engineering **216**, pp.259 (2002).

[59] E. Tagge, G, A. Irish, L, and R. Bailey, A, *Systems study for an integrated digital/elect ric aircraft (idea),* NASA CR 3840 (1985).

[60] H. Qureshi, H, *Collaborative research initiative into secondary power systems. final report of the overall benefits prediction program,* (1992).

[61] T. Jomier, *More open electric technologies (moet),* Airbus Operations S.A.S. and MOET Consortium Partners (2009).

[62] P. Song, F. Mingming, L. Jing, and S. Jun, *A study on container allocation on shipping routes for liner companies,* International Conference on Service Systems and Service Management , 1 (2007).

[63] I. Wilson and P. Roach, *Principles of combinatorial optimization applied to container-ship stowage planning,* Journal of Heuristics **5**, pp.403 (1999).

[64] A. Albano and G. Sapuppo, *Optimal allocation of two-dimensional irregular shapes using heuristic search methods,* IEEE Transactions on Systems, Man, and Cybernetics **10**, pp.242 (1980).

[65] Modelica Association, *Modelica,* [online] Available at: https://www.modelica.org/ (2017), [Accessed November, 2017].